

# Enhancement technologies of ammonia-based carbon capture: A review of developments and challenges



Marta Sibhat<sup>a,b</sup>, Qiuxia Zhu<sup>b</sup>, Gedion Tsegay<sup>a,b</sup>, Guodong Yao<sup>b,c</sup>, Guodong Yin<sup>c</sup>, Yangyuan Zhou<sup>b,c,\*</sup>, Jianfu Zhao<sup>b,c,\*</sup>

<sup>a</sup> UNEP-TONGJI Institute of Environment for Sustainable Development (IESD), College of Environmental Science and Engineering, Tongji University, 1239 Siping Road, Shanghai, 200092, China

<sup>b</sup> Jiaxing-Tongji Environmental Research Institute, 1994 Linggongtang Road, Jiaxing 314051, Zhejiang Province, China

<sup>c</sup> State Key Laboratory of Pollution Control and Resources Reuse, College of Environmental Science and Engineering, Tongji University, 1239 Siping Road, Shanghai, 200092, China

## ARTICLE INFO

### Keywords:

Aqueous ammonia  
Absorption rate  
Mass transfer  
Chemical absorption  
Post-combustion CO<sub>2</sub> capture

## ABSTRACT

Aqueous ammonia is one of the most promising solvents to conventional amine for capturing CO<sub>2</sub> from flue gas and other industrial emissions owing to its high CO<sub>2</sub> loading capacity, low-cost, less corrosive, and low vulnerability to degradation. However, due to the slow absorption rate of CO<sub>2</sub>, the industrial application of ammonia is restricted. The present review mainly focused on the current developments of the aqueous ammonia-based carbon capture process (AAP) and its enhancement technologies to improve the absorption rate performance. The reaction between aqueous ammonia and CO<sub>2</sub>, including reaction mechanism, reaction intermediates, reaction products, and influence of different operational parameters on the absorption performance, are presented. The enhancement technologies, mass transfer coefficients, and perspectives for each potential technology in AAP are reviewed. Furthermore, the recent advances in the potential of ammonia for combined removal of several flue gas components such as; NO<sub>x</sub>, SO<sub>x</sub>, CO<sub>2</sub>, and other pollutants are discussed. Finally, in light of recent advancements and obstacles of AAP, this study provides views and highlights in which future prospective investigation is necessary to improve the absorption rate of aqueous ammonia.

## 1. Introduction

The most significant contributor to climate change is the emission of greenhouse gases (GHGs), which has made it a critical problem for the environment in every region of the globe. Human activities are the leading cause that accounts for 80 % of all GHGs emission and is a major factor in the progression of climate change worldwide (IPCC, 2007). Fossil fuels continue to be seen as the primary energy source of production because of their availability. As a direct consequence of the excessive use of coal, power plants are responsible for around 35 % world's total annual CO<sub>2</sub> emissions (Davidson, 2007). Based on the reports of the Intergovernmental Panel on Climate Change (IPCC), there is an urgent need to cut global emissions of greenhouse gases by 50–80 % to forestall any further deterioration of climate crises (Songolzadeh et al., 2014). Thus, for future sustainability, CO<sub>2</sub> capture technologies should be actively incorporated. Carbon capture and storage (CCS) is an effective strategy for reducing GHGs emissions and coping with climate

change. The process of CCS comprises removing CO<sub>2</sub> from its emission source, compressing it, and delivering it to an appropriate area for its long-term storage (Figueroa et al., 2008).

CCS can be classified into three technological applications: pre-combustion, post-combustion, and oxyfuel combustion capture. Post-combustion capture (PCC) is commercially established and viable technology with a lower risk of technological failure than the other two competing technologies. It is the most practical, near-term technology that may significantly reduce emissions of CO<sub>2</sub> from coal-fired power generation plants. It also has an appealing economic benefit, which can help speed the deployment of CCS (Goto et al., 2013; Liang et al., 2016; Rochelle, 2009; Yang et al., 2014a). PCC can also integrate with renewable technologies; for example, affordable solar repowering might provide energy to regenerate CO<sub>2</sub>. Despite the fact that pre-combustion and oxyfuel capture offers several benefits over post-combustion capture, it is unlikely that either method will replace the PCC on a global scale.

At present, the chemical absorption PCC process has reached its

\* Corresponding authors.

E-mail addresses: [zhouyangyuan@126.com](mailto:zhouyangyuan@126.com) (Y. Zhou), [zhaojianfu@tongji.edu.cn](mailto:zhaojianfu@tongji.edu.cn) (J. Zhao).

Nomenclature	
AAP	Aqueous ammonia capture process.
AIC	Absorber intercooling.
CCS	Carbon Capture and Storage.
CAP	Chilled ammonia process.
e-NRTL	Electrolyte non-random two-liquid.
e-UNIQUAC	Extended Universal Quasi-Chemical.
HIFU	High frequency ultrasonic assisted.
HFMC	Hollow fiber membrane contactor.
IHA	Inter-heated absorber.
MDEA	Methyldiethanolamine.
MEA	Monoethanolamine.
MR	Microchannel.
NH <sub>3</sub>	Ammonia.
NO <sub>x</sub>	Nitrogen Oxides.
SO <sub>x</sub>	Sulphur Oxides.
PCC	Post-combustion CO <sub>2</sub> Capture.
PZ	Piperazine.
RPB	Rotating packed bed.
RSS	Rich solvent splitting.
SFA	Split flow arrangement.
VLE	Vapour-liquid equilibrium.
WWC	Wetted-wall column.
a <sub>v</sub>	Interfacial area per unit volume.
K <sub>Gav</sub>	Overall volumetric mass transfer coefficient.
K <sub>G</sub>	Overall mass transfer coefficient.
k <sub>g</sub>	Gas phase mass transfer coefficient.
k <sub>l</sub>	Liquid phase mass transfer coefficient.
k <sub>m</sub>	Membrane mass transfer coefficients.

technological maturity and has been determined to be the most appropriate technology due to its high CO<sub>2</sub> removal efficiency and cost-saving for large-scale operations (Borhani and Wang, 2019). Many chemical absorbents, such as monoethanolamine (MEA), ammonia (NH<sub>3</sub>), potassium carbonate (K<sub>2</sub>CO<sub>3</sub>), alkaline metal hydroxides (NaOH, KOH),

amino acid, etc., can be used for CO<sub>2</sub> absorption. The benefits and challenges of the most known chemical solvents are summarized in Table 1. Because of its high reactivity, MEA is a widely used sorbent for removing CO<sub>2</sub> from flue gases (Lin and Kuo, 2016). However, there are some weaknesses of MEA including; limited CO<sub>2</sub> capacity, equipment corrosion, the energy requirement of solvent regeneration, and degradation problems.

An aqueous ammonia solution has been suggested as a suitable alternative solvent for CO<sub>2</sub> absorption due to its high capture capacity, lower regeneration energy, and has the capability to remove multi-pollutants (CO<sub>2</sub>, NO<sub>x</sub>, and SO<sub>x</sub>) simultaneously (Han et al., 2013; Yu et al., 2013b; Yu et al., 2012c). Numerous experimental studies have been conducted comparing ammonia and MEA chemical solvents to remove CO<sub>2</sub> (Bai and Yeh, 1997; Puxty et al., 2010; Rivera-Tinoco and Bouallou, 2010; Yeh and Bai, 1999). The experiments revealed that NH<sub>3</sub> has a greater removal efficiency and absorption capacity of CO<sub>2</sub> than MEA. According to the research conducted by Niu et al. (2010), the removal efficiency of CO<sub>2</sub> could be reached 98.4 % with aqueous ammonia. Besides, low regeneration energy is required for NH<sub>3</sub> compared to MEA (Yeh et al., 2005).

Extensive study has been carried out at various scales to comprehend the theoretical and practical components of PCC using aqueous NH<sub>3</sub>. Alstom (Telikapalli et al., 2011), Powerspan (McLarnon and Duncan, 2009), and CSIRO (Yu et al., 2011; Yu et al., 2012a) have each built pilot plants to prove the technological and economic feasibility of AAP. Through these initiatives, it has been demonstrated that the AAP is technically feasible and could reach 90 % efficiency in CO<sub>2</sub> removal and 99 % final purity of CO<sub>2</sub> (Li et al., 2015b). Fig. 1 shows the basic process of CO<sub>2</sub> capture using an ammonia solution.

Despite the benefits outlined above, AAP suffers from some major drawbacks. One of the major challenges is that ammonia has a slow rate of reaction when compared with MEA solution under their respective operational conditions. On the other hand, due to the high vaporization of ammonia, a relatively low NH<sub>3</sub> concentration and low temperature parameter setting is required during absorption (Darde et al., 2009), resulting in a relatively lower absorption rate of CO<sub>2</sub>. Because of these drawbacks, ammonia-based CO<sub>2</sub> capture technology must employ a larger absorption column, which in turn reduces energy efficiency and limits its industrial application.

During the CO<sub>2</sub> separation process, the absorption rate is an important factor to monitor since it has the potential to influence both the operational and capital costs. The rate of CO<sub>2</sub> absorption determines how near the actual quantity of CO<sub>2</sub> that is absorbed may approach the equilibrium value in the packed column. When selecting appropriate chemical absorbents for the removal of CO<sub>2</sub>, rapid CO<sub>2</sub> absorption is recognized as one of the most significant characteristics to consider owing to its number of benefits (Shokrollahi et al., 2022). First, it

**Table 1**  
Benefits and challenges of selected chemical solvents for post combustion capture (Aghel et al., 2022; Borhani et al., 2015; Chu et al., 2021; Rochelle, 2016; Shokrollahi et al., 2022; Zhou et al., 2012).

	Benefits	Challenges
Amines /MEA	<ul style="list-style-type: none"> <li>• High buffering capacity</li> <li>• High reactivity even with low CO<sub>2</sub> concentration</li> <li>• High absorption efficiency</li> <li>• Simple contaminates reclaiming process</li> <li>• Easy to manufacture and cheap</li> </ul>	<ul style="list-style-type: none"> <li>• High rate of corrosiveness</li> <li>• Thermal degradation</li> <li>• Limited CO<sub>2</sub> absorption capacity</li> <li>• High regeneration energy</li> <li>• Unsuitable for high-pressure gaseous stream removal</li> </ul>
Ammonia	<ul style="list-style-type: none"> <li>• Good absorption capacity</li> <li>• Strong thermal-oxidative stability</li> <li>• Low cost compared to MEA</li> <li>• Can capture multi-pollutant gases simultaneously (CO<sub>2</sub>/NO<sub>2</sub>/SO<sub>2</sub> and Hg)</li> <li>• Can form industrially relevant fertilizers</li> </ul>	<ul style="list-style-type: none"> <li>• More complicated procedure than amine</li> <li>• High volatility</li> <li>• Slow rate of reaction</li> <li>• Cannot decrease the CO<sub>2</sub> content to minimum levels in the produced gas</li> </ul>
Alkaline metal solution (NaOH, KOH)	<ul style="list-style-type: none"> <li>• Cheap and easy availability</li> <li>• Non-volatility and lower toxicity</li> </ul>	<ul style="list-style-type: none"> <li>• Hydroxides are not easily generated with a mildly thermal</li> <li>• Precipitation in the pipeline and reboiler of the process</li> <li>• pressure swing compared to carbonates</li> <li>• Low mass transfer and slow reaction rate</li> <li>• Precipitation in pipeline and reboiler of the process</li> <li>• Corrosion of carbon steel problem (less than amines)</li> </ul>
Carbonates	<ul style="list-style-type: none"> <li>• High chemical solubility of CO<sub>2</sub> in solution</li> <li>• Low cost of solvent, less harmful, non-volatile</li> <li>• Low solvent degradation</li> </ul>	<ul style="list-style-type: none"> <li>• Formation of carbonate precipitate at high CO<sub>2</sub> loadings</li> <li>• High energy consumption for desorption</li> </ul>
Amino Acid	<ul style="list-style-type: none"> <li>• More environmentally friendly than amines</li> <li>• Strong stability against oxidative degradation</li> <li>• Low volatility</li> </ul>	<ul style="list-style-type: none"> <li>• Nitrogen Oxides.</li> <li>• Sulphur Oxides.</li> <li>• Post-combustion CO<sub>2</sub> Capture.</li> <li>• Piperazine.</li> <li>• Rotating packed bed.</li> <li>• Rich solvent splitting.</li> <li>• Split flow arrangement.</li> <li>• Vapour-liquid equilibrium.</li> <li>• Wetted-wall column.</li> <li>• Interfacial area per unit volume.</li> <li>• Overall volumetric mass transfer coefficient.</li> <li>• Overall mass transfer coefficient.</li> <li>• Gas phase mass transfer coefficient.</li> <li>• Liquid phase mass transfer coefficient.</li> <li>• Membrane mass transfer coefficients.</li> </ul>

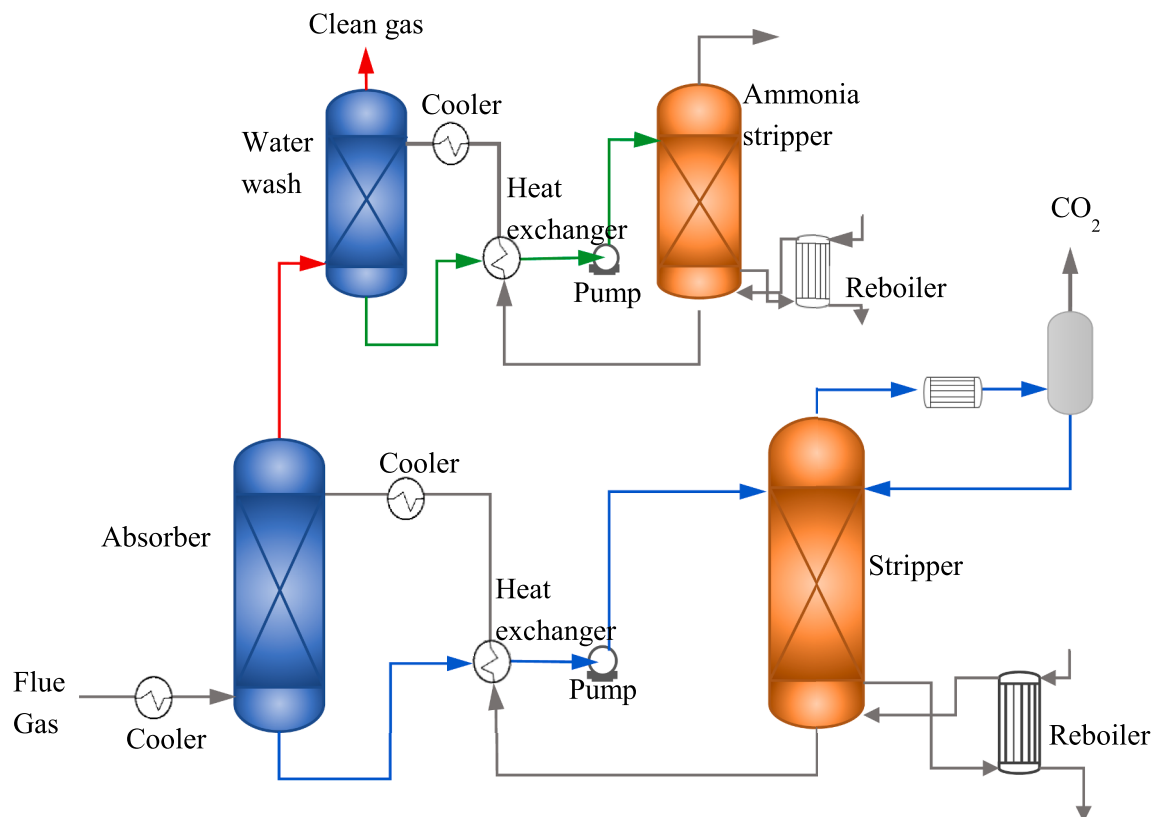


**Fig. 1.** Basic flowsheet of ammonia-based post-combustion carbon capture (Jilvero et al., 2014).

enhances the efficiency with which  $\text{CO}_2$  is absorbed, which ultimately results in improved absorption performance. Second, if the process of  $\text{CO}_2$  absorption is rapid enough, less chemical absorbent will be recirculated throughout the process, which will reduce the energy consumption for solvent regeneration. Both of these aspects contribute to a decrease in operational expenses. Finally, a higher rate of absorption is also required to minimize the height of the absorption column, which lowers the capital expenditure (Oexmann et al., 2012). Therefore, increasing the reaction rate can eliminate this disadvantage, transforming  $\text{NH}_3$  into a good solvent for the absorption of  $\text{CO}_2$  in the process.

The ongoing analysis of relevant academic literature reveals that there is a paucity of material on the topic of the present study. Zhao et al. (2012) examined the progression of fundamental research on AAP, while Han et al. (2013) identified key obstacles hindering AAP, including technical difficulties in the process toward commercialization such as relatively low  $\text{CO}_2$  absorption rate, high ammonia loss, solid precipitation, and inadequate process models. It's worth noting that ammonia escape mechanism and abatement technologies are reviewed by Ma et al. (2013a), Wang et al. (2018) and Yu (2018) emphasized practical applications and specific technological advancements including solid precipitation clogging preventions in the field of aqueous  $\text{NH}_3$ -based  $\text{CO}_2$  capture. Despite this, there remains a gap in a literature regarding mass transfer enhancement technologies for improving the  $\text{CO}_2$  absorption rate performance of aqueous ammonia and energy requirements. The understanding of the underlying mechanisms and the factors impacting the absorption rate of ammonia in carbon capture systems is still relatively limited (Shokrollahi et al., 2022; Yang et al., 2014c). Realizing that the possibility of enhancing the  $\text{CO}_2$  absorption rate of aqueous ammonia required a lot of investigations, this article provides a comprehensive review of the current development and challenges of mass transfer enhancement technologies of AAP, aiming to provide a valuable guide for further development and design of ammonia-based  $\text{CO}_2$  capture absorption processes. Notably, the review

will also briefly discuss  $\text{NH}_3$  slip and solid formation to provide necessary context. The primary emphasis, however, will remain on exploring and addressing the limitations of slow  $\text{CO}_2$  absorption rate associated with ammonia and explore potential solutions to improve its absorption rate performance and the efficiency of  $\text{CO}_2$  capture using aqueous ammonia. The understanding generated from this review aims to serve as a valuable guide for further development and design of efficient ammonia-based  $\text{CO}_2$  capture processes.

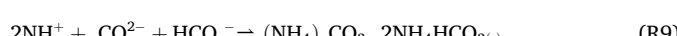
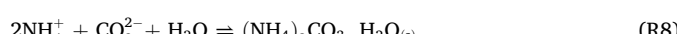
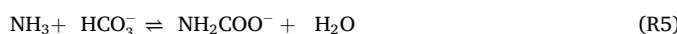
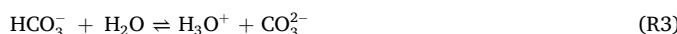
In line with the above objective, **Section 2** mainly explains the AAP's chemistry based on thermodynamic properties, product properties and chemical kinetic parameter. **Section 3** reviews the mass transfer of  $\text{CO}_2$  absorption and the influence of operational conditions, including experimental investigations at various scales and process modeling to evaluate absorption efficiency and energy consumption on the performance of  $\text{CO}_2$  absorption using aqueous ammonia. **Section 4** gives detailed discussions on the development and challenges of  $\text{CO}_2$  absorption rate enhancement technologies of the AAP, i.e., physical, chemical, and combined approaches. **Section 5** reviews the potential of aqueous ammonia in multi-pollutant capture technology and its recent developments. A summary of the major developments and future potential research required for enhancing the rate absorption of  $\text{CO}_2$  using aqueous ammonia is provided in **Section 6**.

## 2. Carbon capture chemistry of aqueous ammonia

### 2.1. General reaction

The absorption of  $\text{CO}_2$  capture using ammonia is usually accompanied by a series of complex multi-step reactions influenced by factors such as concentration, temperature, pressure, and turbulence (Bernardis et al., 1989a; Edwards et al., 1978; Edwards et al., 1975; Göppert and Maurer, 1988; Kurz et al., 1995) indicating the reaction priority varies under different reaction conditions. The absorption of  $\text{CO}_2$  in to

ammonia solution can be described as follows; (Darde et al., 2010)



In recent years, there have been notable advancements in understanding the thermo-chemical properties of the aqueous ammonia-based CO<sub>2</sub> capture system. Extensive experimental and modeling efforts have been carried out, particularly in the last few years, focusing on aspects such as vapor-liquid-solid equilibrium determination, speciation, thermodynamic model development, and reaction kinetics. The research progress and associated challenges in this area are comprehensively reviewed in the following subsection.

## 2.2. Thermodynamics

As the NH<sub>3</sub>-CO<sub>2</sub>-H<sub>2</sub>O system is a mixture of molecular species and non-volatile ionic compounds, a detailed thermodynamic model framework is required to determine the phase behavior and composition. The absorption process is complicated, resulting in the production of different products depending on the CO<sub>2</sub> loadings and temperatures

involved (Darde et al., 2009). The chemical species and phase equilibrium of NH<sub>3</sub> - CO<sub>2</sub>-H<sub>2</sub>O system relevant for the application of aqueous ammonia-based CO<sub>2</sub> capture processes are described in Fig. 2 (Thomsen and Rasmussen, 1999). Theoretically, H<sub>3</sub>O<sup>+</sup>, NH<sub>4</sub><sup>+</sup>, OH<sup>-</sup>, NH<sub>2</sub>COO<sup>-</sup>, HCO<sub>3</sub><sup>-</sup> and CO<sub>3</sub><sup>2-</sup>, ionic species should coexist in the solution according to the reaction mechanism. For the precipitation, although the experimental results from Bai and Yeh (1997) and Chen et al. (2012) indicated that the solid NH<sub>4</sub>HCO<sub>3</sub> was the main component, Darde et al. (2010) suggested that the formation of five different solids should be considered depending on the operation circumstance. These include ammonium bicarbonate (NH<sub>4</sub>HCO<sub>3</sub>), ammonium carbonate monohydrate ((NH<sub>4</sub>)<sub>2</sub>CO<sub>3</sub>·H<sub>2</sub>O), ammonium carbamate (NH<sub>2</sub>COONH<sub>4</sub>), ammonium sesqui-carbonate ((NH<sub>4</sub>)<sub>2</sub>CO<sub>3</sub>·HCO<sub>3</sub>O), and ice (H<sub>2</sub>O).

Thermodynamics plays an important role in modelling CO<sub>2</sub> absorption processes since the absorption process requires thermodynamic data, especially phase equilibria: mean vapour-liquid equilibrium (VLE) and speciation equilibrium (Darde et al., 2012b). Up to now, a number of thermodynamic models has been developed for the NH<sub>3</sub> - CO<sub>2</sub>-H<sub>2</sub>O system due to industrial interests. Pitzer model able to describe both weak and strong electrolytes based on a complex virial model with numerous parameters. Edwards et al. (1978) and Edwards et al. (1975) firstly proposed a thermodynamic model of the NH<sub>3</sub>-CO<sub>2</sub>-H<sub>2</sub>O system using the Pitzer model to represent activity coefficients and the equation of state by Nakamura et al. (1976) for fugacity coefficients. They determined temperature dependent parameters of binary interaction between like undissociated molecules, i.e., of the given electrolyte, from the experimental data for the NH<sub>3</sub>-H<sub>2</sub>O and CO<sub>2</sub>-H<sub>2</sub>O two-component systems and calculated the binary interaction parameters for unlike molecules, i.e., of various electrolytes as arithmetic means of such parameters for like molecules of these electrolytes. Later, this model was extended to the temperature of 423 K by Pawlikowski et al. (1982) based on their experimental results. Although the Edwards model was proved to be reliable in low concentration and applied in waste water treatment (Budzianowski and Koziol, 2005), all the works above were based on a relatively modest experimental database. It was until 1988 that Müller

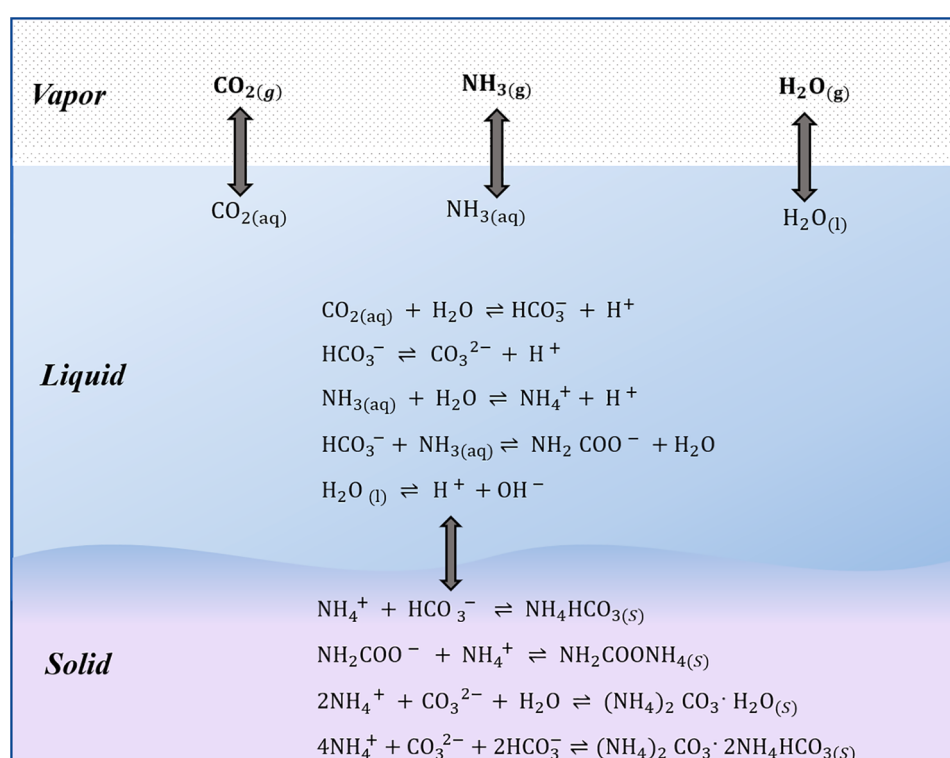


Fig. 2. Vapour-liquid-solid equilibria in the NH<sub>3</sub> - CO<sub>2</sub>-H<sub>2</sub>O system.

et al. (1988), Göppert and Maurer (1988) and Kurz et al. (1995) validated the Pitzer model against experimental data. The studies of Göppert and Maurer (1988) and Müller et al. (1988) was attempted to describe the obtained data by the Edwards model, in which, following the approach of Kawazushi and Prausnitz (1987), the influence of short-range interactions were neglected. Relatively large deviations of the calculated values from the experimental data were however obtained, especially for higher electrolyte concentrations. The experiment done by Kurz et al. (1995) had rejected the interaction parameters between ions of the same sign, found nine binary and ternary interaction parameters including five temperature-dependent that described with good accuracy the experimental data obtained by them and the previous data published by Göppert and Maurer (1988) and Müller et al. (1988).

To upgraded Pitzer thermodynamic model of the NH<sub>3</sub>-CO<sub>2</sub>-H<sub>2</sub>O system Krop (1999) proposed species-group Pitzer activity coefficient model. The species-group Pitzer activity coefficient model relates the parameters to the groups of species instead of real species in the solution, leading to significantly reducing the number of regressed parameters and simplifying the calculation compared to traditional Pitzer model. In another work, a modified species-group Pitzer activity coefficient model has been developed by Xu et al. (2014) to evaluate the solid-liquid equilibria (SLE) of the NH<sub>4</sub>HCO<sub>3</sub>-H<sub>2</sub>O system which needs significantly fewer parameters to be fitted than the traditional models and still is reported to be accurate over wide range of temperatures and concentrations (Gudjonsdottir and Infante Ferreira, 2016).

Later, semi-empirical thermodynamic models for electrolytic solutions based on the concept of local composition, the Universal Quasi-Chemical (UNIQUAC) model (Sander, 1984; Sander et al., 1986) and the Electrolyte Non Random Two Liquid (e-NRTL) model (Chen and Evans, 1986), were proposed to describe the activity coefficient for electrolytic solutions. As presented by Chen and Evans (1986); the e-NRTL model is based on the like-ion repulsion and on local electro-neutrality assumptions. Bernardis et al. (1989a) applied extended UNIQUAC to describe the liquid phase of the ternary system NH<sub>3</sub>-CO<sub>2</sub>-H<sub>2</sub>O. The e-UNIQUAC model is an extension of the original UNIQUAC model (Abrams and Prausnitz, 1975) to further consider electrolytic systems by adding the Debye-Hückel term, which describes the long-range interactions between the species in solution. Unlike the Pitzer model, e-UNIQUAC considers the water dissociation and has a significantly lower number of temperature dependent parameters (Jaworski et al., 2011), which have to be obtained experimentally.

Thomsen and Rasmussen (1999) developed a thermodynamic model to describe behavior of the NH<sub>3</sub>-CO<sub>2</sub>-H<sub>2</sub>O system which includes the aforementioned equilibrium processes under the 0–110 °C range of temperature and 1–10 MPa of the pressure, the ammonia concentration up to 80 molal. The thermal properties of the aqueous electrolyte solution are calculated on the basis of the extended UNIQUAC model and the Soave-Redlich-Kwong equation of state. Later, this model was updated by Darde et al. (2010) to wider range of temperature and pressure and used for evaluating the chilled NH<sub>3</sub> process. On the other hand, Que and Chen (2011) developed e-NRTL activity coefficient model for the NH<sub>3</sub>-CO<sub>2</sub>-H<sub>2</sub>O system. The parameters of the e-NRTL activity coefficient model are identified by fitting against experimental data for various equilibrium and speciation properties of the system. The model is validated with additional data and is shown to satisfactorily represent the thermodynamic properties of the NH<sub>3</sub>-CO<sub>2</sub>-H<sub>2</sub>O system within specified ranges of temperature, pressure, NH<sub>3</sub> concentration, and CO<sub>2</sub> loading. Gudjonsdottir and Infante Ferreira (2016) compared the performance of the e-NRTL model, including modified versions fitted specifically for the NH<sub>3</sub> – CO<sub>2</sub>-H<sub>2</sub>O system and available in Aspen Plus software, with the e-UNIQUAC model for fitting experimental data of the NH<sub>3</sub> – CO<sub>2</sub>-H<sub>2</sub>O mixture. The findings indicated a significant improvement in the modified models over the original e-NRTL model. Additionally, the well-fitted modified models demonstrated comparable performance to the e-UNIQUAC model within its application range.

The two models (e-UNIQUAC and e-NRTL) proposed by Thomsen

and Rasmussen (1999) and Que and Chen (2011) are not only for the vapour-liquid system but also for vapour-liquid-solid equilibrium. The Solid-Liquid equilibria of the NH<sub>3</sub> – CO<sub>2</sub>-H<sub>2</sub>O system has been well experimentally studied by Jänecke (1929), and simulated by Thomsen and Rasmussen (1999). However, all authors did not unanimously agree on the likely salt formation and mixture. In Thomsen and Rasmussen (1999) work, vapor-liquid-solid equilibrium includes the formation of NH<sub>4</sub>HCO<sub>3</sub>, (NH<sub>4</sub>)<sub>2</sub>CO<sub>3</sub>·H<sub>2</sub>O, NH<sub>2</sub>COONH<sub>4</sub> and (NH<sub>4</sub>)<sub>2</sub>CO<sub>3</sub>·2NH<sub>4</sub>HCO<sub>3</sub>. On the other hand, Que and Chen (2011) consider NH<sub>4</sub>HCO<sub>3</sub> to be the sole solid present in the product. In fact, similar conclusion was theoretically supported by an extended UNIQUAC electrolyte model developed by Thomsen and Rasmussen (Darde et al., 2009). Researches have shown that NH<sub>4</sub>HCO<sub>3</sub> is dominant in the total amount of ammonium salts once the CO<sub>2</sub> absorption reaches steady state (Ahn et al., 2011; Kim et al., 2008; Park et al., 2008). Besides the effect of concentrations, the effect of reaction temperature cannot be neglected. The forward reaction is usually dominant at relatively low temperature while backward reaction occurs at relatively high temperature. As the forward reaction proceeds, the concentration of NH<sub>4</sub>HCO<sub>3</sub> by hydrolysis increases gradually (Zhao et al., 2012). Once the NH<sub>4</sub>HCO<sub>3</sub> concentration reaches its saturation solubility at the reaction temperature, the salts would be crystallized. Sutter et al. (2015) provides a very good analysis about the solid formation in the system based on the experimental evidence provided by Jänecke (1929). The author used ternary phase diagrams to represent the thermodynamically stable phases at specific temperature and pressure conditions in the NH<sub>3</sub> – CO<sub>2</sub>-H<sub>2</sub>O system and these diagrams express compositions in weight fractions. This helped to identify critical streams and unit operations at risk of solid formation which is important in designing and optimization of ammonia-based carbon capture process.

The accuracy of vapor-liquid equilibrium prediction in the NH<sub>3</sub> – CO<sub>2</sub>-H<sub>2</sub>O system depends primarily on the activity coefficient model and the vapor phase equation of state played a minor role in prediction accuracy (Rosa et al., 2021). The presence of polar species in the vapor mixture of the system NH<sub>3</sub> – CO<sub>2</sub>-H<sub>2</sub>O have been described by several models such as PC-SAFT (Perturbed-Chain Statistical Associating Fluid Theory (Gross and Sadowski, 2001; Nakamura et al., 1976), and Soave-Redlich-Kwong (Soave, 1972). The PC-SAT equation of state is based on statistical thermodynamics and can be applied for polar and non-polar mixtures. The Nakamura equation, although less complex than the PC-SAFT, still considers the presence of polar and non-polar molecules in the vapor phase.

For the ternary NH<sub>3</sub>-CO<sub>2</sub>-H<sub>2</sub>O system, the predictive ability of liquid species concentrations is another critical reflection of the effectiveness of the thermodynamic model. Different experimental measurement techniques can be used to determine the carbon distribution in the liquid phase. Lichtfers and Rumpf (2004) presented the experimental results of the molalities of CO<sub>2</sub>, HCO<sub>3</sub><sup>-</sup>, CO<sub>3</sub><sup>2-</sup>, NH<sub>3</sub>, NH<sub>4</sub><sup>+</sup>, and NH<sub>2</sub>COO<sup>-</sup> at different CO<sub>2</sub> loadings using ATR-IR spectroscopy, Ahn et al. (2011) and Holmes et al. (1998) have used <sup>13</sup>C NMR, while Halstensen et al. (2017), Jilvero et al. (2015), Wen and Brooker (1995), and Zhao et al. (2011) have used Raman spectroscopy. The studies of Ahn et al. (2011), Holmes et al. (1998), Jilvero et al. (2015), and Wen and Brooker (1995) provide experimental data for the ammonia and carbon dioxide concentrations that are relevant for absorber conditions. The extensive work by Lichtfers and Rumpf (2004) has generated experimental data in the range 40–120 °C, while Ahn et al. (2011), Holmes et al. (1998), Wen and Brooker (1995), and Zhao et al. (2011) have presented experimental data at room temperature (22–25 °C), and Jilvero et al. (2015) in the temperatures range of 10–40 °C. Some of the above speciation studies reported similar results. For example, Mani et al. (2006), Zhao et al. (2011), and Lichtfers and Rumpf (2004) all reported increasing relative concentration for HCO<sub>3</sub><sup>-</sup> but decreasing relative concentration for NH<sub>2</sub>COO<sup>-</sup> as the CO<sub>2</sub> loading increases and the temperature and the NH<sub>3</sub> concentration are fixed. However, these studies do not agree with each other well in values. Wen and Brooker (1995) reported much higher

concentration for bicarbonate and much lower concentration for carbamate in comparison with the results from the other studies. According to the equilibrium speciation data results of [Jilvero et al. \(2015\)](#), CO<sub>2</sub> is predominantly bound as carbamate at low CO<sub>2</sub> loadings. The formation of bicarbonate is the main reaction that increases the CO<sub>2</sub> loading to >0.5. The results of the [Jilvero et al. \(2015\)](#) and [Ahn et al. \(2011\)](#) are very similar particularly in terms of the carbonate and carbamate results for a CO<sub>2</sub>-loading of 0.4, and showed different result in which, [Jilvero et al. \(2015\)](#) detected low concentrations of bicarbonate were for CO<sub>2</sub>-loadings <0.4, whereas in the results presented by [Ahn et al. \(2011\)](#) bicarbonate was present even at low CO<sub>2</sub>-loadings. Similarly, there is no agreement about in the comparison of speciation calculations of models and experimental data, which is the best model to describe the system. [Jilvero et al. \(2015\)](#) and [Darde et al. \(2012b\)](#) compared the models e-UNIQUAC and e-NRTL to describe the liquid phase: [Jilvero et al. \(2015\)](#) observed no significant difference between the models in terms of accuracy, whereas [Darde et al. \(2012b\)](#) concluded that the e-UNIQUAC can more satisfactorily describe the experimental data.

Although different models for describing the non-idealities of the liquid and vapor phases of the ternary system NH<sub>3</sub> – CO<sub>2</sub>–H<sub>2</sub>O have been used in literature, the best model to describe this system is still in research. [Table 2](#) summarizes the most commonly used thermodynamic models in literature to describe the NH<sub>3</sub> – CO<sub>2</sub>–H<sub>2</sub>O system. Recent studies indicate that the e-UNIQUAC model may offer greater accuracy, particularly in replicating experimental data, compared to the e-NRTL model ([Rosa et al., 2021](#)). Based on the current state of research and the challenges identified in modeling the NH<sub>3</sub> – CO<sub>2</sub>–H<sub>2</sub>O ternary system, a potential future suggestion would be to continue exploring and developing thermodynamic models that can effectively address the complexities arising from species dissociation and non-ideal behavior. Further research efforts could focus on refining the existing e-UNIQUAC and e-NRTL models or developing new models that consider the electrolytic term and accurately represent experimental data across a range of conditions.

### 2.2.1. Reaction mechanism

The reaction of ammonia with CO<sub>2</sub> is chemically analogous to the reaction of a primary amine with CO<sub>2</sub> ([Caplow, 1968](#); [Derk and Versteeg, 2009](#)). During the absorption of carbon dioxide into aqueous ammonia, three main reactions should be considered at the gas–liquid interface, on the liquid side.



The production of carbonic acid ([R10](#)) by CO<sub>2</sub> and H<sub>2</sub>O is very slow compared with [Reactions \(R11\)](#) and ([R12](#)), and therefore, is negligible. The carbamate and bicarbonate formation [Reactions \(R11\)](#) and ([R12](#)) are considered to be rate-determining. The carbamate species may undergo hydrolysis to free ammonia and bicarbonate. At low CO<sub>2</sub> loading the carbamate is known to be the dominant species with the equilibria shifting to favour bicarbonate formation at higher loading and lower free ammonia concentration ([Mani et al., 2006](#)).

[Reaction \(R12\)](#) is an overall equation for the reaction between CO<sub>2</sub> and NH<sub>3</sub>. The nature of the reaction could be characterized by either a two-step mechanism ([Pinsent et al., 1956](#)), zwitterion ([Derk and Versteeg, 2009](#)) or termolecular mechanisms ([Qin et al., 2010](#)). The latter two pathways are well-documented and might include fractional orders. In the chemical absorption using amines, the order of a reaction with regard to amine grows from 1 to 2 as the amine concentration increases ([Vaidya and Kenig, 2010](#)). Because of this, it is reasonable to anticipate that the order of the ammonia molecules in an aqueous solution will change depending on the ammonia concentration.

### 1) Simplified two-step pathway

[Pinsent et al. \(1956\)](#) assumed that reaction between CO<sub>2</sub> with NH<sub>3</sub> included two simple reactions. In the initial stage, carbamic acid is formed, and then it will be deprotonated to produce carbamate.



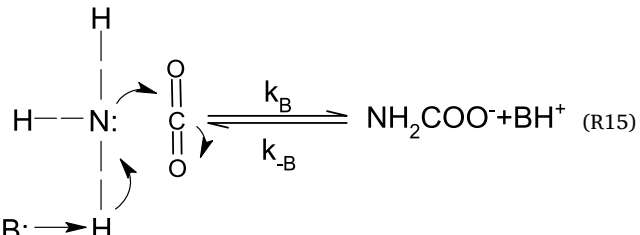
Because the process [Reaction \(R14\)](#) included the transfer of protons, it was believed to take place instantly. All of the hydroxyl ions produced in the [Reaction \(R13\)](#) could be instantly transformed into ammonium ions. Consequently, the rate-determining step was determined by [Reaction \(R13\)](#). The overall rate of reaction is expressed as;

$$-\frac{d[\text{CO}_2]}{dt} = k'_i [\text{CO}_2][\text{NH}_3] \quad (1)$$

Where k'<sub>i</sub> is the velocity constant of [Reaction \(R13\)](#) at ionic strength of I.

### 2) Termolecular

[Crooks and Donnellan \(1989\)](#) suggested a single-step termolecular reaction mechanism and, ([Da Silva and Svendsen, 2004](#)) further expanded it in a research describing the generation of carbamate from alkanol amines and CO<sub>2</sub> using ab initio method. [Reaction \(R15\)](#) shows that it is a mechanism with a single step that works on the assumption that one molecule of ammonia combines with one molecule of CO<sub>2</sub> and one molecule of base simultaneously. In the termolecular reaction between CO<sub>2</sub>, NH<sub>3</sub>, and H<sub>2</sub>O, the generation of ammonium salts predominates instead of zwitterions. The majority of the complexes break down into their component reagent molecules. The molecules of the reagent do not combine with additional amine or water molecule to produce charged species. The formation of chemical bond and separation of charges take place only in stage two.



The rate of reaction in which NH<sub>3</sub> and H<sub>2</sub>O are the predominant bases can be presented as follows;

$$r_{\text{CO}_2}^T = \left( k_{\text{NH}_3}^T [\text{NH}_3] + k_{\text{H}_2\text{O}}^T [\text{H}_2\text{O}] \right) [\text{CO}_2][\text{NH}_3] \quad (2)$$

### 3) Zwitterion reaction mechanism

The zwitterion mechanism is the two-step reaction generally acknowledged for CO<sub>2</sub> absorption into ammonia. In [Reaction \(R16\)](#), the reaction of CO<sub>2</sub> with NH<sub>3</sub> is generates a dipolar ion, which will be deprotonated by any base found in the solution, such as OH<sup>-</sup> ions, ammonia, and water.



In [Reaction \(R17\)](#), deprotonation is the rapid rate at which k<sub>B</sub> ≫ k<sub>-B</sub>. Besides, it is possible that B is a molecule of water, ammonia, or hydroxyl ion presented in the solution. It is important to remember that the hydroxyl ions make only a negligible contribution in the removal of a proton of the dipolar ion in an aqueous ammonia solution. As a result, water and ammonia will serve as primary bases in [Reaction \(R17\)](#) ([Darde et al., 2011](#)). The overall reaction rate is determined from Eq. (3)

**Table 2**Commonly used thermodynamic models in literature to describe the VLE of the ternary system  $\text{NH}_3 - \text{CO}_2 - \text{H}_2\text{O}$ .

Author	Model		Tempreature, pressure and Concentration	Desctption
	Liquid phase	Vapour phase		
Edwards et al. (1975)	Pitzer	Nakamura	$\text{NH}_3$ molality = 1–12 m $\text{CO}_2$ molality = 0–17 m $T = 273\text{--}373\text{ K}$ $P = \leq 0.2\text{ MPa}$	Developed thermodynamic model of to evaluate VLE of $\text{NH}_3 - \text{CO}_2 - \text{H}_2\text{O}$ system
Edwards et al. (1978)	Pitzer	Nakamura	$\text{NH}_3$ molality = 10–20 m $\text{CO}_2$ molality = 0–17 m $T = 273\text{--}433\text{ K}$ $P = \leq 0.2\text{ MPa}$	Extended (Edwards, Newman, and Prausnitz 1975) work to calculate VLE of $\text{NH}_3 - \text{CO}_2 - \text{H}_2\text{O}$ system
Verbrugge (1979)	Pitzer	Nakamura	$\text{NH}_3$ molality = 0.1–49.1 m $\text{CO}_2$ molality = 0–17 m $T = 313\text{--}363\text{ K}$ $P = 0.1\text{--}1\text{ MPa}$	Data of VLE of $\text{NH}_3 - \text{CO}_2 - \text{H}_2\text{O}$ in the given temprature range
Pawlowski et al. (1982)	Pitzer	Nakamura	$\text{NH}_3$ molality = 3–10 m $\text{CO}_2$ molality = 0.3–5.4 m $T = 373\text{--}423\text{ K}$ $P = \leq 1.8\text{ MPa}$	Data of VLE of $\text{NH}_3 - \text{CO}_2 - \text{H}_2\text{O}$ in the given temprature range
Bernardis et al. (1989a)	e-UNIQUAC	Nakamura	$\text{NH}_3$ molality = 3.85–18.3 m $\text{CO}_2$ molality = 0–14 m $T = 414\text{--}473\text{ K}$ $P = 7\text{ kPa}\text{--}20\text{ MPa}$	Calculated the activity coefficients of components in the $\text{NH}_3 - \text{CO}_2 - \text{H}_2\text{O}$ vapor-liquid equilibrium system
Bernardis et al. (1989b)	e-UNIQUAC	Nakamura	$\text{NH}_3$ molality = N/A $T = 414\text{--}473\text{ K}$ $P = 7\text{ kPa}\text{--}20\text{ MPa}$	Described the VLE of $\text{NH}_3 - \text{CO}_2 - \text{H}_2\text{O}$
Müller et al. (1988)	Pitzer	Nakamura	$\text{NH}_3$ molality = 2.4–26 m $\text{CO}_2$ molality = 0–13.3 m $T = 373\text{--}473\text{ K}$ $P = \leq 1\text{ MPa}$	Compared the experimental data with existing correlations
Göppert and Maurer (1988)	Pitzer	Nakamura	$\text{NH}_3$ molality = 0.5–16.5 m $\text{CO}_2$ molality = 0.2–13.5 m $T = 333\text{--}393\text{ K}$ $P = \leq 0.7\text{ MPa}$	Compared the experimental data with existing correlations
Kurz et al. (1995)	Pitzer	Nakamura	$\text{NH}_3$ molality = 6–12.1 m $\text{CO}_2$ molality = 0–9.7 m $T = 313\text{--}353\text{ K}$ $P = \leq 0.7\text{ MPa}$	Validated the model against experimental findings and litrature data (Göppert and Maurer, 1988; Müller et al., 1988)
Krop (1999)	Species-group Pitzer model	Nakamura	$\text{NH}_3$ molality = 0.4–1.7 m $\text{CO}_2$ molality = 0.6–1.9 m $T = 293\text{--}343\text{ K}$ $P = \leq 0.7\text{ MPa}$	Upgraded the Pitzer model
Thomsen and Rasmussen (1999)	e-UNIQUAC	Soave–Redlich–Kwong	$\text{NH}_3$ molality = 80 m $\text{CO}_2$ molality = 9 m $T = 273\text{--}373\text{ K}$ $P = \leq 10\text{ MPa}$	Determined the aqueous-phase activity coefficients and the vapor phase fugacities
Darde et al. (2010)	e-UNIQUAC	Soave–Redlich–Kwong	$\text{NH}_3$ molality = 80 m $\text{CO}_2$ molality = 9 m $T = 273\text{--}333\text{ K}$ $P = \leq 10\text{ MPa}$	Determined the aqueous-phase activity coefficients and the vapor phase fugacities.
Que and Chen (2011)	e-NRTL	PC-SAFT	$\text{NH}_3$ molality = 0–25 m $\text{CO}_2$ loading = 0–1 $T = 273\text{--}473\text{ K}$ $P = \leq 7\text{ MPa}$	Predicted the VLE of $\text{NH}_3 - \text{CO}_2 - \text{H}_2\text{O}$ systems
Darde et al. (2012b)	e-NRTL e-UNIQUAC	Soave–Redlich–Kwong	$\text{NH}_3$ molality = 14.3 m $T = 273\text{--}333\text{ K}$ $P = \leq 14\text{ MPa}$	Compared performance of two thermodynamic models for the system
Freitas et al. (2013)	e-UNIQUAC	Nakamura	$\text{NH}_3$ molality = 16 m and $\text{CO}_2$ molality = 13 m $T = 313\text{--}473\text{ K}$ $P = \leq 7\text{ MPa}$	Predicted the VLE of $\text{NH}_3 - \text{CO}_2 - \text{H}_2\text{O}$ system
Xu et al. (2014)	Spices-group Pitzer	Nakamura	$\text{NH}_3$ Conc. = 58.82 m $\text{CO}_2$ molality = 1.7 m $T = 273\text{--}423\text{ K}$ $P = \leq 0.7\text{ MPa}$	Developed simplified model to reduce regression parameters. Incorporates solid-liquid equilibria of the $\text{NH}_4\text{HCO}_3 - \text{H}_2\text{O}$ system
Jilvero et al. (2015)	e-NRTL e-UNIQUAC	PC-SAFT Soave–Redlich–Kwong	$\text{NH}_3$ molality = 5 wt%–10 wt % $\text{CO}_2$ loading = 0.15–0.75 $T = 283\text{--}310\text{ K}$ $P = 1.13\text{--}1.23\text{ atm}$	Described the VLE of $\text{NH}_3 - \text{CO}_2 - \text{H}_2\text{O}$ systems at low temperature
Gudjonsdottir and Infante Ferreira (2016)	e-NRTL	Soave–Redlich–Kwong	$\text{NH}_3$ molality = 0–25 m $\text{CO}_2$ loading = 0–1 $T = 273\text{--}473\text{ K}$ $P = \leq 7\text{ MPa}$	Significant improvement in the modified models over the original e-NRTL model.
Rosa et al. (2021)	e-NRTL e-UNIQUAC	Nakamura Ideal gas equation	$\text{NH}_3$ molality = 6–12 m $\text{CO}_2$ molality = 10 m $T = 313\text{--}353\text{ K}$ $P = 0.69\text{ MPa}$	e-UNIQUAC model demonstrated greater accuracy in replicating experimental data compared to the e-NRTL model.

(Danckwerts, 1979).

$$r_{\text{CO}_2} = \frac{[\text{CO}_2][\text{NH}_3]}{1/k_2 + k_{-1}(k_2 \sum k_B[B])}, \quad B = \text{NH}_3, \text{H}_2\text{O} \quad (3)$$

$$k_2 \sum [B] \gg k_{-1} r_{\text{CO}_2} = k_2 [\text{CO}_2][\text{NH}_3] \quad (4)$$

Although its complexity frequently poses a challenge for its application in process modeling software, the zwitterion mechanism does provide the most scientific description of reaction pathways for the reaction between  $\text{NH}_3$  and  $\text{CO}_2$ .

In general, the reaction mechanisms of AAP are still controversial. The rate constants of the reaction have been the subject of a few published studies that propose kinetic models. Unfortunately, the studied kinetic models were inconsistent among themselves (Lillia et al., 2016), and the variation may be as significant as many orders of magnitude (Yu et al., 2016a). The research performed by Jilvero et al. (2014), Puxty et al. (2010) and Pinsent et al. (1956) illustrate this. As indicated in Table 3, the discrepancy between previous kinetic data conducted by various researchers may be attributable to distinct absorption processes under the varied reaction circumstances and experimental methodologies. Not all expected reaction orders were supported by experimental results (Qin et al., 2010). In most cases, researchers made assumptions for the reaction orders with respect to the reactants (Gonzalez-Garza et al., 2009; Pinsent et al., 1956). This simple assumption about reaction order may occasionally lead to incorrect conclusions, particularly once the reaction order is fractional. Jilvero et al. (2014) have investigated the apparent reaction rates of chemical reaction of the ammonia-based absorption process using a distinct methodology from prior studies. They developed system design requirements and operational parameters for the absorption column of the ammonia-based absorption process using the Mummorah Aqueous Ammonia pilot plant's design requirement as a baseline Yu et al. (2011). The reaction kinetic data fitted to the pilot plant experimental findings showed a difference in Arrhenius values with the prior literature. The reaction rate inconsistency adds another layer of difficulty to the process of absorption modelling to simulate the performance of capturing  $\text{CO}_2$ . Taking this under consideration, Lillia et al. (2018) proposed a power law equation to fit the data that regenerates experimental findings obtained at various  $\text{CO}_2$  loadings. The constant is developed to correlate the findings among the previous literature with their work since the kinetic models in every study were distinct and were often fitted to the unloaded solutions ( $\text{Loading}_{\text{CO}_2} = 0$ ) data. The experimental data proved that the kinetic model of prior literature is valid across the board for all loading circumstances.

### 2.3. summary on carbon capture chemistry of aqueous ammonia

Efficient design and operation of AAP systems require a comprehensive understanding of the thermodynamic and kinetic aspects. The thermodynamics and kinetics of ammonia-based carbon capture processes (AAP) are complex and require extensive investigation due to several reasons. The complexity of Vapor-Liquid-Solid Equilibrium (VLSE) of  $\text{NH}_3\text{-CO}_2\text{-H}_2\text{O}$  system arises from the presence of multiple chemical species, including gaseous  $\text{CO}_2$ , liquid ammonia, and solid ammonium salts. Previous research has made significant progress in studying the thermodynamics of AAP systems, experimental determination of vapour-liquid-solid equilibrium, speciation, heat of absorption, and the thermodynamic model development to understand the  $\text{CO}_2$  absorption and desorption processes. The availability of thermodynamic models allows the reliable calculation of thermochemical properties of the  $\text{NH}_3\text{-CO}_2\text{-H}_2\text{O}$  system under various conditions, assessment of the energy performance of the capture process and even the definition of the best range of operation conditions. However, improved modeling techniques are needed to better represent the complex behavior of the system and enhance the prediction of thermodynamic equilibrium.

Moreover, the understanding of reaction mechanisms in ammonia-based carbon capture (AAP) is currently a topic of ongoing discussion. Several studies have proposed kinetic models to determine the rate constants of the reaction. However, these models have exhibited inconsistencies and substantial variations, with differences spanning multiple orders of magnitude. There is a need for a more comprehensive understanding of the reaction mechanisms involved in the absorption of  $\text{CO}_2$  by ammonia in the AAP process. It is essential to validate them against experimental data from different sources and under various conditions.

## 3. Mass transfer of $\text{CO}_2$ absorption into aqueous ammonia

The  $\text{CO}_2$  absorption utilizing aqueous ammonia undergoes a gas-liquid chemical reaction. According to two film concept, mass transfer is regarded to occur across the phase gas-liquid boundary (interface) (Lewis and Whitman, 1924). The transfer of  $\text{CO}_2$  is by diffusion, which is associated with the difference in gas concentration between the two phases. There is always some mass transfer resistance throughout the absorption process.

The chemical  $\text{CO}_2$  absorption primarily depends on the mass transfer across the interphase which is performed in a mass transfer apparatus. Researchers conducted studies using these devices for the objective above. Over the last few decades, various separator equipment for the  $\text{CO}_2$  capture process, including packed columns (Zeng et al., 2011a), bubble columns (Chu et al., 2017), and spray columns (Ma et al., 2013b) have been the subject of intensive research. Among these, the packed bed column is a widely applied separator for industrial applications in PCC because of its good mass transfer, no energy consumption for absorption, and easy operation compared with the other two (Chu et al., 2016). It is important to make an accurate estimation of mass transfer coefficients to design an actual size of packing height that is required for the diffusion of gas into liquid body. In previous studies, mass transfer coefficient at a lab scale has been the subject of experimental investigation for aqueous ammonia at a variety of different operating parameters.

### 3.1. Effect of operating parameters on mass transfer of $\text{CO}_2$ in AAP

The mass transfer coefficient is the most significant parameter to design an absorption column and evaluate its rate of  $\text{CO}_2$  absorption. It has a major role in evaluating the effectiveness of the packed column since it provides the actual height of the absorption column. The  $\text{CO}_2$  removal efficiency of amine-based PCC is determined by the gas-liquid contact degree, operational conditions related to the gas and amine solution, hydrodynamics parameters, and amine reactivity level. Understanding of how the overall mass transfer coefficient of various amine solvents differs depending on the operating parameters and reactor design is significant in exploring and optimizing  $\text{CO}_2$  removal processes (Fu et al., 2014). Operating parameters with a significant effect such as; operating temperature,  $\text{NH}_3$  concentration,  $\text{CO}_2$  partial pressure, liquid and gas flow rates, and  $\text{CO}_2$  loading are described under a separate subheading in this section.

#### 3.1.1. Temperature

Temperature is one of the most critical factors affecting the reaction kinetics of aqueous ammonia and  $\text{CO}_2$  reactions. As the ammonia- $\text{CO}_2$  reaction is reversible, the influence of temperature on the  $\text{CO}_2$  absorption efficiency through ammonia is complex, showing a non-linear relationship. This complexity is influenced by factors such as the design of the reactor and various operational parameters. Previous studies have indicated that the forward reactions predominate at ambient temperature (Shale, 1971), whereas the backward reactions take place at temperatures between 311K–333 K (Pelkie et al., 1992). The absorption rate generally increases below 308 K. Empirical findings confirm an optimal critical temperature for absorption. Increasing

**Table 3**Kinetic rate expressions of CO<sub>2</sub> absorption using aqueous ammonia.

Author	Method	Operational condition	Kinetics equation	Reaction Mechanism
Andrew (1954)	Disc Column	NH <sub>3</sub> conc. = 0.25–11 M T = 293–333 K	$k_2 = 1.70 \times 10^{11} \left( \text{m}^3 \cdot \text{mol}^{-1} \text{s}^{-1} \right) \exp \left( - \frac{48819}{RT} \right)$	First-order dependent on NH <sub>3</sub> and CO <sub>2</sub> , respectively
Pinsett et al. (1956)	Thermal method	NH <sub>3</sub> conc.=0.027–0.19 M T = 273–313 K	$k_2 = 1.35 \times 10^{11} \left( \text{m}^3 \cdot \text{mol}^{-1} \text{s}^{-1} \right) \exp \left( - \frac{48436}{RT} \right)$	First-order dependent on NH <sub>3</sub> and CO <sub>2</sub> , respectively
Hsu (2003)	Double stirred tank reactor	NH <sub>3</sub> conc.=3 wt.% CO <sub>2</sub> = 2–15 vol% T = 298–348 K	$k_1 = 1.04 \times 10^3 \exp \left( - \frac{40090}{RT} \right)$	First-order dependent on NH <sub>3</sub> , and zero-order dependent on CO <sub>2</sub>
Diao et al. (2004)	Tray column	NH <sub>3</sub> conc.=0.066 M CO <sub>2</sub> =10–14 vol% T=301–316 K	$k_2 = 2.40 \times 10^5 \left( \text{m}^3 \cdot \text{mol}^{-1} \text{s}^{-1} \right) \exp \left( - \frac{26730}{RT} \right)$	First-order dependent on NH <sub>3</sub> and CO <sub>2</sub> , respectively
Gonzalez-Garza et al. (2009)	Batch thermostatic Stirred cell	NH <sub>3</sub> conc.=2–5 wt.% T= 278–303 K	$k_2 = 2.92 \times 10^5 \left( \text{m}^3 \cdot \text{mol}^{-1} \text{s}^{-1} \right) \exp \left( - \frac{28095}{RT} \right)$	First-order dependent on NH <sub>3</sub> and CO <sub>2</sub> , respectively
Derkx and Versteeg (2009)	Batch thermostatic stirred cell	NH <sub>3</sub> conc.= 0.1–7 M T=278–298 K	$k_x = k_{x-283.15} \exp \left( \frac{A}{283.15} - \frac{A}{T} \right)$ $k_i \text{ at } 283.15 \text{ K } A(K^{-1})$ $k_2 > 7.5 \text{ m}^3 \cdot \text{mol}^{-1} \text{s}^{-1} 3.0 \times 10^3$ $k_{NH_3} \times k_2/k_{-1} 3.8 \times 10^{-4} \text{m}^6 \cdot \text{mol}^{-2} \text{s}^{-1} 8.5 \times 10^3$ $k_{H_2O} \times k_2/k_{-1} 2.6 \times 10^{-6} \text{m}^6 \cdot \text{mol}^{-2} \text{s}^{-1} 5.5 \times 10^3$	Zwitterion
Puxty et al. (2010)	Wetted wall column	NH <sub>3</sub> conc.= 0.6–6 M T= 278–293 K	$k_2 = 915 \left( \text{m}^3 \cdot \text{mol}^{-1} \text{s}^{-1} \right) \exp \left[ - \frac{61000}{R} \left( \frac{1}{T} - \frac{1}{283} \right) \right]$	Carbamic acid
Liu et al. (2011b)	Wetted wall column	NH <sub>3</sub> conc.=1–7.5 wt% T= 283.15–313.15 K	$k_2 = 3.97 \times 10^8 \left( \text{m}^3 \text{mol}^{-2} \text{s}^{-1} \right) \exp \left( - \frac{3861}{T} \right)$ $k_{NH_3}^T = 4.69 \times 10^7 \left( \text{m}^6 \text{kmol}^{-2} \text{s}^{-1} \right) \exp \left( - \frac{3793}{T} \right)$ $k_{H_2O}^T = 4.36 \times 10^6 \left( \text{m}^6 \text{kmol}^{-2} \text{s}^{-1} \right) \exp \left( - \frac{3847}{T} \right)$	Termolecular
Qin et al. (2010)	String of discs contactor	NH <sub>3</sub> conc.=0.9–5.4 M T= 298.3–321.9 K	$k_2 = k_{NH_3}^T c_{NH_3} + k_{H_2O}^T C_{H_2O}$ $k_{NH_3}^T = 3.996 \times 10^8 \left( \text{m}^6 \text{kmol}^{-2} \text{s}^{-1} \right) \exp \left( - \frac{4455.0}{T} \right)$ $k_{H_2O}^T = 47.314 \left( \text{m}^6 \text{kmol}^{-2} \text{s}^{-1} \right) \exp \left( - \frac{306.48}{T} \right)$ $k_2 = 1.7809 \times 10^{23} \left( \text{m}^2 \text{mol}^{-2} \text{s}^{-1} \right) \exp \left( - \frac{9062.0}{T} \right)$ $k_{NH_3}^T = 3.9376 \times 10^8 \left( \text{m}^6 \text{kmol}^{-2} \text{s}^{-1} \right) \exp \left( - \frac{4451.4}{T} \right)$ $k_{H_2O}^T = 47.002 \left( \text{m}^6 \text{kmol}^{-2} \text{s}^{-1} \right) \exp \left( - \frac{303.08}{T} \right)$	Termolecular
Wang et al. (2011)	Stopped flow	NH <sub>3</sub> conc.=2–16 mmol/L T= 288.15–313.15K	$k_2 = 9.17 \times 10^{10} \left( \text{m}^3 \cdot \text{mol}^{-1} \text{s}^{-1} \right) \exp \left( - \frac{5691}{T} \right)$ $k_{-2} = 5.7 \times 10^{13} \left( \text{m}^3 \cdot \text{mol}^{-1} \text{s}^{-1} \right) \exp \left( - \frac{8182}{T} \right)$	Carbamic acid

(continued on next page)

**Table 3 (continued)**

Author	Method	Operational condition	Kinetics equation	Reaction Mechanism
Kim et al. (2014)	Wetted wall column	NH <sub>3</sub> conc.=5–10 wt.%, 12–15 wt.%, Loading <sub>CO<sub>2</sub></sub> =0 and 0.1 T= 288–303 K	$k_{\text{NH}_3} = 2.17 \times 10^2 (\text{m}^3 \text{mol}^{-2} \text{s}^{-1}) \exp\left(-\frac{530}{T}\right)$ $k_{\text{H}_2\text{O}} = 1.13 \times 10^7 (\text{m}^3 \text{mol}^{-2} \text{s}^{-1}) \exp\left(-\frac{4410}{T}\right)$	Termolecular
Darde et al. (2011)	Wetted wall column	NH <sub>3</sub> conc.= 1–10 wt.% Loading <sub>CO<sub>2</sub></sub> = 0–44.44 mol% T=279–304 K	$k_2 = 4900 (\text{m}^6 \text{mol}^{-2} \text{s}^{-1}) \exp(-14000(1/T - 1/283))$ $\frac{k_2 k_{\text{NH}_3}}{k_{-1}} = 210 \exp(m^6 \text{mol}^{-2} \text{s}^{-1})(-2200(1/T - 1/283))$ $\frac{k_2 k_{\text{H}_2\text{O}}}{k_{-1}} = 0.71 \exp(m^6 \text{mol}^{-2} \text{s}^{-1})(-18000(1/T - 1/283))$	Zwitterion
Yu et al. (2016a)	Double stirred tank reactor	NH <sub>3</sub> conc.= 0.42–7.67 kmol/m <sup>3</sup> T=273.15–293.15 K	$k_{\text{NH}_3}^T = 7.6089 \times 10^8 (\text{m}^6 \text{mol}^{-2} \text{s}^{-1}) \exp\left(-\frac{4018.4}{T}\right)$ $k_{\text{H}_2\text{O}}^T = 7.9161 \times 10^7 (\text{m}^6 \text{mol}^{-2} \text{s}^{-1}) \exp\left(-\frac{4356.4}{T}\right)$	Termolecular
Lillia et al. (2018)	Wetted wall column	NH <sub>3</sub> conc.=5–10 wt.%, Loading <sub>CO<sub>2</sub></sub> =0.2 and 0.6 T= 288–308 K	$k_{\text{NH}_3} = 1.41 \times 10^8 (\text{m}^3 \text{mol}^{-1.89} \text{s}^{-1}) \exp\left(-\frac{60680 \text{ Jm}^{-1}}{RT}\right)$	Zwitterion

temperature leads to a higher reaction rate constant and faster diffusion, benefiting absorption efficiency. However, the absorption rate declines beyond 313 K due to impacts on CO<sub>2</sub> solubility and ammonium bicarbonate breakdown, affecting absorption efficiency and mass transfer. Beyond the critical temperature, a contrasting trend may arise, with limited data showing increased efficiency at higher temperatures (Zhao et al., 2012). Comprehensive temperature analysis is essential for determining the optimal reaction temperature for maximizing CO<sub>2</sub> absorption efficiency.

### 3.1.2. Ammonia concentration

Ammonia concentration is another essential factor related to the mass transfer of AAP. Experimental findings from many researchers have shown that the NH<sub>3</sub> concentration significantly affects the K<sub>Gav</sub>. According to Li et al. (2014b), the K<sub>Gav</sub> value is maximized by half as NH<sub>3</sub> concentration raised from  $2.7 \times 10^{-4}$  kmol/L to  $6.3 \times 10^{-4}$  kmol /L. This is because of the generation of a greater quantity of active NH<sub>3</sub> that may spread to the interfacial area and be combined with CO<sub>2</sub>, resulting high enhancement factor of chemical absorption, that decreases the resistance of the liquid phase, which in turn causes K<sub>Gav</sub> to increase.

However, because of high vapor pressure of NH<sub>3</sub>, a high concentration results in NH<sub>3</sub> escape problem in the treated gas stream. Moreover, it can also relate with the liquid viscosity, that have a detrimental influence on the K<sub>Gav</sub>. Nevertheless, the observation that K<sub>Gav</sub> rises with ammonia concentration differs from MEA CO<sub>2</sub> absorption (Demontigny et al., 2005). The value of mass transfer coefficient diminishes when the MEA concentration exceeds 5.0 mol/L. This is due the solution viscosity, which reduces the rate of molecular diffusion (Demontigny et al., 2005; Strigle, 1987). Additionally, the rising viscosity tends to reduce the effective gas-liquid contacting area in the packed column (Strigle, 1987). On the other hand, the fact that the increasing of K<sub>Gav</sub> value as a result of the rising concentration of aqueous ammonia is that it has a smaller influence on the viscosity of the liquid compared to the influence of the concentration of MEA (Pérez-Calvo et al., 2021a).

### 3.1.3. CO<sub>2</sub> partial pressure

Following the two-film model, there will be a reduction in gas phase resistance as the CO<sub>2</sub> partial pressure rises. This is because more

molecules of CO<sub>2</sub> move from the bulk gas to the interfacial area, resulting in enhanced absorption performance. Nevertheless, the phenomenon of CO<sub>2</sub> transfer in the gas phase is not the only factor that affects the rate at which gases are absorbed, it is also crucial throughout the liquid phase since the movement of the solvent through the liquid body is relatively hindered.

The mass transfer rate is strongly correlates to the liquid mass transfer coefficient (k<sub>l</sub>). The k<sub>l</sub> is mainly affected by the viscosity and diffusivity coefficient of liquid phase, in which increasing either of these components raises the k<sub>l</sub> and further accelerates the overall mass transfer. When CO<sub>2</sub> partial pressure in the exhaust gas is excessively high, the absorbent content throughout the liquid phase dramatically decreases, resulting in a reduction in enhancement factor and the k<sub>l</sub>, which inhibits overall mass transfer. This indicates that the liquid phase resistance mainly regulates the mass transfer performance of the absorption process.

### 3.1.4. Liquid and gas flow rates

The liquid flow rate affects the overall absorption rate and mass transfer performance. Increasing the flow rate of a liquid, would result in a tremendous amount of liquid being dispersed over the packing surface, which would cause an increase in the interfacial area of the two phases. This leads to a higher k<sub>l</sub>, that strongly related to K<sub>Gav</sub> value in a liquid-phase controlled mass transfer (Javed et al., 2006; Javed et al., 2010). Moreover, intense atomization pressure that limits droplets' initial average diameter is required for a high liquid flow rate. Nevertheless, the residence duration of the droplets is shortened as a result of an increase in first injection velocity due to higher atomization pressure.

Gas flow rate is another important parameter that should be examined in the CO<sub>2</sub> removal process using aqueous ammonia. When gas flow rate increases, the velocity of gas increases, which causes reduced layer thickness and higher interface turbulence intensity. Each of these factors contribute to a higher gas-film mass transfer coefficient (k<sub>G</sub>), which can improve the K<sub>Gav</sub>. Furthermore, increasing gas flow rate may rapidly replace CO<sub>2</sub> at the interfacial area, hence supporting in the maintenance of a greater CO<sub>2</sub> partial pressure. The rate of CO<sub>2</sub> absorption is strongly correlated to the K<sub>Gav</sub> and the partial pressure of bulk gas. The results of Zeng et al. (2011a) and Zeng et al. (2011b) revealed that increasing the

gas flow rate may result in a greater  $K_{Gav}$  value, especially at small gas flow rates. This might be because of a greater quantity of  $\text{CO}_2$  is available for absorption under specific circumstances, resulting a larger  $K_{Gav}$ . However, as numerous studies have highlighted (DeMontigny et al., 2006; Kuntz and Aroonwilas, 2009), the  $K_{Gav}$  is dependent not simply on gas flow rate only, but also factors including; ammonia concentration and liquid flow rate are important to take into consideration. According to Li et al. (2014b), the effect of gas flow rate on  $K_{Gav}$  is quite small under conditions of higher gas flow rates and lower ammonia concentrations. Other studies reported that when the gas flow rate increases, the quantity of  $\text{CO}_2$  entering the column increases, while the content of ammonia molecules in the solution doesn't change (Qing et al., 2011). Consequently, the molar ratios of  $\text{NH}_3/\text{CO}_2$  decrease which negatively affects the  $\text{CO}_2$  absorption. It is essential to keep the  $\text{NH}_3/\text{CO}_2$  ratio at an appropriate point to retain the removal efficiency of  $\text{CO}_2$  at a high level. Moreover, as the gas flow rate increases, the duration of gas stays in the absorption column is reduced, resulting lower likelihood of  $\text{CO}_2$  and ammonia molecules would react.

### 3.1.5. $\text{CO}_2$ loading

An increase of  $\text{CO}_2$  loading in amine solutions leads to a decrease in the existing active amine concentration, which consequently decreases  $K_{Gav}$  and the absorption rate (Afkhamipour and Mofarahi, 2017). When the  $\text{CO}_2$  loading of absorbent increases in AAP, the free-state ammonia will decrease. The mole ratio of the ammonia solution to  $\text{CO}_2$  goes down with the increase of the inlet  $\text{CO}_2$  volume fraction, which is disadvantageous to the absorption of  $\text{CO}_2$  (Darde et al., 2011). At low  $\text{CO}_2$  loading the carbamate is known to be the dominant species with the equilibria shifting to favour bicarbonate formation at higher loading and lower free ammonia concentration (Mani et al., 2006). Studies have shown that gas loading has little influence on  $K_{Gav}$ , and the  $\text{CO}_2$  removal efficiency and overall mass transfer coefficient show inconspicuous variations with the inlet  $\text{CO}_2$  volume fraction (Li et al., 2014b)

## 3.2. Empirical correlation of operating parameters for investigation of $K_{Gav}$

Empirical correlations for investigating  $K_{Gav}$  have been derived using the relation and influence of operational conditions in absorption columns. Zeng et al. (2011b) have developed an empirical correlation  $\text{CO}_2$  absorption process between the mass transfer coefficient and working conditions of mass fraction of ammonia and liquid flow. Their empirical correlation is given by;

$$K_{Gav} = 3.24L^{0.52}C_{\text{NH}_3}^{0.9} \quad (5)$$

Li et al. (2014b) have developed an empirical correlation of the  $K_{Gav}$  ammonia-based carbon-capturing process in a structured packing column. Major parameters including, the  $\text{NH}_3$  concentration, liquid flow, and  $\text{CO}_2$  partial pressure rate, are involved in the correlation as follows;

$$K_{Gav} = 0.0767 \frac{L^{0.442}C^{0.495}}{P_{\text{CO}_2}^{0.194}} \quad (6)$$

In addition, the modelling of  $\text{CO}_2$  removal using  $\text{NH}_3$  solution was conducted using a computational mass transfer model to evaluate and optimize the reactor design and its operational parameters. The authors Li et al. (2014b) applied the computational mass transfer method with an established empirical relation of  $K_{Gav}$ . (Eq.(6)). They did not reveal the variance between the produced correlation and the empirical studies, but the correlation's trends indicated a minor error in contrast to the experimental result. Chu et al. (2016) applied advanced computational modelling of  $\text{CO}_2$  removal using aqueous ammonia in packed column of a pilot carbon capture plant. The modeling was validated with the experimental data of  $K_{Gav}$  from Li et al. (2014b), Zeng et al. (2011b) and Zeng et al. (2013) simulation results were found in good agreement compared to experimental data, demonstrating the validity of the

computational modeling for predicting the mass transfer coefficient. Moreover, Liu et al. (2018) investigated the effect of packed column's geometry and observed that following the normal distribution of porosity improves the performance absorption process.

The mass transfer performance, hydrodynamic characteristics, energy demand, and of a bubble column in the AAP are investigated by Chu et al. (2017). Although the geometry of the bubble column reactor is relatively straightforward, it is challenging to determine the mass transfer and energy intake that takes place within the bubble column reactor because of the complex nature of multi-phase flow and the mechanisms of the subsequent chemical reaction. The operational conditions, liquid and gas properties, and arrangement significantly affect the mass transfer and amount of energy required. The performance of  $\text{CO}_2$  capture could be improved by maintaining similar intake gas velocity while increasing the height to the diameter ratio of the bubble column. Besides, the energy usage reduces as the orifice at the base of the column lowers.

Spray reactor is another important equipment for  $\text{CO}_2$  absorption process with less susceptible to corrosion due to the lack of column internals, less pressure drop, suitable for treating large volumes of flue gas, greater tolerance to solid precipitation, and lack expensive packing materials, which is expected to result in lower capital costs compared to packed columns (Kayahan et al., 2023). However, the gas-liquid mass transfer performance of spray column is lower compared to packed column. This is attributed to the limited gas-liquid contact area in the absorption tower, as the spray column lacks the filler present in the packed tower, which is essential for effectively increasing the gas-liquid contact area (Ma et al., 2013b). Empirical relationships describing the capture efficiency using aqueous ammonia droplets in a single-nozzle spray tower in terms of the four operating parameters were developed by Lim et al. (2013). Higher efficiency was observed at low gas flow rates and high liquid flow rates, as well as at low  $\text{CO}_2$  concentrations and high  $\text{NH}_3$  concentrations. The empirical relation is given by;

$$\eta = 1 - \exp(-AX) \quad (7)$$

where,

$$X = \left( \frac{Q_L C_L}{Q_G C_G} \right)^{0.7} (C_L C_G)^{0.3} \quad (8)$$

$X$  is a dimensionless number representing the combined impact of all four operational parameters, while Parameter A is an empirical factor indicating the system design's effectiveness in terms of droplet distribution and relative capture performance under specific operating conditions.

The performance of spray absorbers has been characterized using absorption ratio, mean droplet diameter, pressure drop, and mass transfer coefficient, respectively. Atomization of solution in spray absorbers can either initiate at the nozzle exit or is an outcome of liquid sheet break up s that maximum mass transfer occurred during the deceleration of the droplets. Also, the mass transfer performance of a spray absorber with droplet diameter of 400  $\mu\text{m}$  was better than a falling film with a film thickness of 400  $\mu\text{m}$ . However, superior mass transfer performance in spray absorbers leads to a high pressure drop penalty, which leads to high pumping power (Sehgal et al., 2021). The single stage spraying used in most of the studies proved unfavorable to enhancement of mass transfer due to a reduction of the absorbent concentration gradient, and also reduction of the wall-film effect due to diffusion of the cone-jet atomization (Zhao et al., 2016a).

To improve the performance of spray reactor absorption, Xu et al. (2018) proposed a computational fluid dynamics model incorporating the hydrodynamics characteristics and reaction pathways of the AAP. They employed the Eulerian-Lagrangian method to study hydrodynamics. At the same time, thermodynamic and reaction kinetic properties were examined to understand the conversion system of  $\text{CO}_2$ . It has been found that significant droplet's temperature and  $\text{CO}_2$  loading are

due to higher droplets absorption time and gas flow rate, whereas an increasing ammonia concentration of the solution has the potential to significantly improve the  $K_{Gav}$ . For this reason, hydrodynamics should be considered while designing a spray reactor to get optimal results in terms of gas flow temperature and  $\text{CO}_2$  and  $\text{NH}_3$  concentration. The mechanisms responsible for enhanced absorption performance still need to be elucidated through more rigorous numerical simulations. Future numerical studies should make sure of pertinent experimental data for validation purposes.

Moreover, the hydrodynamic conditions within the  $\text{CO}_2$  absorber can also strongly influence by the density and by the transport properties of the aqueous solution, among which viscosity and  $\text{CO}_2$  diffusivity have the greatest impact. Stec et al. (2019) presented method for determining  $\text{CO}_2$  loading using pH and density measurements at 293 K for aqueous solutions containing apparent concentrations of  $\text{NH}_3$  up to  $7\text{ mol}_{\text{NH}_3}\text{ Kg}_{\text{H}_2\text{O}}^{-1}$ . The density model proved to be the most accurate in terms of mean absolute error but lacks the robustness of the pH model, expressed as the insensitivity on ammonia concentration determination errors. Pérez-Calvo et al. (2021a) measured the densities and viscosities of aqueous solutions containing ammonia and carbon dioxide at atmospheric pressure, temperatures between 278 and 318 K, apparent  $\text{NH}_3$  concentrations between 4 and  $10\text{ mol}_{\text{NH}_3}\text{ Kg}_{\text{H}_2\text{O}}^{-1}$  and apparent  $\text{CO}_2$  concentrations up to  $5.2\text{ mol}_{\text{CO}_2}\text{ Kg}_{\text{H}_2\text{O}}^{-1}$ . The experimental measurements have been used for the development of empirical models that are able to reproduce the experimental density and viscosity values with an average absolute relative deviation of 0.3 % and 3.5 %, respectively.

In conclusion, the aforementioned studies have provided valuable insights into optimizing reactor designs, operational conditions, and the physiochemical properties of ammonia solutions in amine-based carbon capture processes. Future research should focus on refining and expanding empirical correlations and computational models, with the aim of improving overall efficiency and performance. Additionally, further investigations into properties such as  $\text{CO}_2$  loading and ammonia solution transport properties can contribute to more accurate process design and optimization.

### 3.3. Simulation studies of $\text{CO}_2$ absorption

It is generally accepted that the development of precise, comprehensive, and robust plant design modelling is necessary to analyze different operational parameters in a manner that does not put the actual system plant at risk, saving a lot of time and cost. The preferred model should be rigorous and capable of handling all parts of the process while also being simple enough to be readily applied (Koronaki et al., 2015). Many studies were conducted on the simulations, numerical modelling, and optimization of  $\text{CO}_2$  absorption. Popular optimization simulation tools and programs include; Aspen Plus, HYSYS, COMSOL, etc. (Mores et al., 2018). There are two different approaches for modelling, i.e., equilibrium and rate model (Sultan et al., 2021). The equilibrium stage model implies a rapid and transient mass transfer that ensures vapor and liquid are thoroughly mixed at all levels (Koronaki et al., 2015). The equilibrium model applies Murphree efficiencies and a theoretical number of plates that increased the accurateness of the model. Stags are related to either theoretical or actual trays for a column (Koronaki et al., 2015). The efficiency measures are supposed to reveal how much the actual column function deviates from the theoretical. It is presumed that effectiveness is consistent throughout the board. This method helps to conduct rapid evaluations of the different process components. However, since the rate of the absorption process is restricted by liquid phase mass transfer, the equilibrium model gives unduly optimistic predictions (Mathias et al., 2010).

On the other hand, rate-based modelling, also known as non-equilibrium modelling comprises well-established equations used to predict the absorber's actual performance. The rate-based model uses the two-film concept employed to simulate the interfacial transfer of mass and energy in the two phases (see Fig. 3). It shows more accurate prediction but is complicated compared to equilibrium model. The occurrence is frequently investigated using an enhancement factor, which is derived from theoretical or empirical observations using simple model parameters.

Rate-based models explicitly state the gas flux across the interface of the two phases of the absorber. Besides, the controlling heat and mass transfer equations (MESH equations) are numerically solved. Thus, this

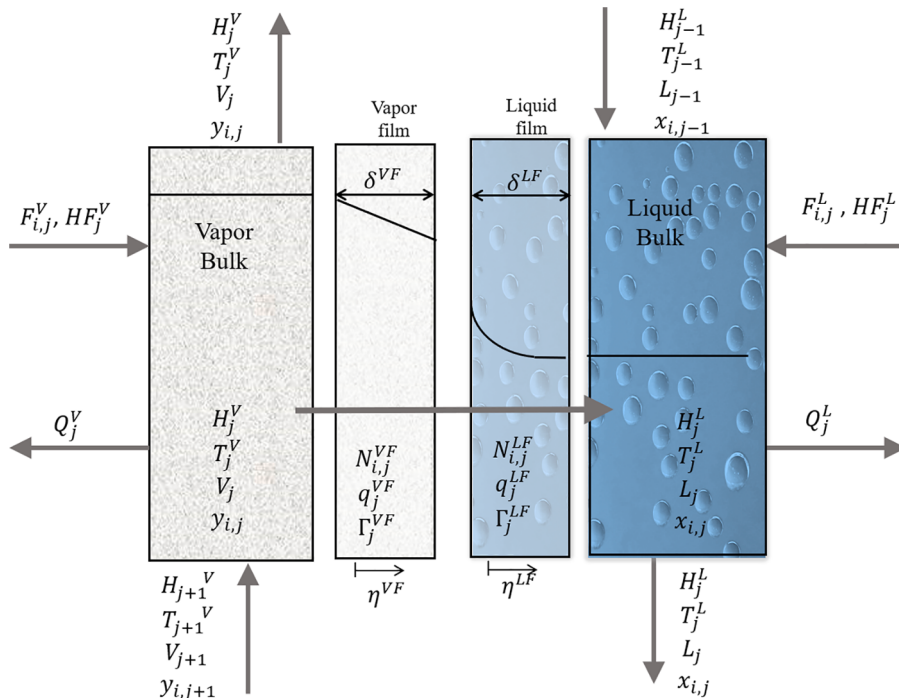


**Fig. 3.** Illustrative diagram of rate-based model (Liu et al., 2015).

model can better explain an actual process since it requires physical properties, kinetics data, and reactor details. Maxwell-Stefan equations are used to calculate the mass fluxes through the films, which is given by Taylor and Krishna (1993);

$$\Gamma_j^{VF} \left( \langle y \rangle_j^V - y_j^V \right) + R_j^{VF} \left( N_j^{VF} - N_T^{VF} y_j^V \right) = 0 \quad (9)$$

$$\Gamma_j^{LF} \left( x_j^L - \langle x \rangle_j^L \right) + R_j^{LF} \left( N_j^{LF} - N_T^{LF} x_j^L \right) = 0 \quad (10)$$

Where  $N$  is the overall molar transfer rate,  $\Gamma$  and  $\Gamma'$  are thermodynamic matrices in non-ideal adjustments,  $(\langle y \rangle_j^V - y_j^V)$  and  $(x_j^L - \langle x \rangle_j^L)$  are driving factors in which determination can be influenced by the Flow Model selection.  $L$ ,  $V$  are the molar flow rates of liquid and vapor, respectively,  $F$  is the molar flow rate of feed,  $R$  the resistance factor across the films.

Different operating parameters optimization ammonia-based carbon capture systems have been studied to enhance their efficiency and reduce energy consumption. Darde et al. (2009) applied the extended UNIQUAC model to simulate the stripper, which was used to regenerate the  $\text{NH}_3$  absorbent, and reported that the regeneration energy was 2.1 GJ/ton-CO<sub>2</sub>. Subsequently, the abatement duty of controlling ammonia slip was reported by Darde et al. (2012a) to be ca. 0.2–0.4 GJ/ton-CO<sub>2</sub> by using 7.8 wt.%  $\text{NH}_3$  absorbent. The overall energy consumption required with 7.8 wt.%  $\text{NH}_3$  absorbent was lower than that required with 30 wt.% MEA absorbent, which was reported as 4 GJ/ton-CO<sub>2</sub> (Alie et al., 2005). Mathias et al. (2010) simulated the CAP using the equilibrium model of Aspen Plus with 26 wt.%  $\text{NH}_3$  absorbent and reported that the stripper duty was 2.3 GJ/ton-CO<sub>2</sub> and the  $\text{NH}_3$  abatement duty was 2.4 GJ/ton-CO<sub>2</sub>, which is significantly larger than the results reported by Darde et al. (2012a) due to the high concentration of ammonia used. Han et al. (2014) and Rhee et al. (2011) evaluated the technical performance of AAP at relatively lower ammonia concentration (10 wt. %) in iron and steel industry which has a higher concentration CO<sub>2</sub> concentration 20–25 wt.% compared to the exhaust gas from power plants. It was found higher capture CO<sub>2</sub> rate of 90 % with the purity of 99 % and significant reduction in ammonia slip in the product CO<sub>2</sub> stream. Versteeg and Rubin (2011) also used Aspen Plus to simulate the CAP model using an  $\text{NH}_3$  concentration of 14.4 wt.% in order to evaluate the power penalty and the capture cost. The respective power penalties obtained by 30 wt.% MEA and CAP are 30.4 and 28.6 %. Furthermore, the differences between the total capital cost and the operating cost per year for the two processes are approximately 5 and 1 %, respectively. They concluded that the absorber cooling requirements and the ammonia clean up system significantly increased the energy loads and capital costs for the CAP. However, in the aforementioned CAP simulations, the reaction kinetics and the vapor-to-liquid mass transfer rate were not taken into consideration.

Because CO<sub>2</sub> absorption is limited by mass transfer in the liquid phase, the evaluation results achieved with the equilibrium model of Aspen Plus are overly optimistic (Mathias et al., 2010). Niu et al. (2012) performed conducted a laboratory-scale CO<sub>2</sub> absorption experiments and used the results to develop a model in Aspen plus. They conclude that if the operating conditions are optimized to 5–7 wt.%  $\text{NH}_3$  concentration and 0.12–0.15 CO<sub>2</sub>-lean loading, it could attain CO<sub>2</sub> removal efficiencies of over 90 %. When the concentration of  $\text{NH}_3$  increases above 7 wt.%, the influence on the CO<sub>2</sub> removal efficiency is negligible, but there is a considerable rise in the amount of ammonia slip. Zhang and Guo (2013a) adapted Niu et al. (2012) model parameters to develop AAP in a 500 MW power plant. To attain the desired 90 % removal efficiency of CO<sub>2</sub>, they indicated that the absorber's packed height and diameter must be 72 m and 40 m, respectively. They minimized the packing height and diameter of 20 m and 12 m, respectively. However, the removal efficiency was reduced to 51 % under optimum operational parameters NH<sub>3</sub> concentration (5 wt.%) and CO<sub>2</sub>-lean loading (0.23). However, the cost of CO<sub>2</sub> capture increases the Levelized cost of

electricity (LCOE) beyond that of a plant without CO<sub>2</sub> capture when the CO<sub>2</sub> removal efficiency falls below 90 % (Versteeg and Rubin, 2011). Based on the economic analysis, the proposed design by Zhang and Guo (2013a) cannot be implemented.

Qi et al. (2013) applied a rigorous model for AAP based on trials of a pilot plant at the Munmorah power station (Yu et al., 2011). The model finding agreed with pilot plant results and found that 15 % relative difference between anticipated and experimental data for rate absorption of CO<sub>2</sub>, and below 10 % for NH<sub>3</sub> slip. Similarly, the absorption modelling of Jililvero et al. (2014) has been validated using data from Yu et al. (2011). They revealed that under the optimal working parameters of the NH<sub>3</sub> concentration 5.6 M and the lean loading of solvent 0.225 molCO<sub>2</sub>/molNH<sub>3</sub>, the removal efficiency of CO<sub>2</sub> has reached 85 %.

However, the established optimal operational parameters for AAP were not consistent. The proposed NH<sub>3</sub> concentrations vary among Zhang and Guo (2013a), Niu et al. (2012), and Jililvero et al. (2014) and substantially differ in absorber's diameters. The absence of a widely accepted and verified simulation model is likely one of the contributing factors that result in such divergent findings. The selection of mass transfer correlations, kinetic models, and operating parameters affects the Aspen plus rate-based simulation modelling outcomes (Liu et al., 2015). Despite the modelling efforts to describe the efficiency of packed column depending on fundamental thermodynamic, kinetic, and mass transfer correlations, there were still some factors that need to be changed experimentally. Consequently, Liu et al. (2015) applied a model by modifying the operating conditions in accordance with many possible combinations of thermodynamics, kinetics, and correlations for mass transfer coefficients. This CO<sub>2</sub> absorption model is shown to be able to accurately describe the experimental results at the lab-scale and validated by the results of Yu et al. (2011). A rate-based model has been validated to simulate the CO<sub>2</sub> absorber of the CAP for cement plant-like flue gas composition by Pérez-Calvo et al. (2017) in order to optimize the process. They found optimal operating conditions and achieved 85.2 % CO<sub>2</sub> capture with a minimum exergy requirement of 0.92 MJ/kgCO<sub>2</sub>. The impact of various variables on CO<sub>2</sub> capture performance is investigated and establish a reliable model applicable to a wide range of experimental conditions (Pérez-Calvo et al., 2018).

Moreover, Liu and Chen (2017) used an integrated systematic method of separate studies (Jililvero et al., 2014; Zhang and Guo, 2013a; Zhang and Guo, 2013b) and factors that influence the simulation of AAP to determine the size of the packing heights of the 500 MW power plant of AAP. The staged CO<sub>2</sub> absorber's column height were found reduced specified to be 5 m and 6 m, and the removal efficiency of CO<sub>2</sub> (90 %) has been enhanced dramatically compared to Zhang and Guo (2013a) as the lean solvent inlet temperatures and the exhaust gas were reduced.

Sutter et al. (2016) applied a multi-variable sensitivity analysis that allowed to identify the set of operating conditions that minimized the energy consumption of the capture process for two different process configurations of the Chilled Ammonia Process (CAP): one configuration was free of solids, whereas the other exploited controlled solid formation. Despite the complexities associated with the CO<sub>2</sub>-NH<sub>3</sub>-H<sub>2</sub>O system and its challenges in process simulation convergence (Sutter et al., 2015), Sutter et al. (2016) successfully determined the optimal operating conditions for each configuration, resulting in minimized energy consumption during the capture process. More recently, Pérez-Calvo et al. (2020) developed a methodology for the heuristic optimization of solvent-based CO<sub>2</sub> capture processes, using the Chilled Ammonia Process (CAP) as a case study. Their methodology includes multi-objective optimization of the capture process, aiming to minimize energy consumption and maximize productivity within a certain range of CO<sub>2</sub> capture efficiencies. They provide guidelines for the selection, development, and validation of the process mode used in the optimization. This comprehensive approach enables researchers and engineers to effectively optimize solvent-based CO<sub>2</sub> capture processes, such as the CAP, and improve their overall performance.

### 3.4. Summary on the mass transfer of CO<sub>2</sub> absorption in to aqueous ammonia

The determination of mass transfer coefficients of CO<sub>2</sub> absorption has been reviewed over a range of operating parameters in absorber columns. Normally, in the absorption process the mass transfer process in CO<sub>2</sub> absorption into aqueous ammonia solution is mainly controlled by the resistance in the liquid phase and the ammonia concentration has a great effect on the overall mass transfer coefficient. However, high concentration of ammonia can lead to ammonia escape. Generally, in most studies, authors showed that the effect of temperature, liquid flow rate, partial pressure of CO<sub>2</sub>, and ammonia concentration on the overall mass transfer coefficient is significant, whereas the gas flow rate and CO<sub>2</sub> loading only has a little effect.

Computational models have been used to predict the mass transfer coefficient and validate experimental data. The hydrodynamic characteristics and energy demand of different reactor designs, such as absorption columns, bubble columns, and spray reactors, have also been studied. The density, viscosity, and CO<sub>2</sub> diffusivity of aqueous ammonia solutions have been investigated to improve accuracy in process design. Overall, the studies provide valuable insights for optimizing reactor designs, operational conditions, and the properties of ammonia solutions in ammonia-based carbon capture processes, with scope for further refinement and expansion of empirical correlations and computational models. These models can help optimize reactor designs, predict performance under different operating conditions, and guide process optimization efforts.

Moreover, developed rate-based models for the capture of CO<sub>2</sub> in absorber columns which are validated against experimental results were also reviewed. Optimization of operating parameters in ammonia-based carbon capture systems to helps to improve efficiency and reduce energy consumption. However, there is inconsistency among the optimal operational parameters suggested by various studies, indicating the need for a widely accepted and verified simulation model. A modified model was applied to the the operating conditions inaccordance with many possible combinations of thermodynamics, kinetics, and correlations for mass transfer coefficients, which shows a significant reduction of absorber column height to be 5 m and 6 m, and the found removal efficiency of CO<sub>2</sub> (90 %) of AAP. This would enable more reliable optimization and provide guidelines for the design and operation of these systems to achieve high CO<sub>2</sub> removal efficiency while minimizing energy consumption and capital costs. Future research should investigate the scalability of the optimized parameters to larger-scale applications. This would provide valuable insights into the practical implementation and economic viability of these systems.

## 4. Mass transfer enhancement technologies of AAP

Aqueous ammonia has a relatively slower reaction kinetic towards CO<sub>2</sub> due to liquid phase absorption rate limitation that affects the mass transfer. Various methods have been evaluated to improve the current approaches of CO<sub>2</sub> removal using ammonia solution, including; physical/mechanical, chemical, and combined measures, as illustrated in Fig. 4.

### 4.1. Physical/mechanical method

#### 4.1.1. Mass transfer intensifying technologies

Various separation devices for CO<sub>2</sub> capture processes enhance the absorption rate by maximizing the gas-liquid interfacial area. Nevertheless, there are still significant obstacles in the mass transfer enhancement and process intensification of traditional mass transfer devices. This is due to mass transfer restrictions that inhibit the enhancement of the CO<sub>2</sub> removal process and limit the reduction of the packing column size. Therefore, mass transfer intensifying absorbers, which can provide high performance and throughput, are necessary. Microchannel, rotating packed bed, high frequency ultrasonic assisted reactor, and membrane contactors are among the main intensification technologies that have introduced a new idea in this field.

##### 1) Microchannel reactor (MR)

Microchannel is one of the potential intensification technologies in the absorption process. Compared to the conventional reactors, the microchannel has micro-thin channels that help to shorten the transfer distances and increase the surface-to-volume ratio (Lam et al., 2013), which results in faster reaction rates, heat transfer, and mass transfer (Khatoon and Alam, 2022).

Asgarifard et al. (2021) have employed a microchannel reactor to analyze the CO<sub>2</sub> capturing efficiency of aqueous ammonia. The absorption efficiency of AAP has reached 96.48 % as the best output using comprehensive numerical optimization. They also investigated parameters that affect CO<sub>2</sub> absorption efficiency, such as; concentration of solvent, gas flow rate, and temperature. They found that solvent concentration had a significant effect compared to other parameters.

##### 2) Rotating packed beds (RPB)

One of the most suitable apparatuses designed to relax limitations of mass transfer and intensify the absorption process by achieving high gravity conditions is rotating packed beds (RPB), also called “HiGee” (Ramshaw, 1983). The high gravity situation is formed using the centrifugal forces that accelerate mass transfer competence (Wang et al., 2015). The interface area of the liquid-gas increases as a result of liquid dispersion into droplets due to high rotator speed. RPB could also be potentially managed at higher liquid and/or gas flow rates since it has a

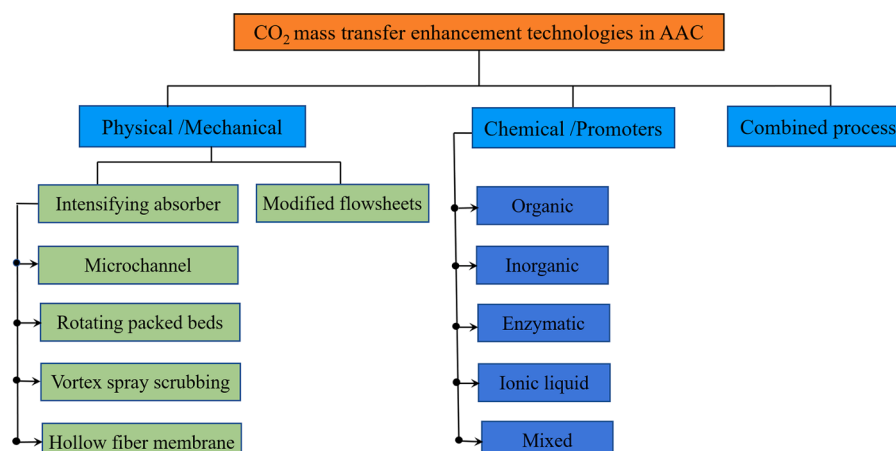


**Fig. 4.** Enhancement methods of ammonia-based CO<sub>2</sub> capture.

**Table 4**The overall volumetric mass transfer coefficient of conventional to intensified technologies of CO<sub>2</sub> absorption using aqueous ammonia.

Author	Reactor	Experimental conditions			Volumetric mass transfer coefficients K <sub>GCO<sub>2</sub></sub> a <sub>V</sub> (kmol /m <sup>3</sup> h kPa)
		Type	Size		
Conventional/traditional					
Qiu et al. (2011)	Packed column	Di: 50 mm	NH <sub>3</sub> conc.= 1.5–5 Wt.%, CO <sub>2</sub> = 8–16 vol.%, LFR=0.0018 – 0.0078m <sup>3</sup> /h, GFR= 0.6m <sup>3</sup> /h, Pressure = 3 KPa		0.33–1.17
Zeng et al. (2011a)	Packed column with ceramic Raschig ring	Ht:400 mm Di: 100 mm	NH <sub>3</sub> conc.= 2–16 Wt.%, CO <sub>2</sub> = 5–15 kpa, LFR=0.76 – 3.06m <sup>3</sup> /m <sup>2</sup> h, GFR= 61 – 214m <sup>3</sup> /m <sup>2</sup> h, T=293–328 K		0.1–08
Zeng et al. (2011b)	Packed column	Ht:400 mm Di: 100 mm	NH <sub>3</sub> conc.= 2–8 Wt.%, CO <sub>2</sub> =15 Vol.%, LFR =0.0162m <sup>3</sup> /h GFR = 0.96 – 1.68m <sup>3</sup> /h, Pressure = 0.1 MPa, T=293 K		0.09–0.20
Zhongli et al. (2012)	Packed column	Ht: 2400 mm Di: 150 mm	NH <sub>3</sub> conc.= 0.36–0.72 M, CO <sub>2</sub> =2.8–8 Vol.%, LFR = 0.1098 – 0.2202m <sup>3</sup> /h, GFR = 7.9 – 12.7m <sup>3</sup> /h, P <sub>CO<sub>2</sub></sub> = 0.1 MPa, T=300 K		0.31–0.22
Zeng et al. (2013)	Packed column with ceramic raschig ring	Ht: 600 mm Di: 100 mm	NH <sub>3</sub> conc.=2–16 Wt.%, CO <sub>2</sub> =5–15 Vol.%, LFR = 0.008 – 0.024m <sup>3</sup> /h, GFR= 0.6 – 1.68m <sup>3</sup> /h, P <sub>CO<sub>2</sub></sub> = 5–15 KPa, T=293–328 K		0.09–0.42
Ma et al. (2013b)	Spray tower	Ht: 350 mm Di: 55 mm	NH <sub>3</sub> conc.= 1–7 Wt.%, CO <sub>2</sub> =10–20 Vol.%, LFR= 0.09 – 0.18m <sup>3</sup> /h, GFR=0.2 – 0.4m <sup>3</sup> /h, P <sub>CO<sub>2</sub></sub> =0.1 MPa, T = 293–323 K		0.08–0.17
Nair and Selvi (2014)	Structured packed column	Ht: 600 mm Di: 100 mm	NH <sub>3</sub> conc.= 2–6 Wt.%, CO <sub>2</sub> =10–20 Vol.%, LFR = 0.75 – 3.06m <sup>3</sup> /m <sup>2</sup> h, GFR = 61 – 214m <sup>3</sup> /m <sup>2</sup> h, P <sub>CO<sub>2</sub></sub> up to 16 Kpa, T=293–323 K		0.043–0.733
Li et al. (2014b)	Structured packing with division windows	Ht: 2000 mm D:150 mm	NH <sub>3</sub> conc.= 2.27–0.72 M, CO <sub>2</sub> =2.2–8 kpa, LFR = 20–39m <sup>3</sup> /m <sup>2</sup> h, GFR = 0.393 – 0.629m <sup>3</sup> /s, P <sub>CO<sub>2</sub></sub> = 1 atm, T=300 K		0.12–0.250
Chu et al. (2016)	Structured packing column	Ht: 2000 mm Di: 150 mm	NH <sub>3</sub> conc.=2–10 Wt.%, CO <sub>2</sub> =5–21 Vol.%, LFR = 14 – 24m <sup>3</sup> /m <sup>2</sup> h, GFR=1600–2600m <sup>3</sup> /m <sup>2</sup> h, P <sub>CO<sub>2</sub></sub> =1 atm, T=293.15 K		0.2–0.7
Ma et al. (2016)	Bubble column	Ht: 305 mm Di: 42 mm	NH <sub>3</sub> conc.= 0–9 Wt.%, CO <sub>2</sub> =0–15 Vol.%, Liquid volume= 0.15 L, GFR= 0.06m <sup>3</sup> /h, P <sub>CO<sub>2</sub></sub> = 100 MPa, T=283–313 K		0.103–0.644
Intensified					
Zhao et al. (2016a)	Multistage spraying tower	Ht: 540 mm Di: 50 mm	NH <sub>3</sub> conc.= 10–20 Wt.%, CO <sub>2</sub> =10–20 Vol.%, LFR= 0.0696 – 0.1296m <sup>3</sup> /h, GFR=1.8 – 3.6m <sup>3</sup> /h, P <sub>CO<sub>2</sub></sub> = 0.7–1 MPa, T=293 K		1.116–1.764
Kittiampon et al. (2017)	Microchannel	Dimension = 60 × 0.5 × 0.5mm <sup>2</sup>	NH <sub>3</sub> conc.= 4–10 Wt.%, CO <sub>2</sub> =10 Vol.%, LFR= 0.00012 – 0.0003m <sup>3</sup> /h, GFR=0.0285m <sup>3</sup> /h, P <sub>CO<sub>2</sub></sub> = 141–401 KPa, T=293–303 K		32.44–115.67
Feng et al. (2018)	Bubbling reactor under magnetic static	Ht =305 mm	NH <sub>3</sub> conc.= 6–15 Wt.%, CO <sub>2</sub> =0–20 Vol.%, GFR=0.036 – 0.084m <sup>3</sup> /h, P <sub>CO<sub>2</sub></sub> = 0.1 MPa, T=288–313 K		0.302–0.673

Note: Ht = packing height, Di = inner diameter, LFR = liquid flow rate, GFR = gas flow rate,

slower tendency to flood than a conventional packed bed. Consequently, an increase in mass transfer by a factor of 10–100 would be achieved and reduced equipment size considerably (Ramshaw, 1983).

Few studies have been done on AAP using RBP. Kang et al. (2014) examined the performance of a packed bed and RPB and compared the effectiveness of the particular absorbers in AAP. The range of the height of transfer unit of each seems to be between 0.35–1.96 m and 0.08–0.40 m, respectively. In their later work, Kang et al. (2016) applied a model to evaluate the efficiency of RPB to capture 1000 tons per day of CO<sub>2</sub>, with a composition of CO<sub>2</sub> (15 %) and aqueous ammonia concentration (3 wt. %). They used the experimental result of Kang et al. (2014) in the validation of the modelling result, and revealed that ammonia intensification is more effective than MEA solution. In MEA, the mass transfer rate enhanced but the concentration difference that drives the mass transfer declined. This is because of the proximity of MEA operational loading to be saturated and low average rate of reaction at this stage. As the mass transfer increases, the diffusion of free CO<sub>2</sub> across the interface increases, which minimizes the driving force. Nevertheless, due to operating loading being far from saturation, the aqueous ammonia process may still achieve an adequate reaction rate to convert the free CO<sub>2</sub>.

However, although RPB is excellent for the enhancement of mass transfer rates over the conventional mass transfer device, it does have certain drawbacks, including energy intensive, a sharp drop in pressure, and maintenance problems (Tay et al., 2019).

3) High frequency ultrasonic assisted reactor (HIFU)

The development of a high frequency ultrasonic assisted reactor (HIFU) emerges as a promising technique for intensifying the CO<sub>2</sub> absorption process, as its good mass transfer is powered by the sono-physical effect. The principle of this technology has been demonstrated by utilizing an ultrasonic cleaning bath in which the whole bath serves as the reactor (Tay et al., 2016). However, the optimal intensification factor might be restricted by the slower reaction rate of the solvent. Meanwhile, HIFU offers a direct impact by means of ultrasonic fountain generation, results reducing the liquid phase mass transfer resistance. Furthermore, it is possible to create sonochemical impact for the enhancement of chemical reactions through the microturbulent and ultrasonic cavitation phenomena (Gielen et al., 2015). Thus, an ultrasonic reactor may be used with solvents having a slow kinetic rate. In addition, this technique may circumvent the size constraint of physical intensification methods. The standard thickness of the ultrasonic discs used in HIFU is less than 2 mm which is determined by the ultrasound frequency. Consequently, the ultrasonic transducer is connected to the plate column while only requiring a small amount of space. However, the potential benefits of utilizing HIFU with an aqueous ammonia solvent have not been definitively determined.

In summary, the process intensification approaches mentioned above have grown rapidly over the past two decades and have become crucial technologies for PCC. However, the study that has been done on the experimental and modelling of AAP using intensification technologies is insufficient. The conventional and intensified systems employed in AAP are summarized in Table 4.

#### 4) Membrane technology

Membrane technology is a viable alternative to packed columns which is recently taking a crucial role in the advancement of modern CO<sub>2</sub> separation technology. The membrane-based absorption system is an arrangement of a conventional gas separation and mass transfer with membrane. Membrane contactors provide several benefits including, high interfacial area, operational flexibility, simple scaling, and independent gas and liquid operation (Li and Chen, 2005). Thus, they are able to offer a larger mass transfer and accomplish a quicker rate of mass transfer, reducing NH<sub>3</sub> loss in the AAP (Wang et al., 2018).

Typically, the mass transfer characteristics in membrane gas absorption have three stages. Firstly, the CO<sub>2</sub> moves from the bulk gas(g) to the interface of gas/membrane(gm); secondly, it migrates to the liquid/membrane(lm) interface across the membrane pores, finally, moves from liquid/membrane interface to the liquid(l) body. Porous membranes of hollow fiber membrane contactors (HFMC) are used for partitioning the gas-liquid phases while still allowing mass transfer between them, as shown in Fig. 5. The Molar flux (N) is given by:

$$N = k_g (P_g - P_{gm}) = k_m (P_{gm} - P_{lm}) = k_l (C_{lm} - C_{lb}) \quad (11)$$

Where k<sub>g</sub>, k<sub>m</sub>, and k<sub>l</sub> represent individual mass transfer coefficients for gas, membrane, and liquid, respectively. P and C are the partial pressure and amine concentration, respectively.

Generally, the overall mass transfer coefficient (K<sub>G</sub>) for membrane contractor gas absorption is given by (Lin et al., 2009):

$$\frac{H}{K_G d_i} = \frac{H}{k_g d_0} + \frac{H}{k_m d_{ln}} + \frac{1}{k_l^o E d_i} \quad (12)$$

Where H is Henry's Law constant, E is the enhancement factor, respectively. d<sub>0</sub>, d<sub>i</sub>, and d<sub>ln</sub> are the average diameters of the outer, inner, and logarithmic of the non-wetted part of the membrane, respectively.

Employing a membrane for gas absorption provides a third mass transfer resistance which is additional to the resistance of the gas side and liquid side (Rejl et al., 2016). The gas side resistance has minimal effect and could be almost insignificant compared to the liquid side resistance. The membrane resistance can also be quite low in comparison to liquid side resistance of a non-wetted membrane. However, in the case when the membrane becomes wet, the membrane resistance will dramatically increase (Wang et al., 2005).

Few researchers investigated the potential of adopting membrane contactors to improve the mass transfer of the AAP. Makhloifi et al. (2014) was first examined the potential of employing HFMC for AAP. They used composite membranes, i.e., custom Teflon and standard TPXs (Polymethylpentene). The results of the experiments showed that a stable and good functionality is observed, with a smaller ammonia escape and enhanced mass transfer in comparison to a standard absorption column. Accordingly, it is found that the size of the gas separator device can be reduced by 3× with HFMC made of polypropylene microporous membranes (McLeod et al., 2014), up to 4× with commercial composite membranes, and 5× with composite membranes fabricated in-house (Makhloifi et al., 2014). The impact of different parameters such as ammonia vaporization, ammonia concentration, and solvent temperature in a HFMC was examined by Mehdipour et al. (2014). They employed two-dimensional modelling to investigate CO<sub>2</sub> removal by aqueous NH<sub>3</sub> and revealed that the rate of absorption increases exponentially with ammonia concentration and temperature of the ammonia solution. Molina and Bouallou (2015) studied how the material composition of a membrane and operational parameters affected the removal efficiency of CO<sub>2</sub> and ammonia loss. When the gas velocity is kept low, the CO<sub>2</sub> removal efficiency may exceed 99.9 %, while ammonia loss can be minimized to less than 1 %.

The primary technical challenge of the HFMC is when liquid amine penetrates the membrane pores, commonly called "membrane wetting." This problem limits the practical deployment of membrane contactors in PCC industries. Even minor membrane wetness considerably increased

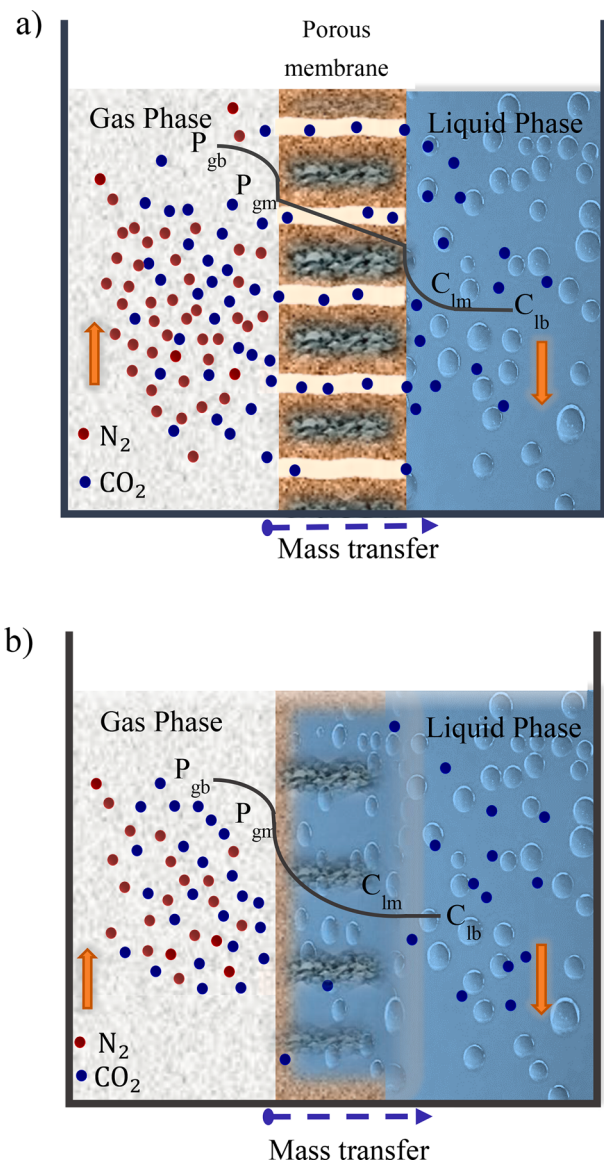


**Fig. 5.** Schematic diagram of hollow fiber membrane mass transfer mechanism (a)non-wetted (b)Wetted. Reprinted in modified form with permission from (Zhao et al., 2016b).

the resistance in the mass transfer. Although membrane fiber wetting is only 5 %, the overall mass transfer rate would decrease by approximately 20 % (Wang et al., 2005). For an extended period of operation, a HFMC made with good hydrophobicity might experience three forms of wetting. Absorption efficiency is high during the first few hours because the membrane separation unit is likely to be non-wetted (Fig. 5(a)). Within a couple of days, the membrane may get progressively wet (i.e., partly wet), which significantly diminishes its absorption effectiveness. Over a long period, the membrane pores eventually become entirely clogged with the liquid absorbent (Fig. 5 (b)), resulting in high mass transfer resistance.

When aiming to ensure optimal and stable mass transfer of CO<sub>2</sub> absorption, it is necessary to regulate the wettability of the membrane. Coating microporous support with a dense thin film that acts as a protective border exposing to the liquid phase prevents the membrane contactors from being wet (Favre and Svendsen, 2012; Simons et al., 2009). In addition, the composite fibers with several thick layers have been effectively employed and evaluated (Chabanon et al., 2011a; Chabanon et al., 2011b). If a proper dense layer is selected, the wetting

will be reduced, and the effectiveness of mass transfer is equivalent to the one obtained in microporous membrane contactors (Makhloufi et al., 2014; Nguyen et al., 2011). In comparison to the packed column, dense layer membranes showed stable functionality and enhanced CO<sub>2</sub> mass transfer (Karami et al., 2013). Toro Molina and Bouallou (2016) proposed the use of a thin hydrophobic dense layer of composite hollow fibers and higher gas permeance to avoid membrane wetting. As compared to the packed column, the intensification factor of the membrane's overall absorption rate has reached 5. The estimation of the intensification factor for CO<sub>2</sub> absorption is to calculate the values from the experimental results. If a membrane's intensification factor is larger than 1, it is preferable to packed absorption column.

Cui and deMontigny (2017) evaluated the membrane CO<sub>2</sub> absorption capability and overall mass transfer performance of aqueous ammonia in hollow fiber PTFE membranes at room temperature. Their result showed that the value of K<sub>GAv</sub> ranged from  $1.06 \times 10^{-4}$ m/s to  $2.89 \times 10^{-4}$ m/s. They also investigated the effect of operating parameters and demonstrated that at the highest liquid flow rate, the absorption performance NH<sub>3</sub> may reach 98 % of MEA. As shown in Fig. 6, Even though NH<sub>3</sub> has slow kinetics reaction with CO<sub>2</sub>, the large diffusivity of NH<sub>3</sub> allows it to provide a similar mass transfer performance as MEA. The K<sub>GAv</sub> of NH<sub>3</sub> at the highest possible liquid flow rate is only 2 % lower than MEA, but it is still within the same magnitude range. However, the author (Cui and deMontigny, 2017) found that the membrane wetness caused the absorption efficiency to decline progressively after 60 min of use. The generation of ammonium bicarbonate precipitate along the boundary of the membrane induced noticeable membrane fouling, lowered the membrane surface's hydrophobic nature, and further enabled membrane wetting.

Process performance should be studied under real industrial operating conditions to develop CO<sub>2</sub> capture technology in industries with practical applications. Investigations modelling and simulation studies of membrane contactors in ammonia-based CO<sub>2</sub> absorption processes are scarce. Villeneuve et al. (2018) developed a membrane gas absorption model in the Aspen Custom Modeler (ACM) with industrially applicable operating conditions to examine the capacity of composite membrane contactors with non-selective and selective dense layers in AAP. The maximum CO<sub>2</sub> specific absorption capacity of the contactors with handmade selective membranes was found to be 2.7 mol/m<sup>3</sup>/s, providing 20× larger than results for the simulations in packed columns,

allowing for significant process intensification via reactor volume reduction. Hughes et al. (2022) demonstrated the high potential of membrane-assisted ammonia-based CO<sub>2</sub> capture systems in reducing energy penalties. Rigorous rate-based models were developed for post-combustion CO<sub>2</sub> capture using chilled aqueous ammonia. The study showed that the membrane can considerably lower the reboiler, cooler, and condenser duties in the NH<sub>3</sub> abatement section, but with higher water removal, there is a steeper rise in the required membrane area. Thus, the use of NH<sub>3</sub> as a potential option to more conventional amines in the HFMC for absorption of CO<sub>2</sub> might prove to be quite effective by addressing potential issues such as solid precipitation and membrane wetting.

#### 4.1.2. Modified process flowsheets

The conventional equipment configuration used for ammonia-based carbon dioxide capture lends itself well to several structural adaptations. To discover ideal configurations, a systematic technique should assess the potential of several alternative alterations and pairings of modifications at the same time. This is accomplished by constructing a superstructure that contains several distinct potential alterations that may be simulated and improved to discover the best optimal configuration for a certain CO<sub>2</sub> capture process (Oh et al., 2016). Modifying the process is accompanied by three process schemes (Le Moullec et al., 2014; Wang et al., 2017b): (a) absorption enhancement in which CO<sub>2</sub> loading is increased in rich solution near to the bottom of the absorber to increase the solvent capacity and decrease the reboiler duty, includes modifications such as; absorber intercooling (AIC), rich solvent splitting (RSS), split flow arrangement (SFA), and inter-heated absorber (IHA) (b) heat integration in which waste heat can be recovered by transferring heat between the streams to minimize heat losses in the reboiler includes modifications such as; rich solvent splitting (RSS), inter-heated stripper (IHS), vacuum operated stripper (VOC), multi-effect stripper (MES) (c) heat pump in which heat quality is improved at the expense of extra mechanical work includes lean vapor compression (LVC), rich vapor compression (RVC), multi-pressure stripper (MPS).

"Absorption enhancement" is one of the modifying process schemes that focus on increasing the rate or effectiveness of CO<sub>2</sub> removal (Le Moullec et al., 2014). These changes have the capacity to minimize heat consumption and/or boost the energy consumption of CO<sub>2</sub> removal. In the AIC configuration, the CO<sub>2</sub> absorption equilibrium shifted back by cooled solvent's a lower temperature (Feron, 2016). Since CO<sub>2</sub> absorption with chemical solvents is inherently exothermic, removing heat to a level that does not significantly decrease the reaction kinetics is favorable for the CO<sub>2</sub> absorption equilibrium. This results in the process to use less solvent for a given amount of CO<sub>2</sub> removed (Le Moullec and Kaniche, 2011), and consequently, save energy being required for solvent regeneration. Jilvero et al. (2014) adapted the two-stage absorption design incorporated with the intermediate cooling process to advance the AAP. Compared with a one-absorber setup, two-stage absorption is advantageous in terms of absorber column height reduction, capture efficiency and minimizing ammonia slip. In stage 1 absorption process, the lean solvent (rich in free NH<sub>3</sub>) is introduced to the middle of the absorber to achieve fast CO<sub>2</sub> absorption, and then enters the top of the column to recover NH<sub>3</sub> from the gas (Stage 2 absorption). Following the intercooling process, the semi-rich solvent was taken from the bottom of the absorber and injected from the top. Since most of the NH<sub>3</sub> molecules reacted with CO<sub>2</sub> in the first stage of the absorption, the vapor pressure of NH<sub>3</sub> at the top of the absorber only depended on the temperature of the solvent after intercooling. A cooling step between the two absorbers enhances absorber performance in terms of the levels of CO<sub>2</sub> capture and ammonia slip. The NH<sub>3</sub> slip in the absorption process is reduced by more than 50 % compared with single-stage absorption (Li et al., 2016c). Elevating CO<sub>2</sub> absorption temperature to ambient conditions (20–30 °C) and using relatively high NH<sub>3</sub> concentrations (6–10 wt.%) can avoid both solid precipitation and the substantial energy input for solvent chilling while also improving the CO<sub>2</sub> absorption rate.

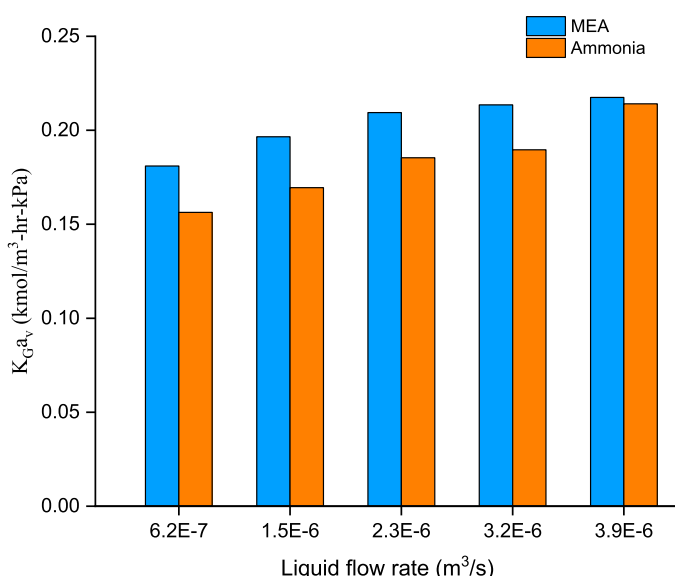


**Fig. 6.** Mass transfer of CO<sub>2</sub> absorption using hollow fiber membrane performance comparison of aqueous ammonia and MEA. Reprinted with permission from (Cui and deMontigny, 2017).

Various heat integration process modifications and designs that are vital to recover the heat loss of absorbent regeneration and advance the NH<sub>3</sub>-based CO<sub>2</sub> capture process have been studied. These advanced processing configurations can decrease the energy penalty of absorbent regeneration, and a combination of these processes improves energy performances. Li et al. (2015a) developed and evaluated the advanced AAP process based on the platform of ASPEN Plus. By applying multi-modification including rich solvent split and inter-heated stripper, the reboiler duty can be significantly reduced to 2.46 MJ/kg CO<sub>2</sub> from their base case of 3.27 MJ/kg CO<sub>2</sub> and carbon capture rate of 84.7 % at the NH<sub>3</sub> concentration of 6.8 wt.% and the CO<sub>2</sub> loading of 0.225 mol CO<sub>2</sub>/mol NH<sub>3</sub>. The total energy saving is found to be 24.8 %. Jiang et al. (2017) developed the NH<sub>3</sub>-based process by applying the advanced flash stripper configuration. They showed that the reboiler duty can be further reduced to 1.86 MJ/kg CO<sub>2</sub> at the elevated stripper pressure of 12 bar, in which the carbon capture rate is 85 % and total energy saving of 28.5 %, at NH<sub>3</sub> concentration and lean loading of 10.2 wt.% and 0.28 mol/mol, respectively. It was very much lower than the regeneration energy obtained at Munmorah pilot plant and the typical MEA processes. In addition, process modifications that include rich solvent split, lean vapor compression, and rich vapor compression using aqueous ammonia were reported in the literature. These process modifications enhance the efficiency of the process while requiring an acceptable amount of electricity and can reduce the energy requirement remarkably. Nguyen and Wong (2019) proposed new stripper configuration based on the LVR concept when applying to the AAP process and found the total energy saving of 7.69 %. They claimed that the need of reboiler can be eliminated completely and the total equivalent work consumption of 0.167 kW h/kg CO<sub>2</sub> captured can be achieved. Obek et al. (2019) compared different configurations of an ammonia-based carbon capture system. In terms of energy savings, the LVC configuration demonstrated the highest reduction in energy consumption at 34.5 %, followed by a 6.4 % reduction for RSS and a slight increase of 0.3 % for RVC.

Liu et al. (2020) expanded on the comparison of different configurations over the research article explained above by Obek et al. (2019) where they have included two more possible configurations for ammonia-based carbon capture systems, which are cold split bypass (CSB), and the combination of CSB and LVC. Their simulation results show that using the CSB configuration decreases energy requirements by a significant amount at a reduction value of 34.2 % compared to a typical ammonia-based system. Furthermore, the combination of CSB and LVC does not give noticeable energy reductions as it only reduces the energy requirements by an additional 0.2 % to get a value of 34.4 %. This combination does not seem like a viable option since using two configurations in a single system increases the capital costs and does not offer any energy savings potential.

Furthermore, Nguyen and Wong (2021) developed and optimized a novel low-energy process called the combined rich and lean vapor recompression (RLVR) process for post-combustion carbon capture (PCC) using dilute aqueous ammonia (NH<sub>3</sub>) as the solvent. By integrating rich vapor recompression (RVR) and lean vapor recompression (LVR) approaches, the RLVR process achieved a remarkable reduction in total equivalent work required for CO<sub>2</sub> capture, with a specific energy penalty of only 0.123 kWh/kg of CO<sub>2</sub> captured.

A distinct method has been adopted where the ammonia-based carbon capture system reduces the energy requirements by using ammonia to provide some of the cooling needed by the typical chilled ammonia process. Wang et al. (2017a) developed a system that integrates an ammonia-based carbon capturing unit with an absorption chiller for supplying a cooling load. This cooling load provides a useful commodity that can be sold to cover some of the costs of operating the carbon capture system. The authors have conducted a thermodynamic analysis on this integrated system and found that the system can reach a rate of CO<sub>2</sub> removal of 90 %, while the specific regeneration energy and the cooling load are 3.4 MJ/kg of CO<sub>2</sub>, and 113.3 MW, respectively. Sutter

et al. (2017) designed a chilled ammonia process that could avoid the solid formation and inhibit the NH<sub>3</sub> loss. In addition, Sutter et al. (2016) proposed an improved chilled ammonia process that utilized the solid ammonium bicarbonate formed in the regeneration section for increasing the CO<sub>2</sub> concentration in the product stream. The improved process was used for precipitation, and to separate and dissolve the solid phase, thereby freeing the packed absorption and desorption columns of solids. A comparison of Controlled Solid Formation- Chilled Ammonia Process (CSF-CAP) was carried out with conventional CAP (L-CAP) technology since a solid handling section, and from the scrutinized comparison it was found that in the CSF-CAP process reduction of steam, the requirement was minimized by 30 % for CO<sub>2</sub> desorption and the SPECCA (Specific Primary Energy Consumption for CO<sub>2</sub> Avoided) by 17 %. The separation of CO<sub>2</sub> absorption and solid formation in different process units enables heat integration between precipitation and dissolution including the enthalpy of crystallization and the utilization of low-grade heat at temperatures below 50 °C. Such heat integration is essential for the performance of the CSF-CAP.

It can be noted that the most advanced industrial processes are designed around combined multiple process modifications. Ullah et al. (2019) introduced a combined modification of the typical ammonia-based carbon capture system to reduce the energy requirements and compared to the typical system as well as other modifications. They combined RVC (which was introduced earlier) with cold solvent split (CSS) processes. Their simulation results show that this new combination reduced the energy requirements by 20.2 % compared to the typical chilled ammonia process and this is a much better reduction than other modifications, such as RSS which gives an 11.6 % reduction, and inter-heating processes which provide only an 8.26 % reduction. Also, the authors conducted a capital cost estimate to see if the additional components for this combined modification would save money. Their findings show that the combined modification of RVC and CSSP saves about \$707 thousand every year. Therefore, the proposed modification is economically justifiable.

Ishaq et al. (2021) proposed another energy saving modification for NH<sub>3</sub>-based absorption-desorption process in which the heat integration is performed with a rich solvent split and absorption enhancement is done with split flow arrangement. The rich solvent split and split flow process reduced the reboiler duty by 15.8 % and 32.8 %, respectively. Split-flow arrangement(SFA) is most recommended process configuration which combines the split-flow of solvent from the stripper with a staged feed of the absorber has an impact on the absorption performance (Aroonwilas and Veawab, 2007). The SFA provides better absorption of CO<sub>2</sub> either by reducing the driving force in the absorber section or by maximizing the CO<sub>2</sub> loading in the bottom absorber's section. As shown in Fig. 7, the process functions by enabling the recovered amine separate into two or more streams: a semi-lean amine stream is supplied to the midsection of the absorption column, and a lean amine stream is supplied to the upper part of the absorption column. The semi-lean amine solution is cooled prior to its being introduced into the absorber. Thus, it cools in the absorber and able to make use of the inter-cooling that occurs. This intercooling process causes a reduction of the reboiler heat duty. Moreover, the effect of intercooling that is produced when the cooled semi-lean amine is supplied into the lower column section slightly decreases the equilibrium CO<sub>2</sub> partial pressure. These results increase gas uptake in the liquid amine, leading to a faster rate of reaction and rich amine loading. Besides, when a semi-lean amine flows through the lower part of the absorption, showed the impact of SFA process flowsheet on the temperature gradient is significant, which can enhance the absorption rate.

More recently Pérez-Calvo et al. (2021b) developed advanced process configurations for CO<sub>2</sub> capture using aqueous ammonia as an absorbent. They optimized ten different configurations with specific goals: controlling NH<sub>3</sub> emissions, minimizing capital costs, and reducing energy demand. They proposed a new benchmark configuration that combines the Chilled Ammonia Process with innovative components of a

multi-pressure desorber with recycled vapor compression, a vacuum integrated stripper using low-temperature steam, and a flue gas water-wash column for NH<sub>3</sub> reduction without an acid-wash column. The proposed benchmark configuration, based on the Chilled Ammonia Process, demonstrated significant improvements. The multi-pressure desorber with recycled vapor compression achieved steam requirements as low as 1.1 MJ/kg CO<sub>2</sub> captured at temperatures of 140–160 °C. The vacuum integrated stripper utilized low-temperature steam below 100 °C for solvent recuperation. Additionally, the flue gas water-wash column effectively reduced NH<sub>3</sub> concentration in the CO<sub>2</sub>-depleted flue gas to below 10 ppmv without an acid-wash column. These numerical results highlight the potential for energy savings, cost reduction, and improved NH<sub>3</sub>-based CO<sub>2</sub> capture efficiency with the proposed benchmark configuration.

In summary, almost all studies related to process modification evaluation of AAP have been performed through process modeling and there is a clear lack of pilot plant scale evaluation of these modifications. It appears that some modifications have been widely studied such as intercooled absorber, lean vapor compression or rich solvent split, whereas others have only been evaluated by individual authors. Moreover, all these process modifications always require extra devices, introducing more complicated processes and higher operating costs. When evaluating several process configurations based on energy requirements, it is also important to consider the additional cost incurred compared to the conventional process configuration. Few publications addressing the cost of modification are available in the current literature. Economic evaluations are needed to assess the trade-off between technical improvement and the associated economic burden. Li et al. (2016a), Li et al. (2016b) and Li et al. (2016c) comprehensively evaluated the NH<sub>3</sub> and MEA-based PCC systems and their process improvements integrated with a coal-fired power plant using a validated techno-economic model. They concluded that the cost benefits from energy saving can offset the increased capital cost, owing to the CO<sub>2</sub> avoided cost being the largest contributor to energy consumption (55–75 %) in these processes. With the implementation of process modifications, an overall energy reduction of 13.5 % in the MEA process and 20.2 % in the NH<sub>3</sub> process were achieved, decreasing the CO<sub>2</sub> avoided cost by 13.1 % and 20.9 %, respectively. It demonstrated that reducing energy consumption is the top priority in the advancement of PCC techno-economic performance. However, a case-by-case investigation for different process modifications is required to gain a detailed understanding of the trade-off between technical improvements and economic burden. In addition to the cost, each additional process modification increases the overall complexity of the process and therefore reduces its operability and possibly its reliability. Some process modifications may improve operability, such as RSS. This is due to the

additional degree of freedom they build into the process, providing the ability to cope with process instabilities; however, most modifications will reduce the energy consumption at the cost of increased complexity.

#### 4.2. Chemical enhancement method

The chemical enhancement method is the use of various types of chemical solvents to enhance the absorption rate and carbon capture efficiency. Chemicals added to a solvent in order to improve the reaction rates of the absorption are called promoters. The approach has the ability to exploit and merge the good features of each solvent in the mixture while minimizing their drawbacks. Thus, the effectiveness of the resulting blends may be much superior to that of the individual solvents.

##### 4.2.1. Types of promoters

In past decades, various types of promoters are explored to improve the performance of mass transfer CO<sub>2</sub> absorption using aqueous ammonia solutions. These are categorized into 5 major groups; organic promoter, inorganic promoter, enzymatic promoter, ionic liquid promoter, and mixed promoter. The vast majority of researchers have used organic promoters to improve the absorption of AAP. Nowadays, new inorganic promoters such as nanoparticles are investigated to increase kinetic limited aqueous ammonia solution.

Organic type promoters such as amine and amino acid salts were studied widely to improve the absorption rate of AAP. Table 5 presents the types of promoters and the relevant research in the enhancement rate of AAP. Amines are effective promoters for increasing reaction rates due to the wide availability of amines and the apparently limitless capacity to optimize a solvent and minimize regeneration costs by leveraging the various features and benefits of different amines. When choosing amine promoters, it is widely acknowledged that chemical properties such as rapid absorption rate and high CO<sub>2</sub> absorption capacity should be prioritized. Cyclic amine has been identified as a desirable class of absorbents because of their rapid kinetics toward CO<sub>2</sub> (Conway et al., 2013; Jackson, 2014). Among them, Piperazine (PZ) is the most extensively studied in AAP and often exhibits high capture capacity, faster reaction rates, stability, and thermal degradation (Freeman et al., 2010). Alstom (Gal et al., 2012) carried out experimental investigations of the chilled ammonia process and revealed that PZ can be employed as an effective rate booster of the process. In comparison to ammonia solutions without a promoter, the removal efficiency of CO<sub>2</sub> improved by 31–43 % when 0.45 M PZ was added at different CO<sub>2</sub> loadings. This CO<sub>2</sub> removal efficiency could be equivalent to the MEA (Yu et al., 2016b).

Another type of suitable organic promoters studied to enhance the rate of absorption in AAP is amino acid salts. They are inexpensive, safe for the environment, have high absorption rates, and lower vapor pressure (Feron and ten Asbroek, 2005). Although adding amino acid salts improved K<sub>G</sub>, the NH<sub>3</sub> vaporization raised dramatically (Yang et al., 2013; Yang et al., 2014b).

##### 4.2.2. Thermodynamics and kinetics properties of promoted aqueous ammonia

Understanding the thermodynamics and kinetic properties and the capability to simulate the system behavior is essential for developing, designing, and optimizing the process. The selection of an improper thermodynamic model will result in substantial convergence difficulty and erroneous numerical simulations (Edwards et al., 1975). An effective thermodynamic model is obligatory to characterize the phase equilibria, estimate the CO<sub>2</sub> partial pressure and thermodynamic datasets, including fugacity, Gibbs free energy ( $\Delta G$ ), enthalpy ( $\Delta H$ ), entropy ( $\Delta S$ ), and volume. The most commonly applied thermodynamic models for chemical absorption used in literature are outlined in Koronaki et al. (2015).

On the other hand, in a complicated promoted aqueous ammonia

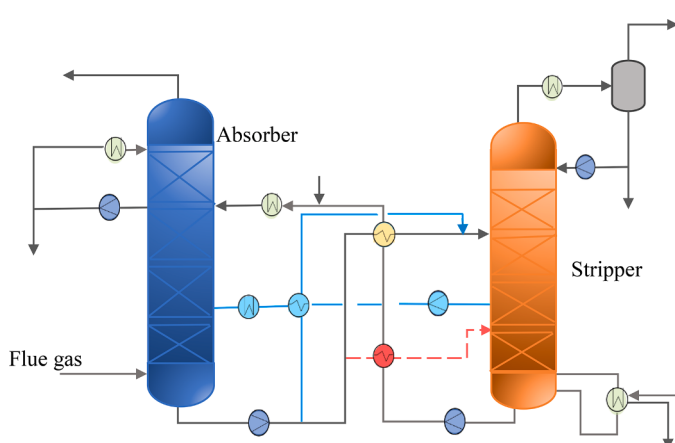


**Fig. 7.** Flow diagram of conventional split-flow process (SFA) modification (Le Moulléc et al., 2014).

**Table 5**Summarized studies of promoted aqueous ammonia for CO<sub>2</sub> capture and their operating condition.

Author	Promoter	Group	Reactor	Experimental conditions	Key finding	Challenge
You et al. (2008)	2-amino-2-methyl-1-propanol (AMP) 2-amino-2-ethyl-1,3-propandiol (AEPD) 2-amino-2-methyl-1,3-propandiol (AMPD) Tri(hydroxymethyl) aminomethane (THAM)	Organic	Bubbling Reactor	NH <sub>3</sub> conc. = 10 % Promoter conc. = 1 % T = 298 K	CO <sub>2</sub> removal capacities: NH <sub>3</sub> < (NH <sub>3</sub> + AMPD) < (NH <sub>3</sub> + AEPD) < (NH <sub>3</sub> + AMP) < (NH <sub>3</sub> + THAM)	Low CO <sub>2</sub> absorption rate enhancement
Rowland et al. (2011)	Piperazine (PZ) Glycine Boric acid	Organic Inorganic base	WWC	NH <sub>3</sub> conc. = 3 M PZ conc. = 0.5 M NH <sub>3</sub> conc. = 3.35 M Glycine conc. = 0.5 M NH <sub>3</sub> conc. = 3 M Boric acid conc. = 0.5 M For all experiment; Loading <sub>CO<sub>2</sub></sub> = 0 – 2.8 mol T = 288 K	Increased CO <sub>2</sub> absorption rate at 0-0.8 loadings Increased CO <sub>2</sub> absorption rate at 0-0.45 loadings No increase in absorption rate	
Collett et al. (2011)	Bovine carbonic anhydrase (BCA)	Enzyme	CSTR Bubble column	NH <sub>3</sub> conc. = 4 M BCA conc. = 360 mg/L  NH <sub>3</sub> conc. = 2 M BCA conc. = 154 mg/L	Increased 21.1 % in the hydration rate of CO <sub>2</sub> as pH drops from 9.4 to 8.5. Increased 34.1 % in the hydration rate of CO <sub>2</sub> as pH drops from 9.6 to 8.6.	Operation under rigorously regulated conditions.
Yu et al. (2012b)	MEA PZ 1-methylpiperazine 4-aminopiperidine Sarcosine Taurine Glycine MEA PZ 1-methyl piperazine Sarcosinate Taurinate Glycinate	Organic	WWC	NH <sub>3</sub> conc. = 3 M Promoter conc. = 0.3 M T = 288 K	PZ, 1-methylpiperazine, and sarcosine have high K <sub>G</sub> with promotion factor more than 20 %.	NH <sub>3</sub> -promoter absorption interaction unclear.
Fang et al. (2015)		Organic	WWC	NH <sub>3</sub> conc. = 3 M Promoter conc. = 0.3 M T = 279–298 K	K <sub>G</sub> increased by three to fourfold with addition of PZ.	
Yang et al. (2014d)	Sarcosine Proline Taurine	Organic	WWC	NH <sub>3</sub> conc. = 3 M Promoter conc. = 0.3-3 M T = 288 K	NH <sub>3</sub> neutralized taurine is most suitable for increasing K <sub>G</sub> .	
Xu et al. (2015)	[EtOHMim][PF <sub>6</sub> ] [EtOHMim][BF <sub>4</sub> ] [EtOHMim]Cl [Choline][PF <sub>6</sub> ] [Choline][BF <sub>4</sub> ] [Choline]Cl	Ionic liquids	Bubble reactor	NH <sub>3</sub> conc.=2 M Promoter conc.= 0.2 M	Anions improved CO <sub>2</sub> removal: [PF <sub>6</sub> ] <sup>-</sup> > [BF <sub>4</sub> ] <sup>-</sup> > [Cl] <sup>-</sup>	Limited mass transfer
Xu et al. (2019)	PZ	Organic	Spray tower	NH <sub>3</sub> conc. = 5 wt.% PZ conc. = 0.1 M CO <sub>2</sub> conc. = 15 vol% GFR= 1.25–2.5 L/s LFR = 0.025–0.05 L/s T = 293 K	K <sub>Gav</sub> increase as the 0.497, 0.355 and 0.397 powers of the NH <sub>3</sub> Conc., the PZ conc., and the liquid flow rate.	Ammonia loss increases.
Zhang et al. (2020)	Fe <sub>3</sub> O <sub>4</sub>	Inorganic	Bubbling reactor	NH <sub>3</sub> conc. = 2–5 wt.% Nanoparticle loading= 0–0.5 g/L CO <sub>2</sub> conc. =9.2–20.1 % GFR = 0.025–0.05 L/s	K <sub>Gav</sub> = 5.6 × 10 <sup>-5</sup> mol/m <sup>3</sup> s Pa Increased by 14.5 % compared to without nanoparticles.	Nanoparticle's precipitation increases with nanoparticle loading.
Al-Sudani (2020)	MEA + PZ MEA + potassium arginat(ArgK) PZ + ArgK	Mixed promoters of amine and amino acid	Packed column	MEA+ PZ=0.3M + 0.1,0.5,0.7M) MEA + ArgK = 0.3M + (0.1,0.5,0.7M) PZ+ArgK= 0.3M+ (0.1,0.5,0.7M) For all, NH <sub>3</sub> conc. = 8 wt.% LFR = 0.00416–0.01416 L/s, GFR = 0.0833–0.25 L/s, T = 298	MEA+ ArgK promoter was performed 123.23 % higher than the other two mixed promoters The absorption rate rises with initial partial pressure and liquid flow rate.	
Rashidi et al. (2022)	Glycerol	Organic	Microchannel	NH <sub>3</sub> conc.= 4 – 10 wt.% Glycerol conc. = 1–3 wt.% LFR=0.05–0.15 ml/s CO <sub>2</sub> conc. = 10 vol% T = 293–313 K	K <sub>Gav</sub> = 49.4 kmol/m <sup>3</sup> h kPa. K <sub>Gav</sub> increased by 4.8 % with 2–3 wt.% glycerol.	

$\text{CO}_2$  absorption, a detailed reaction mechanism is required owing to the existence of several intermediates that might or might not participate in the reaction. The absorption process includes several reversible interactions and protonation equilibrium. Some species connected by protonation including carbonate, amine, and carbamate. A primary goal of reaction mechanism research includes the determination of basic chemical reaction pathways, model validating, and resulting reaction rate constant for individual species from the evaluation of fast stopped-flow records.

A wetted-wall column (WWC) is a commonly used technique by scholars to quantify the equilibrium constant or  $\text{CO}_2$  absorption rate. The  $K_G$ , derived from the rate of reaction, is a significant indicator of the effectiveness of a possible promoter for enhancing AAP. As a result, the  $\text{CO}_2$  absorption rate of both promoted and unpromoted ammonia solutions will be evaluated using the  $K_G$  recordings from the WWC. As the effect of promoter addition on the  $K_G$  processes is a crucial criterion, basic knowledge of the kinetic reactions that take place in the solution is also equally important. The stopped-flow is a powerful experimental method used to examine the chemical reaction mechanisms of the liquid phase of promoted ammonia solution with  $\text{CO}_2$  in milliseconds. This certainly helps to understand the experimental findings of the WWC.

The thermodynamic and kinetic properties of the absorption process using PZ as a promoter in ammonia solution are examined by Li et al. (2015c), Li et al. (2013), and Liu et al. (2012b). These investigations proved that the addition of a small quantity of PZ could remarkably promote the absorption process. The promotion may be attributed to two reasons (Rowland et al., 2011). The first reason is due to the higher reaction rate of PZ, and the second one is that  $\text{NH}_3$  has more proton acceptor, which helps to buffer the absorption of PZ. Liu et al. (2012a) used a reaction calorimetry to measure the absorption heats, and results revealed that applying little quantity of PZ seemed to have minimal influence on the heat of absorption of  $\text{CO}_2$  and little impact on  $\text{NH}_3$  escape (Liu et al., 2011a). In general, the experimental kinetics and equilibrium studies about promoted  $\text{NH}_3$  solution for  $\text{CO}_2$  absorption are summarized in Table 6.

#### 4.2.3. Simulation and modelling of promoted aqueous ammonia

It is essential that a comprehensive understanding of the entire behavior of blended  $\text{NH}_3$ /promoter solvent for  $\text{CO}_2$  capture be attained to make possible the future commercial use of the solvent. A rigorous evaluation is needed to successfully determine a system's fundamental properties, including; phase equilibria, equilibrium constant and its kinetic properties such as mass transfer, heat transfer, energy balance, and reaction pathways.

Some simulation studies have been conducted on  $\text{CO}_2$  absorption using PZ-promoted ammonia solution. Yu et al. (2016b) conducted a lab-scale study of  $\text{NH}_3$ /PZ-based  $\text{CO}_2$  absorption in a packed column, and experimental data is used to validate a simulation result. When 5 wt.% PZ applied to a 5 wt.%  $\text{NH}_3\text{H}_2\text{O}$  at loading <sub>$\text{CO}_2$</sub>  of 0.2 mol $\text{CO}_2$ /mol $\text{NH}_3$ , a removal efficiency of  $\text{CO}_2$  that is equivalent to MEA (30 wt.%, loading <sub>$\text{CO}_2$</sub>  of 0.2 mol $\text{CO}_2$ /molMEA) solution was obtained. Lu et al. (2017) uses a rate-based model to simulate the  $\text{NH}_3$ -PZ- $\text{CO}_2$ - $\text{H}_2\text{O}$  system and evaluated the results against a variety of experimental date. They demonstrated that the presence of PZ may significantly speed up the absorption rate of AAP, hence reducing the absorber size and reach high  $\text{CO}_2$  removal efficiency. Due to PZ's high heat absorption, the temperature all the way down the column is high, which is favored for the reaction kinetics. In the reactions that took place throughout the packed absorber, the interaction between  $\text{NH}_3$  carbamate and PZ carbamate in the upper part of the absorption column causes extra free ammonia into the solution.

To further optimize the process, Jiang et al. (2018) incorporated RSS and advanced stripper configuration with the solvent recovery system. They analyzed the significant parameters, such as promoter concentration, pressure, and  $\text{CO}_2$  lean loading. The addition 0.25 mol of PZ per

kilogram of  $\text{H}_2\text{O}$  into the  $\text{NH}_3$  solution showed a reduction of packing height by 35 % when compared to which did not include PZ. Xu et al. (2021) used a sophisticated computational fluid dynamics program incorporated with the solvent characteristics to simulate the removal of  $\text{CO}_2$  using PZ based promoted aqueous ammonia in a spray column. The hydrodynamics characteristics, absorbent temperature, and reactive species concentration on mass transfer performance are investigated. The upward spraying showed higher removal efficiency of  $\text{CO}_2$  when the spray droplet volume fraction and residence time increased compared to downward spraying.

The characterizations of  $\text{CO}_2$  capture with promoted absorbents for industrial use, particularly AAP, are rare. The majority of studies are relevant exclusively to laboratory/bench-scale studies and simulations. Recently Zhao et al. (2021) demonstrated the feasibility of the blended aqueous absorbents of PZ and aqueous ammonia in 430 MW commercial power plant compared with other PZ-promoted amine solvents with specified 85 % carbon capture efficiency. This may to serve as a constructive reference and helpful benchmark for process development and optimization and evaluate the techno-economic performances of the industrial AAP.

#### 4.3. Combined enhancement method

The combined enhancement technique is the combination of using both physical/mechanical and chemical technologies to enhance the  $\text{CO}_2$  absorption performance. By leveraging the strengths of chemical promoters and physical modifications, the combined system maximizes efficiency, improves overall performance, and represents a promising approach for enhancing ammonia-based carbon capture processes. Some promoters are viscous and are challenging to manage efficiently in traditional packed column devices. New designs/intensification technologies must therefore be developed for these solvents. Nowadays, researchers are exploring the effect of combining potential promoters and intensification technology to enhance absorption rate performance of carbon capture (Kiani et al., 2022).

#### 4.4. summary on the enhancement technologies of ammonia-based carbon capture

Researchers investigate alternative physical, chemical and combined enhancement technologies to improve ammonia-based carbon capture, these findings can be directly applied to AAP technologies. Physical modification that includes mass transfer intensifying absorbers and modified configuration has been studied. These include microchannel, rotating packed bed, high-frequency ultrasonic-assisted reactor, and hollow fiber membrane, that can significantly enhance  $\text{CO}_2$  absorption in AAP. Microchannel offers the highest mass transfer coefficient and absorption efficiency (96 %), while RPB addresses equipment size challenges. Further research is needed to minimize energy consumption in RPB and explore the benefits of ultrasonic-assisted reactors and membrane contactors. Future studies should focus on experimental and modeling investigations of these technologies under different conditions, while addressing challenges like membrane wetting in contactors.

Extensive research has been conducted on physical process modifications to enhance the ammonia-based carbon capture process. These modifications aim to improve  $\text{CO}_2$  absorption and desorption rates while reducing energy consumption. Promising technologies include two-stage absorption columns, absorber intercooling, and split-flow configurations. The Lean Vapor Compression (LVC) configuration has shown the highest energy reduction, while combined configurations like split-flow and rich splitting offer significant energy savings. However, there are still underexplored modifications that require further investigation, such as split flow with overhead heat exchanger and heat-integrated stripper. Future research should focus on pilot plant-scale evaluations and comprehensive techno-economic analyses to identify efficient and cost-effective solutions for maximizing  $\text{CO}_2$  absorption and minimizing

**Table 6**

Thermodynamic and kinetic studies of promoted ammonia solution.

Author	System	Kinetics		Thermodynamic	
		Method	Reaction Mechanism	Model/Method	Parameters
Li et al. (2015c), Liu et al. (2012b)	PZ-NH <sub>3</sub> -CO <sub>2</sub> -H <sub>2</sub> O	WWC Stopped-flow spectrophotometry	'Ternary-termolecular' reaction mechanism PZ + H <sub>2</sub> O + CO <sub>2</sub> ↔ PZCOO <sup>-</sup> + H <sub>3</sub> O <sup>+</sup> (R1 <sub>PZ</sub> ) CO <sub>2</sub> + NH <sub>3</sub> + H <sub>2</sub> O + ↔ NH <sub>2</sub> COO <sup>-</sup> + H <sub>3</sub> O <sup>+</sup> (R2 <sub>PZ</sub> ) $r_{CO_2-NH_3}^T = (k_{NH_3}^T [NH_3] + k_{H_2O-NH_3}^T [H_2O] + k_{int-PZ}^T) [NH_3][CO_2]$ $r_{CO_2-PZ}^T = (k_PZ^T [PZ] + k_{H_2O-PZ}^T [H_2O] + k_{int-NH_3}^T) [PZ][CO_2]$ Interaction effect, $r_{CO_2-NH_3/PZ}^T = r_{CO_2-NH_3}^T + r_{CO_2-PZ}^T + r_{CO_2-int}^T$ kinetic constants $k_i = a_i \exp(-b_i/T)$ $k_{2-NH_3} [m^3/kmol/s] = a_1 = 1.541 \times 10^8, b_1 = 3535$ $k_{2-PZ} [m^3/kmol/s] = a_2 = 1.1201 \times 10^{12}, b_2 = 5318$ $k_{int} [m^6/kmol^2/s] = a_3 = 5.946 \times 10^{11}, b_3 = 4926$ PZCO <sub>2</sub> <sup>-2</sup> /PZCO <sub>2</sub> H has essential function in the promoting process.	Modified Stokes-Einstein	- Diffusion coefficient of CO <sub>2</sub> - Correlations for densities and viscosities - Solubility of CO <sub>2</sub> - Henry constant
Li et al. (2013)	PZ-NH <sub>3</sub> -CO <sub>2</sub> -H <sub>2</sub> O	WWC	Zwitterion mechanism is rate determining CO <sub>2</sub> + NH <sub>3</sub> ↔ NH <sub>3</sub> <sup>+</sup> COO <sup>-</sup> (R <sub>Pz1</sub> ) NH <sub>3</sub> <sup>+</sup> COO <sup>-</sup> + NH <sub>3</sub> ↔ NH <sub>3</sub> <sup>+</sup> + NH <sub>2</sub> COO <sup>-</sup> (R <sub>Pz2</sub> ) PZ + CO <sub>2</sub> ↔ PZH <sup>+</sup> COO <sup>-</sup> (R <sub>Pz3</sub> ) PZ <sup>+</sup> COO <sup>-</sup> + CO <sub>2</sub> ↔ PZH <sup>+</sup> (COO <sup>-</sup> ) <sub>2</sub> (R <sub>Pz4</sub> ) $k_{2,NH_3} = 1.1451 \times 10^9 \exp\left(\frac{-34193}{RT}\right)$ $k_{PZ} = 1631 \times 10^8 \exp\left(\frac{-20139}{RT}\right)$	ENRTL Stokes-Einstein	- Speciation distribution - NH <sub>3</sub> partial pressure - Diffusion constant for CO <sub>2</sub> - Viscosities - Diffusivity in liquid phase - Viscosity in liquid phase
Jeon et al. (2013)	Hydroxyl group-NH <sub>3</sub> -CO <sub>2</sub> -H <sub>2</sub> O ↓ Ethylene glycol Glycerol 2-amino-2-methyl-1-propanol (AMP)	Stirred-cell reactor	Zwitterion mechanism CO <sub>2</sub> + RNH <sub>2</sub> ↔ RNH <sub>2</sub> <sup>+</sup> COO <sup>-</sup> (R1 <sub>H</sub> ) RNH <sub>2</sub> <sup>+</sup> COO <sup>-</sup> + B ↔ RNHC <sub>OO</sub> <sup>-</sup> + B H <sup>+</sup> (R2 <sub>H</sub> ) Deprotonation reaction RNH <sub>2</sub> + RNH <sub>2</sub> <sup>+</sup> COO <sup>-</sup> ↔ RNH <sub>3</sub> <sup>+</sup> + RNHC <sub>OO</sub> <sup>-</sup> (R3 <sub>H</sub> ) H <sub>2</sub> O + RNH <sub>2</sub> <sup>+</sup> COO <sup>-</sup> ↔ H <sub>3</sub> O <sup>+</sup> + RNHC <sub>OO</sub> <sup>-</sup> (R4 <sub>H</sub> ) OH <sup>-</sup> + RNH <sub>2</sub> <sup>+</sup> COO <sup>-</sup> ↔ H <sub>2</sub> O + RNHC <sub>OO</sub> <sup>-</sup> (R5 <sub>H</sub> ) The reaction rate constants: $k_{2,NH_3/AMP} = 4.565 \times 10^5 \exp(-1396.5/T)$ $k_{2,NH_3/ethy.gly} = 1.499 \times 10^6 \exp(-1978.7/T)$ $k_{2,NH_3/gly.} = 7.078 \times 10^6 \exp(-2413.3/T)$		
Xiang et al. (2013) and Yang et al. (2014b)	SAR <sup>-</sup> -NH <sub>3</sub> -CO <sub>2</sub> -H <sub>2</sub> O	WWC Stopped-flow spectrophotometers	Chemical equilibrium Debye-Hückel	- Species distribution - Activity coefficients	
Yu et al. (2018)	TAU <sup>-</sup> -NH <sub>3</sub> -CO <sub>2</sub> -H <sub>2</sub> O	Stopped-flow spectrophotometry	Van't Hof	- Equilibrium constant	
Li et al. (2019)	4-AMTHP-NH <sub>3</sub> -CO <sub>2</sub> -H <sub>2</sub> O	WWC Stopped-flow spectrophotometry	Debye-Hückel	- Activity coefficients	

The experimentally measured and calculated kinetic data successfully agreed.

energy consumption in ammonia-based carbon capture.

Chemical promoters are highly effective solvents that greatly enhance CO<sub>2</sub> absorption in aqueous ammonia for ammonia-based carbon capture processes. Cyclic amines like piperazine exhibit significant improvements, and amino acids also show promise as enhancers in AAP. However, a common drawback of many promoters is increased ammonia loss. Further research is necessary to explore alternative promoters and gather more data on their properties. Additionally, it is crucial to develop technologies that can simultaneously control ammonia loss. Combining chemical promoters and physical process modifications in ammonia-based carbon capture systems might enhances CO<sub>2</sub> capture rates, reduces ammonia loss, and offers flexibility.

## 5. Simultaneous multi-pollutant (CO<sub>2</sub>, NO<sub>x</sub>, SO<sub>x</sub>) capture using aqueous ammonia

### 5.1. Process description

The typical post-combustion exhaust gas contains 10–20 % (by volume) of CO<sub>2</sub>, approximately 0.05–0.5 % sulfur oxide (SO<sub>x</sub>) and nitric oxide (NO<sub>x</sub>), and 10–9 g/m<sup>3</sup> mercury (Zhao et al., 2012). The gas pollutants NO<sub>x</sub>, SO<sub>x</sub>, and other pollutants adversely affect the CO<sub>2</sub> capture process using amine solvents. For example, the reaction of SO<sub>2</sub> with amine form undesired irreversible compounds, decreasing the capacity of the solvent; the interaction of NO<sub>x</sub> with amine causes the formation of carcinogenic nitrosamine and nitramine, which are environmental hazards (Dai and Mitch, 2014). A number of distinct procedures, such as selective catalytic reduction (SCR) remove NO<sub>x</sub>, flue gas desulfurization (FGD) technology for SO<sub>x</sub> treatment, and carbon capture technologies (CCS) for CO<sub>2</sub> Capture are used in a traditional way to reduce the emission of gaseous pollutants from the power plant. An enormous financial outlay is required for each part of the treatment process. The use NH<sub>3</sub>-based technique is capable of overcoming the difficulties that most amine absorbents face because of its high chemical stability. Notably, the NH<sub>3</sub> scrubbing process is used to simultaneously treat NO<sub>x</sub> and SO<sub>x</sub> gases and form useful byproducts that can be employed as agriculture fertilizers and have economic support.

Many articles have analyzed the feasibility and process development of ammonia-based simultaneous capture of multiple gas emissions (CO<sub>2</sub>, SO<sub>x</sub>, and NO<sub>x</sub>) targeted at minimizing the economic penalty (Choi et al., 2009; Ciferno and Dipietro, 2005; Resnik et al., 2004). US Department of Energy (Ciferno and Dipietro, 2005) revealed several pollutants (CO<sub>2</sub>, SO<sub>2</sub>, NO<sub>x</sub>, and Hg) could be removed simultaneously in an effective way using ammonia scrubbing and reduce capital expenditure by 14 % compared to capturing each pollutant separately. According to Li et al. (2016c), the integration of the pretreatment of SO<sub>2</sub> and CO<sub>2</sub> capture method with ammonia scrubbing system can reduce the capital expenditure by 13.1 % in a 650 MW power plant. A novel aqueous NH<sub>3</sub>-based capture process was also presented by Qi et al. (2013), which can treat CO<sub>2</sub> and SO<sub>2</sub> in a single absorber and lower overall costs by 17.4 % compared to the cost of a separate gas capturing system. Powerspan Corp (McLarnon and Duncan, 2009) developed the ECO<sub>2</sub> process coupled with the Electrocatalytic oxidation (ECO) air pollutant-removing technology. ECO<sub>2</sub> is a technology that utilizes aqueous ammonia bicarbonate to remove CO<sub>2</sub>, while ECO removes multi-pollutants (NO<sub>x</sub>, SO<sub>2</sub>, Hg) from flue gases. Yu et al. (2011), Yu et al. (2013a) ammonia-based air-pollutant capture in a real coal-fired power station and revealed the effects of ammonia flow rate and CO<sub>2</sub> loading on the removal efficiency of CO<sub>2</sub> and ammonia slip.

The features and effect of different operational parameters on the aqueous NH<sub>3</sub>-based simultaneous multiple gas pollutants absorption mechanism have been investigated. Qiu et al. (2011) conducted a small-scale test in a packed column to assess the feasibility of a simultaneous CO<sub>2</sub>/SO<sub>2</sub> removal process using aqueous ammonia. They revealed that high ammonia concentration is advantageous for the simultaneous absorption of CO<sub>2</sub> and SO<sub>2</sub>. It contributes more favorably

and speeds up the carbamate formation reaction, increasing the CO<sub>2</sub> mass transfer coefficient. Li et al. (2014a) used bubble column utilizing Ammonium sulfite solvent to study the SO<sub>2</sub> absorption under varied circumstances in a simultaneous capture system. The removal efficiency of SO<sub>2</sub> increased from 60 to 96 %. Qi et al. (2012) demonstrated that the value of K<sub>G</sub> can be dropped by 50 % when the concentration of SO<sub>2</sub> rises, and the SO<sub>2</sub> loading also has a detrimental effect. When the concentration of SO<sub>2</sub> increases from 0 to 0.4 % in NH<sub>3</sub> solvent of 0.581 M, it causes increase in the liquid phase resistance, hence k<sub>L</sub>(mol/Pa/cm<sup>2</sup>/s) declines from 0.44 to 0.22 (Qi et al., 2015b). This implies that the SO<sub>2</sub> absorption into NH<sub>3</sub> creates a competitive environment with CO<sub>2</sub> and restricts the CO<sub>2</sub> mass transfer in the liquid phase. Moreover, as the SO<sub>2</sub> loading rose, it excreted a higher equilibrium partial pressure of CO<sub>2</sub> in the system, resulting in a decrease in the amount of CO<sub>2</sub> that could be absorbed (Qi et al., 2015a). However, as the temperature increases, the liquid phase mass transfer resistance decreases (Qi et al., 2015b). This happens because of higher activation energy at higher temperature accelerates the rate-determining step of carbamate formation.

### 5.2. Modelling of the simultaneous multi-pollutant capture process

In literature, modelling studies on the multiple pollutant (CO<sub>2</sub>, SO<sub>2</sub>, NO<sub>2</sub>) simultaneous capture using an aqueous ammonia process were also reported. Asif and Kim (2014) modelled the combined SO<sub>2</sub>/ CO<sub>2</sub> removal process and investigated the operational parameters to optimize the process. They revealed that the SO<sub>2</sub> capture efficiency could reach 53–90 % at high level of concentration (~9000 ppm) and CO<sub>2</sub> capture efficiency of ≥90 %. Yu and Wang (2015) adopted a rate-based model of a novel ammonia-based CO<sub>2</sub>/SO<sub>2</sub> capture process in Aspen Plus. Their novel method includes multi-functions, including SO<sub>2</sub> pretreatment, CO<sub>2</sub> absorption, NH<sub>3</sub> abatement, CO<sub>2</sub> regeneration, and product purity, that could reduce the overall energy consumption by ~32 %. Li et al. (2015b) simulated the technical performance of SO<sub>2</sub> removal and ammonia recycling integrated with the AAP process using a Pitzer thermodynamic model in aspen plus. This process absorbs SO<sub>2</sub> and CO<sub>2</sub> from flue gas more than 99.5 % and 85 %, respectively. In addition, the rate of CO<sub>2</sub> absorption could be improved by either raising ammonia concentration (Jiang et al., 2017) or adding a promoter such as PZ (Jiang et al., 2018; Lu et al., 2017) that consequently decreases the column height and its associated capital costs.

Qi and Wang (2017b) developed an e-NRTL thermodynamic model of the NH<sub>3</sub>-CO<sub>2</sub>-SO<sub>2</sub>-K<sub>2</sub>SO<sub>4</sub>-H<sub>2</sub>O process in Aspen Plus that could successfully evaluate the CO<sub>2</sub> absorption heat, SO<sub>2</sub> removal, and phase equilibria of the system. The simulation analyzes the primary difficulties of high initial investment of the removal of SO<sub>2</sub>, the presence of remaining SO<sub>2</sub> leaving to the absorption column, and the challenges of coordinating the operations of the SO<sub>2</sub> absorption and the CO<sub>2</sub> capture process in an integrated system. In their later work Qi and Wang (2017a) proposed a new multiple air pollutant removal process that both CO<sub>2</sub>/SO<sub>2</sub> simultaneously absorbed by a lean ammonia solution in the packing column. The CO<sub>2</sub>-rich solvent is heated to regenerate the solvent in a stripper and release the captured CO<sub>2</sub>. The SO<sub>2</sub> in the aqueous ammonia solution may undergo forced oxidation flushing and then precipitate by mixing with potassium hydroxide to form potassium sulfate (K<sub>2</sub>SO<sub>4</sub>) (Qi and Wang, 2017b).

Recently, Jiang et al. (2020a) designed a system that integrates a supercritical power plant with the process of removing NO<sub>x</sub>/SO<sub>x</sub>/CO<sub>2</sub> simultaneously using the NH<sub>3</sub>-based capture technology (see Fig. 8) The capital cost estimation analysis showed that it is a cost-effective design, showing 20–30 % reduction in capital investments comparing to the conventional MEA absorption process integrated with traditional flue gas desulfurization and denitrification technologies. By exploring novel process designs and concepts that can improve the efficiency, selectivity, and economic viability of simultaneous pollutant capture using aqueous ammonia. Consider innovative approaches such as advanced solvent regeneration techniques, hybrid systems, or alternative promoters,

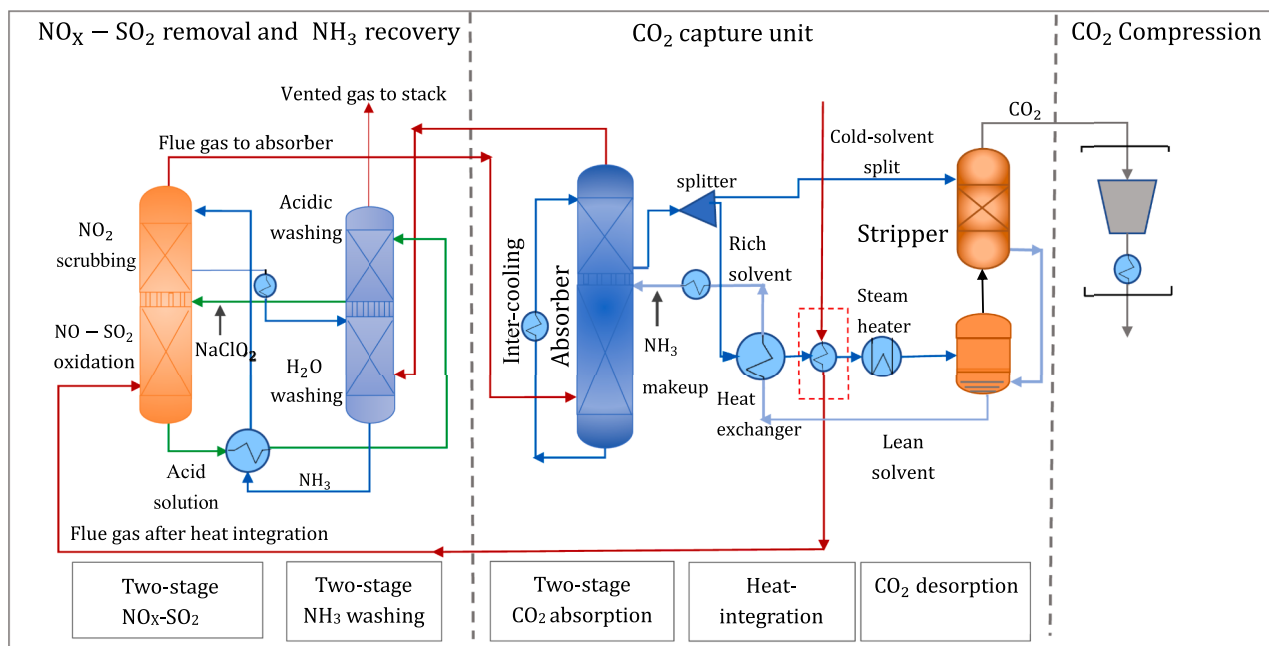


**Fig. 8.** Simultaneous  $\text{NO}_x/\text{SO}_2/\text{CO}_2$  removal using aqueous ammonia scrubbing. Reprinted with permission from (Jiang et al., 2020a).

leading to more effective and sustainable solutions for air pollution control.

In their subsequent work, Jiang et al. (2020b) investigated important factors, including temperature, ammonia concentration, and  $\text{NO}_x/\text{SO}_2$  concentrations, to optimize the process. The increase in  $\text{NH}_3$  concentration and low absorption temperature are suggested to reduce the height of the column. Besides, using the two-stage integrated with the intercooling process improved the  $\text{CO}_2$  absorption performance, which resulted in reduced column height. Compared with the reference  $\text{NH}_3$  process, the absorber size was reduced by 6.5 %. In summary, the technological and economic adaptability of this ammonia-based simultaneous multi-pollutant removal procedure to different concentrations of  $\text{NO}_x/\text{SO}_2$  in flue gas can make it applicable in different industries.

## 6. Conclusions and prospects

Ammonia is among the most cost-effective sorbent with high  $\text{CO}_2$  loading capacity for the  $\text{CO}_2$  separation. However, low  $\text{CO}_2$  absorption rates and limited  $\text{CO}_2$  mass transfer hinder its industrial application. Enhancement of  $\text{CO}_2$  absorption is one of the crucial aspects of  $\text{CO}_2$  capture technology in reducing operating and capital costs. A higher  $\text{CO}_2$  absorption rate increases the  $\text{CO}_2$  absorption efficiency, reduces chemical absorbent circulated throughout the process, and minimizes the size of the absorber column. In this paper, we have reviewed various mass transfer enhancement technologies and their development in AAP. Here are the main conclusions:

- The complex nature of the  $\text{CO}_2\text{-NH}_3\text{-H}_2\text{O}$  system, including vapor-liquid-solid equilibrium (VLSE) complexity, presents challenges in modeling and predicting system behavior. While progress has been made in studying thermodynamics and developing models, further research is required to validate and improve the accuracy of thermodynamic and kinetic predictions in AAP systems. Enhanced modeling techniques are needed to better capture the intricate behavior of the system and improve predictions of thermodynamic equilibrium and reaction kinetics.
- The determination of  $\text{CO}_2$  mass transfer coefficients in absorber columns has been extensively reviewed, considering various operating parameters. The mass transfer coefficient is influenced by factors such as ammonia and  $\text{CO}_2$  concentrations, gas and liquid

flowrates, and reaction temperature. Computational models have been used to predict mass transfer coefficients and validate experimental data, aiding in reactor design optimization and process efficiency improvement. However, there is a need for a widely accepted simulation model that incorporates thermodynamics, kinetics, and correlations for mass transfer coefficients. Further research should focus on scaling up the optimized parameters for larger-scale applications to enhance practical implementation and economic viability.

- The  $\text{CO}_2$  absorption rate performance can be remarkably enhanced using physical, chemical, and combined technologies. Some of the physical intensification technologies that have been developed for absorption process includes; microchannel, rotating packed bed, high-frequency ultrasonic-assisted reactor, and hollow fiber membrane. The studied volumetric mass transfer coefficient showed that they can significantly reduce the absorber volume and consequently enhance absorption performance of AAP compared to conventional packed column. Microchannel offers the highest overall volumetric mass transfer coefficient and  $\text{CO}_2$  absorption efficiency compared with other intensification absorbers. Alternatively, RPB demonstrated that can improve overall volumetric mass transfer coefficients and overcome the technical challenge of needing large equipment sizes in conventional absorbers. However, the energy consumption for this technology must be further minimized. The benefits of using HIUF over conventional absorbers with aqueous ammonia solvent have not been determined. As a promising technology, the membrane contactor has attracted considerable interest for  $\text{CO}_2$  capture, principally because it integrates the benefits of both liquid absorption (high selectivity) and membrane separation (modularity and compactness). Most research on membrane contactors  $\text{CO}_2$  capture is still conducted at the laboratory scale, because of the critical challenge from membrane wetting. Even slight wetting can significantly increase the mass transfer resistance, reducing  $\text{CO}_2$  absorption performance. For future research direction the experimental and modelling of these mass transfer intensifying absorbers at different operating properties and energy consumption should be considered.
- Various physical process modifications have been extensively studied to improve the ammonia-based carbon capture process. These modifications involve absorption enhancement, heat integration, heat pumps, and novel process configurations, aiming to enhance

$\text{CO}_2$  absorption and desorption rates while minimizing energy consumption. Technologies like two-stage absorption columns, absorber intercooling, and split-flow configurations have shown promise in improving  $\text{CO}_2$  absorption rate. The Lean Vapor Compression (LVC) configuration has demonstrated the highest energy reduction at 34.5 %, while combined configurations, such as split-flow and rich splitting, offer substantial energy savings. Process modification such as; LVR, RVR, LVC, RSS have been widely studied compared to some other modifications that are only done by single researchers (eg. vacuum integrated stripper, multi pressure desorber and split flow.) In conclusion, while significant progress has been made in optimizing the ammonia-based carbon capture process through physical process modifications, future research should focus on exploring underexplored modifications (eg. split flow with overhead heat exchanger, heat integrated stripper etc.), conducting pilot plant-scale evaluations, and performing comprehensive techno-economic analyses to identify efficient and cost-effective solutions for maximizing  $\text{CO}_2$  absorption and minimizing energy consumption.

- Efficient solvents, known as promoters, can enhance the absorption rate of  $\text{CO}_2$  in aqueous ammonia solutions. These promoters can be classified into five major categories: organic, inorganic, enzymatic, ionic liquids, and mixed promoters. Among them, cyclic amines like piperazine have shown the highest improvement in  $\text{CO}_2$  mass transfer of AAP. However, the use of piperazine can result in ammonia loss which is a drawback to consider. While some studies have explored the simulation and modeling of piperazine with aqueous ammonia, further efforts are needed to investigate other blended solvents. Limited data on vapor-liquid equilibrium, thermodynamic properties, and physical properties have constrained the modeling of these blended solvents. This presents an opportunity for future research to investigate and develop efficient solvent blends that can enhance the absorption rate of  $\text{CO}_2$  in aqueous ammonia. Additionally, it is crucial to consider technologies that control ammonia loss in conjunction with the use of promoters for effective ammonia-based carbon capture.
- Studies incorporating multi-functions, such as  $\text{SO}_2$  pretreatment,  $\text{CO}_2$  absorption,  $\text{NH}_3$  abatement,  $\text{CO}_2$  regeneration, and product purity, have shown potential for reducing overall energy consumption by approximately 32 %. The technical performance of  $\text{SO}_2$  removal and ammonia recycling integrated with the AAP process has demonstrated high removal efficiencies of over 99.5 % for  $\text{SO}_2$  and 85 % for  $\text{CO}_2$ . Further investigate and optimize the operational parameters such as ammonia concentration, temperature, gas loading, and promoter effect will provide more accurate data and insights into the performance and scale up of the aqueous ammonia processes. This will help to maximize pollutant capture efficiency while minimizing energy consumption and operational costs using aqueous ammonia.
- Implementing a combined system that incorporates both chemical promoters and physical process modifications in ammonia-based carbon capture can be advantageous compared to using either approach individually. The synergistic effects of the combined system enhance  $\text{CO}_2$  capture rates, mitigate ammonia loss, and provide flexibility in adapting to different operating conditions. However, it is important to consider the challenges and limitations associated with compatibility, process complexity, cost, system performance, and scale-up. These limitations should be addressed in future studies to further optimize and validate the efficacy of the combined approach in ammonia-based carbon capture systems.
- Finally, Future studies and research efforts should focus on further optimizing the interconnection between chemical and physical enhancement technologies in ammonia-based multi-pollutant absorption systems. This includes investigating the compatibility of different chemical promoters, exploring novel additives or promoters for specific pollutants, and optimizing the system design and

integration to achieve optimal performance and make the technologies more competitive.

## CRediT authorship contribution statement

**Marta Sibhat:** Writing – original draft, Methodology, Formal analysis, Conceptualization. **Qiuxia Zhu:** Writing – review & editing, Visualization, Software, Data curation. **Gedion Tsegay:** Writing – review & editing, Data curation. **Guodong Yao:** Writing – review & editing, Methodology. **Guodong Yin:** Writing – review & editing, Supervision. **Yangyuan Zhou:** Writing – review & editing, Supervision, Conceptualization. **Jianfu Zhao:** Writing – review & editing, Supervision, Methodology, Funding acquisition, Conceptualization.

## Declaration of competing interest

The authors declare that they have no known competing financial interests or personal relationships that could have appeared to influence the work reported in this paper.

## Data availability

Date is available in different published articles searched and analyzed from web of science, google scholar, (public domain resources) etc.

## Acknowledgements

The authors acknowledge the financial support of the National Key Research and Development Project of China (2018YFC1902103).

## References

- aiAbrams, D.S., Prausnitz, J.M., 1975. Statistical thermodynamics of liquid mixtures: a new expression for the excess Gibbs energy of partly or completely miscible systems. *AIChE J.* 21 (1), 116–128. <https://doi.org/10.1002/aic.690210115>.
- Afkhamipour, M., Mofarahi, M., 2017. Review on the mass transfer performance of  $\text{CO}_2$  absorption by amine-based solvents in low-and high-pressure absorption packed columns. *RSC Adv.* 7 (29), 17857–17872. <https://doi.org/10.1039/C7RA01352C>.
- Aghel, B., Janati, S., Wongwises, S., Shadloo, M.S., 2022. Review on  $\text{CO}_2$  capture by blended amine solutions. *Int. J. Greenh. Gas Control* 119, 103715. <https://doi.org/10.1016/j.ijggc.2022.103715>.
- Ahn, C.K., Lee, H.W., Chang, Y.S., Han, K., Kim, J.Y., Rhee, C.H., et al., 2011. Characterization of ammonia-based  $\text{CO}_2$  capture process using ion speciation. *Int. J. Greenh. Gas Control* 5 (6), 1606–1613. <https://doi.org/10.1016/j.ijggc.2011.09.007>.
- Al-Sudani, F.T., 2020. Absorption of carbon dioxide into aqueous ammonia solution using blended promoters (MEA, MEA+PZ, PZ+ArgK, MEA+ArgK). *Eng. Technol. J.* 38 (9), 1359–1372. <https://doi.org/10.30684/etj.v38i9A.876>.
- Alie, C., Backham, L., Croiset, E., Douglas, P.L., 2005. Simulation of  $\text{CO}_2$  capture using MEA scrubbing: a flowsheet decomposition method. *Energy Convers. Manage.* 46 (3), 475–487. <https://doi.org/10.1016/j.enconman.2004.03.003>.
- Andrew, S., 1954. A rapid method of measuring absorption rates and its application to  $\text{CO}_2$  absorption into partially carbonated ammonia liquor. *Chem. Eng. Sci.* 3 (6), 279–286. [https://doi.org/10.1016/0009-2509\(54\)80009-1](https://doi.org/10.1016/0009-2509(54)80009-1).
- Aroonwilas, A., Veawab, A., 2007. Integration of  $\text{CO}_2$  capture unit using single-and blended-amines into supercritical coal-fired power plants: implications for emission and energy management. *Int. J. Greenh. Gas Control* 1 (2), 143–150. [https://doi.org/10.1016/S1750-5836\(07\)00011-4](https://doi.org/10.1016/S1750-5836(07)00011-4).
- Asgarifard, P., Rahimi, M., Tafreshi, N., 2021. Response surface modelling of  $\text{CO}_2$  capture by ammonia aqueous solution in a microchannel. *Can. J. Chem. Eng.* 99 (2), 601–612. <https://doi.org/10.1002/cje.23881>.
- Asif, M., Kim, W.S., 2014. Modeling and simulation of the combined removal of  $\text{SO}_2$  and  $\text{CO}_2$  by aqueous ammonia. *Greenh. Gas.: Sci. Technol.* 4 (4), 509–527. <https://doi.org/10.1002/ghg.1420>.
- Bai, H., Yeh, A.C., 1997. Removal of  $\text{CO}_2$  greenhouse gas by ammonia scrubbing. *Ind. Eng. Chem. Res.* 36 (6), 2490–2493. <https://doi.org/10.1021/ie960748j>.
- Bernardis, M., Carvoli, G., Delogu, P., 1989a.  $\text{NH}_3$ ,  $\text{CO}_2$ ,  $\text{H}_2\text{O}$  VLE calculation using an extended UNIQUAC equation. *AIChE J.* 35 (2), 314–317. <https://doi.org/10.1002/aic.690350217>.
- Bernardis, M., Carvoli, G., Santini, M., 1989b. Urea- $\text{NH}_3$ - $\text{CO}_2$ - $\text{H}_2\text{O}$ : VLE calculations using an extended UNIQUAC equation. *Fluid Phase Equilib.* 53, 207–218. [https://doi.org/10.1016/0378-3812\(89\)80088-3](https://doi.org/10.1016/0378-3812(89)80088-3).
- Borhani, T.N., Wang, M., 2019. Role of solvents in  $\text{CO}_2$  capture processes: the review of selection and design methods. *Renew. Sustain. Energy Rev.* 114, 109299.

- Borhani, T.N.G., Azarpour, A., Akbari, V., Alwi, S.R.W., Manan, Z.A., 2015. CO<sub>2</sub> capture with potassium carbonate solutions: a state-of-the-art review. *Int. J. Greenh. Gas control* 41, 142–162. <https://doi.org/10.1016/j.ijggc.2015.06.026>.
- Budzianowski, W., Kozioł, A., 2005. Stripping of ammonia from aqueous solutions in the presence of carbon dioxide: effect of negative enhancement of mass transfer. *Chem. Eng. Res. Des.* 83 (2), 196–204. <https://doi.org/10.1205/cherd.03289>.
- Caplow, M., 1968. Kinetics of carbamate formation and breakdown. *J. Am. Chem. Soc.* 90 (24), 6795–6803. <https://doi.org/10.1021/ja01026a041>.
- Chabanon, E., Bouallou, C., Remigy, J.-C., Lasseguette, E., Medina, Y., Favre, E., et al., 2011a. Study of an innovative gas-liquid contactor for CO<sub>2</sub> absorption. *Energy Proc.* 4, 1769–1776. <https://doi.org/10.1016/j.egypro.2011.02.052>.
- Chabanon, E., Roizard, D., Favre, E., 2011b. Membrane contactors for postcombustion carbon dioxide capture: a comparative study of wetting resistance on long time scales. *Ind. Eng. Chem. Res.* 50 (13), 8237–8244. <https://doi.org/10.1021/ie200704h>.
- Chen, C.C., Evans, L.B., 1986. A local composition model for the excess Gibbs energy of aqueous electrolyte systems. *AIChE J.* 32 (3), 444–454. <https://doi.org/10.1002/aic.690320311>.
- Chen, H., Dou, B., Song, Y., Xu, Y., Wang, X., Zhang, Y., et al., 2012. Studies on absorption and regeneration for CO<sub>2</sub> capture by aqueous ammonia. *Int. J. Greenh. Gas Control* 6, 171–178. <https://doi.org/10.1016/j.ijggc.2011.11.017>.
- Choi, W.-J., Min, B.-M., Shon, B.-H., Seo, J.-B., Oh, K.-J., 2009. Characteristics of absorption/regeneration of CO<sub>2</sub>-SO<sub>2</sub> binary systems into aqueous AMP+ ammonia solutions. *J. Ind. Eng. Chem.* 15 (5), 635–640. <https://doi.org/10.1016/j.jiec.2009.09.034>.
- Chu, F., Jon, C., Yang, L., Du, X., Yang, Y., 2016. CO<sub>2</sub> absorption characteristics in ammonia solution inside the structured packed column. *Ind. Eng. Chem. Res.* 55 (12), 3696–3709. <https://doi.org/10.1021/acs.iecr.5b03614>.
- Chu, F., Xiao, G., Yang, G., 2021. Mass transfer characteristics and energy penalty analysis of MEA regeneration process in packed column. *Sustain. Energy Fuels* 5 (2), 438–448. <https://doi.org/10.1039/dose01251c>.
- Chu, F., Yang, L., Du, X., Yang, Y., 2017. Mass transfer and energy consumption for CO<sub>2</sub> absorption by ammonia solution in bubble column. *Appl. Energ.* 190, 1068–1080. <https://doi.org/10.1016/j.apenergy.2017.01.027>.
- Ciferno J.P., Dipietro P. 2005, An economic scoping study for CO<sub>2</sub> capture using aqueous ammonia, <https://api.semanticscholar.org/CorpusID:130201660>.
- Collett, J.R., Heck, R.W., Zwoster, A.J., 2011. Dissolved carbonic anhydride for enhancing post-combustion carbon dioxide hydration in aqueous ammonia. *Energy Proc.* 4, 240–244. <https://doi.org/10.1016/j.egypro.2011.01.047>.
- Conway, W., Fernandes, D., Beyad, Y., Burns, R., Lawrence, G., Puxty, G., et al., 2013. Reactions of CO<sub>2</sub> with aqueous piperazine solutions: formation and decomposition of mono- and dicarboxylic acids/carbamates of piperazine at 25.0°C. *J. Phys. Chem. A* 117 (5), 806–813. <https://doi.org/10.1021/jp310560b>.
- Crooks, J.E., Donnellan, J.P., 1989. Kinetics and mechanism of the reaction between carbon dioxide and amines in aqueous solution. *J. Chem. Soc. Perkin Transac. 2* (4), 331–333. <https://doi.org/10.1039/p29890000331>.
- Cui, Z., deMontigny, D., 2017. Experimental study of carbon dioxide absorption into aqueous ammonia with a hollow fiber membrane contactor. *J. Membr. Sci.* 540, 297–306. <https://doi.org/10.1016/j.memsci.2017.06.013>.
- Da Silva, E.F., Svendsen, H.F., 2004. Ab initio study of the reaction of carbamate formation from CO<sub>2</sub> and alkanolamines. *Ind. Eng. Chem. Res.* 43 (13), 3413–3418. <https://doi.org/10.1021/ie030619k>.
- Dai, N., Mitch, W.A., 2014. Effects of flue gas compositions on nitrosamine and nitramine formation in postcombustion CO<sub>2</sub> capture systems. *Environ. Sci. Technol.* 48 (13), 7519–7526. <https://doi.org/10.1021/es501864a>.
- Danckwerts, P., 1979. The reaction of CO<sub>2</sub> with ethanolamines. *Chem. Eng. Sci.* 34 (4), 443–446. [https://doi.org/10.1016/0009-2509\(79\)85087-3](https://doi.org/10.1016/0009-2509(79)85087-3).
- Darde, V., Maribo-Møgensen, B., van Well, W.J., Stenby, E.H., Thomsen, K., 2012a. Process simulation of CO<sub>2</sub> capture with aqueous ammonia using the extended UNIQUAC model. *Int. J. Greenh. Gas Control* 10, 74–87. <https://doi.org/10.1016/j.ijggc.2012.05.017>.
- Darde, V., Thomsen, K., van Well, W.J., Bonalumi, D., Valenti, G., Macchi, E., 2012b. Comparison of two electrolyte models for the carbon capture with aqueous ammonia. *Int. J. Greenh. Gas Control* 8, 61–72. <https://doi.org/10.1016/j.ijggc.2012.02.002>.
- Darde, V., Thomsen, K., van Well, W.J., Stenby, E.H., 2009. Chilled ammonia process for CO<sub>2</sub> capture. *Energy Proc.* 1 (1), 1035–1042.
- Darde, V., Van Well, W.J., Fosboel, P.L., Stenby, E.H., Thomsen, K., 2011. Experimental measurement and modeling of the rate of absorption of carbon dioxide by aqueous ammonia. *Int. J. Greenh. Gas Control* 5 (5), 1149–1162. <https://doi.org/10.1016/j.ijggc.2011.07.008>.
- Darde, V., van Well, W.J., Stenby, E.H., Thomsen, K., 2010. Modeling of carbon dioxide absorption by aqueous ammonia solutions using the extended UNIQUAC model. *Ind. Eng. Chem. Res.* 49 (24), 12663–12674. <https://doi.org/10.1021/ie1009519>.
- Davison, J., 2007. Performance and costs of power plants with capture and storage of CO<sub>2</sub>. *Energy* 32 (7), 1163–1176. <https://doi.org/10.1016/j.energy.2006.07.039>.
- DeMontigny, D., Aboudheir, A., Tontiwachwuthikul, P., Chakma, A., 2006. Using a packed-column model to simulate the performance of a membrane absorber. *Ind. Eng. Chem. Res.* 45 (8), 2580–2585. <https://doi.org/10.1021/ie050568m>.
- Demontigny, D., Tontiwachwuthikul, P., Chakma, A., 2005. Comparing the absorption performance of packed columns and membrane contactors. *Ind. Eng. Chem. Res.* 44 (15), 5726–5732. <https://doi.org/10.1021/ie040264k>.
- Derkx, P., Versteeg, G., 2009. Kinetics of absorption of carbon dioxide in aqueous ammonia solutions. *Energy Proc.* 1 (1), 1139–1146. <https://doi.org/10.1016/j.egypro.2009.01.150>.
- Diao, Y.-F., Zheng, X.-Y., He, B.-S., Chen, C.-H., Xu, X.-C., 2004. Experimental study on capturing CO<sub>2</sub> greenhouse gas by ammonia scrubbing. *Energ. Convers. Manage.* 45 (13-14), 2283–2296. <https://doi.org/10.1016/j.enconman.2003.10.011>.
- Edwards, T., Maurer, G., Newman, J., Prausnitz, J., 1978. Vapor-liquid equilibria in multicomponent aqueous solutions of volatile weak electrolytes. *AIChE J.* 24 (6), 966–976. <https://doi.org/10.1002/aic.690240605>.
- Edwards, T.J., Newman, J., Prausnitz, J.M., 1975. Thermodynamics of aqueous solutions containing volatile weak electrolytes. *AIChE J.* 21 (2), 248–259. <https://doi.org/10.1002/aic.690210205>.
- Fang, M., Xiang, Q., Yu, C., Xia, Z., Zhou, X., Cai, D., et al., 2015. Experimental study on CO<sub>2</sub> absorption by aqueous ammonia solution at elevated pressure to enhance CO<sub>2</sub> absorption and suppress ammonia vaporization. *Greenh. Gas.: Sci. Technol.* 5 (2), 210–221. <https://doi.org/10.1002/ghg.1463>.
- Favre, E., Svendsen, H., 2012. Membrane contactors for intensified post-combustion carbon dioxide capture by gas-liquid absorption processes. *J. Membr. Sci.* 407, 1–7. <https://doi.org/10.1016/j.memsci.2012.03.019>.
- Feng, D., Gao, J., Zhang, Y., Li, H., Du, Q., Wu, S., 2018. Mass transfer in ammonia-based CO<sub>2</sub> absorption in bubbling reactor under static magnetic field. *Chem. Eng. J.* 338, 450–456. <https://doi.org/10.1016/j.cej.2018.01.061>.
- Feron, P., 2016. Absorption-based Post-Combustion Capture of Carbon dioxide. Woodhead publishing. <https://doi.org/10.1016/C2014-0-03382-5>.
- Feron, P.H., ten Asbroek, N., 2005. New solvents based on amino-acid salts for CO<sub>2</sub> capture from flue gases. In: *Greenhouse Gas Control Technologies*, 7. Elsevier, pp. 1153–1158. <https://doi.org/10.1016/B978-008044704-9/50121-X>.
- Figueroa, J.D., Fout, T., Plasynski, S., McEvried, H., Srivastava, R.D., 2008. Advances in CO<sub>2</sub> capture technology—the US department of energy's carbon sequestration program. *Int. J. Greenh. Gas Control* 2 (1), 9–20. [https://doi.org/10.1016/S1750-5836\(07\)00094-1](https://doi.org/10.1016/S1750-5836(07)00094-1).
- Freeman, S.A., Dugas, R., Van Wagener, D.H., Nguyen, T., Rochelle, G.T., 2010. Carbon dioxide capture with concentrated, aqueous piperazine. *Int. J. Greenh. Gas Control* 4 (2), 119–124. <https://doi.org/10.1016/j.ijggc.2009.10.008>.
- Freitas, D., Costa, G., Guerrini, Y., 2013. Expanding Aspen Plus® applications with the use of external models, case study: thermodynamic models for electrolyte solutions, Proceedings of the 13th International Conference on Properties and Phase Equilibria for Products and Process Design.
- Fu, K., Chen, G., Liang, Z., Sema, T., Idem, R., Tontiwachwuthikul, P., 2014. Analysis of mass transfer performance of monoethanolamine-based CO<sub>2</sub> absorption in a packed column using artificial neural networks. *Ind. Eng. Chem. Res.* 53 (11), 4413–4423. <https://doi.org/10.1021/ie403259g>.
- Gal, E., Bade, O.M., Jayaweera, I., Krishnan, G., 2012. Promoter Enhanced Chilled Ammonia Based System and Method for Removal of CO<sub>2</sub> from Flue Gas Stream. Google Patents.
- Gielen, B., Jordens, J., Janssen, J., Pfeiffer, H., Wevers, M., Thomassen, L., et al., 2015. Characterization of stable and transient cavitation bubbles in a milliflow reactor using a multibubble sonoluminescence quenching technique. *Ultrason. Sonochem.* 25, 31–39. <https://doi.org/10.1016/j.ulsonch.2014.08.013>.
- Gonzalez-Garza, D., Rivera-Tinoco, R., Bouallou, C., 2009. Comparison of ammonia, monoethanolamine, diethanolamine and methyldiethanolamine solvents to reduce CO<sub>2</sub> greenhouse gas emissions. In: *12th International Conference on Process Integration, Modelling and Optimisation for Energy Saving and Pollution Reduction, PRES'09*. <https://doi.org/10.3303/CET0918044>.
- Göppert, U., Maurer, G., 1988. Vapor—liquid equilibria in aqueous solutions of ammonia and carbon dioxide at temperatures between 333 and 393 K and pressures up to 7 MPa. *Fluid Phase Equilib.* 41 (1-2), 153–185. [https://doi.org/10.1016/0378-3812\(88\)80042-6](https://doi.org/10.1016/0378-3812(88)80042-6).
- Goto, K., Yogo, K., Higashii, T., 2013. A review of efficiency penalty in a coal-fired power plant with post-combustion CO<sub>2</sub> capture. *Appl. Energ.* 111, 710–720. <https://doi.org/10.1016/j.apenergy.2013.05.020>.
- Gross, J., Sadowski, G., 2001. Perturbed-chain SAFT: an equation of state based on a perturbation theory for chain molecules. *Ind. Eng. Chem. Res.* 40 (4), 1244–1260. <https://doi.org/10.1021/ie0003887>.
- Gudjonsdottir, V.I., Ferreira, C., 2016. Comparison of models for calculation of the thermodynamic properties of NH<sub>3</sub>-CO<sub>2</sub>-H<sub>2</sub>O mixture, <http://docs.lib.psu.edu/iracc/1641>.
- Halstensen, M., Jilvero, H., Jinadasa, W.N., Jens, K.-J., 2017. Equilibrium measurements of the NH<sub>3</sub>-CO<sub>2</sub>-H<sub>2</sub>O system: speciation based on Raman spectroscopy and multivariate modeling. *J. Chem.* 2017 (1), 7590506. <https://doi.org/10.1155/2017/7590506>.
- Han, K., Ahn, C.K., Lee, M.S., 2014. Performance of an ammonia-based CO<sub>2</sub> capture pilot facility in iron and steel industry. *Int. J. Greenh. Gas Control* 27, 239–246. <https://doi.org/10.1016/j.ijggc.2014.05.014>.
- Han, K., Ahn, C.K., Lee, M.S., Rhee, C.H., Kim, J.Y., Chun, H.D., 2013. Current status and challenges of the ammonia-based CO<sub>2</sub> capture technologies toward commercialization. *Int. J. Greenh. Gas Control* 14, 270–281. <https://doi.org/10.1016/j.ijggc.2013.01.007>.
- Holmes, P.E., Naaz, M., Poling, B.E., 1998. Ion concentrations in the CO<sub>2</sub>–NH<sub>3</sub>–H<sub>2</sub>O system from <sup>13</sup>C NMR spectroscopy. *Ind. Eng. Chem. Res.* 37 (8), 3281–3287. <https://doi.org/10.1021/ie9707782>.
- Hsu, C., 2003. Study on Carbon dioxide Removals from Flue Gas using Chemical Absorption Method. Cheng Kung University, Taiwan. <https://doi.org/10.1080/10473289.2003.10466139>.
- Hughes, R., Kotamreddy, G., Bhattacharyya, D., Omell, B., Matuszewski, M., 2022. Modeling and Bayesian uncertainty quantification of a membrane-assisted chilled ammonia process for CO<sub>2</sub> capture. *Ind. Eng. Chem. Res.* 61 (11), 4001–4016. <https://doi.org/10.1021/acs.iecr.1c04601>.

- [ IPCC, Core Writing Team, 2007. Climate change 2007: synthesis report. Contribution of working groups I, II and III to the fourth assessment report of the intergovernmental panel on climate change. In: Pachauri, R.K., Reisinger, A. (Eds.), United Nations Intergovernmental Panel on Climate Change. PCC, Geneva, Switzerland, p. 104.
- Ishaq, H., Ali, U., Sher, F., Anus, M., Imran, M., 2021. Process analysis of improved process modifications for ammonia-based post-combustion CO<sub>2</sub> capture. *J. Environ. Chem. Eng.* 9 (1), 104928. <https://doi.org/10.1016/j.jece.2020.104928>.
- Jackson, P., 2014. Experimental and theoretical evidence suggests carbamate intermediates play a key role in CO<sub>2</sub> sequestration catalysed by sterically hindered amines. *Struct. Chem.* 25, 1535–1546. <https://doi.org/10.1007/s11224-014-0431-5>.
- Jänecke, E., 1929. Über das system H<sub>2</sub>O, CO<sub>2</sub> und NH<sub>3</sub>, Zeitschrift für Elektrochemie und angewandte physikalische. Chemie 35 (9), 716–728. <https://doi.org/10.1002/bbpc.192900060>.
- Javed, K., Mahmud, T., Purba, E., 2006. Enhancement of mass transfer in a spray tower using swirling gas flow. *Chem. Eng. Res. Des.* 84 (6), 465–477. <https://doi.org/10.1205/cherd.05119>.
- Javed, K., Mahmud, T., Purba, E., 2010. The CO<sub>2</sub> capture performance of a high-intensity vortex spray scrubber. *Chem. Eng. J.* 162 (2), 448–456. <https://doi.org/10.1016/j.cej.2010.03.038>.
- Jaworski, Z., Czernuszewicz, M., Gralla, Ł., 2011. A comparative study of thermodynamic electrolyte models applied to the Solvay soda system. *Chem. Process Eng.* 32, 135–154. <https://doi.org/10.2478/V10176-011-0011-9>.
- Jeon, S.-B., Seo, J.-B., Lee, H.-D., Kang, S.-K., Oh, K.-J., 2013. Absorption kinetics of carbon dioxide into aqueous ammonia solution: Addition of hydroxyl groups for suppression of vaporization. *Korean J. Chem. Eng.* 30 (9), 1790–1796. <https://doi.org/10.1007/s11814-013-0105-9>.
- Jiang, K., Li, K., Yu, H., Chen, Z., Wardhaugh, L., Feron, P., 2017. Advancement of ammonia based post-combustion CO<sub>2</sub> capture using the advanced flash stripper process. *Appl. Energ.* 202, 496–506.
- Jiang, K., Li, K., Yu, H., Feron, P.H., 2018. Piperazine-promoted aqueous-ammonia-based CO<sub>2</sub> capture: Process optimisation and modification. *Chem. Eng. J.* 347, 334–342. <https://doi.org/10.1016/j.cej.2018.04.103>.
- Jiang, K., Yu, H., Chen, L., Fang, M., Azzi, M., Cottrell, A., et al., 2020a. An advanced, ammonia-based combined NO<sub>x</sub>/SO<sub>x</sub>/CO<sub>2</sub> emission control process towards a low-cost, clean coal technology. *Appl. Energ.* 260, 114316. <https://doi.org/10.1016/j.apenergy.2019.114316>.
- Jiang, K., Yu, H., Yu, J., Li, K., 2020b. Advancement of ammonia-based post-combustion CO<sub>2</sub> capture technology: process modifications. *Fuel Process. Technol.* 210, 106544. <https://doi.org/10.1016/j.fuproc.2020.106544>.
- Jilvero, H., Jens, K.-J., Normann, F., Andersson, K., Halstensen, M., Eimer, D., et al., 2015. Equilibrium measurements of the NH<sub>3</sub>–CO<sub>2</sub>–H<sub>2</sub>O system—measurement and evaluation of vapor–liquid equilibrium data at low temperatures. *Fluid Phase Equilib.* 385, 237–247. <https://doi.org/10.1155/2017/7590506>.
- Jilvero, H., Normann, F., Andersson, K., Johnsson, F., 2014. The rate of CO<sub>2</sub> absorption in ammonia implications on absorber design. *Ind. Eng. Chem. Res.* 53 (16), 6750–6758. <https://doi.org/10.1021/ie403346a>.
- Kang, J.-L., Luo, Z.-J., Liu, J.-L., Sun, K., Wong, D.S.-H., Jang, S.-S., et al., 2014. Experiment and modeling studies on absorption of CO<sub>2</sub> by dilute ammonia in rotating packed bed. *Energy Proc.* 63, 1308–1313. <https://doi.org/10.1016/j.egypro.2014.11.139>.
- Kang, J.-L., Wong, D.S.-H., Jang, S.-S., Tan, C.-S., 2016. A comparison between packed beds and rotating packed beds for CO<sub>2</sub> capture using monoethanolamine and dilute aqueous ammonia solutions. *Int. J. Greenh. Gas Control* 46, 228–239. <https://doi.org/10.1016/j.ijggc.2016.01.017>.
- Karami, M., Keshavarz, P., Khorram, M., Mehdipour, M., 2013. Analysis of ammonia separation from purge gases in microporous hollow fiber membrane contactors. *J. Hazard. Mater.* 260, 576–584. <https://doi.org/10.1016/j.jhazmat.2013.06.002>.
- Kawazuishi, K., Prausnitz, J.M., 1987. Correlation of vapor-liquid equilibria for the system ammonia–carbon dioxide–water. *Ind. Eng. Chem. Res.* 26 (7), 1482–1485.
- Kayahan, E., Di Caprio, U., Van den Bogaert, A., Khan, M.N., Bulut, M., Braeken, L., et al., 2023. A new look to the old solvent: mass transfer performance and mechanism of CO<sub>2</sub> absorption into pure monoethanolamine in a spray column. *Chem. Eng. Process.-Process Intensific.* 184, 109285. <https://doi.org/10.1016/j.cep.2023.109285>.
- Khatoon, B., Alam, M.S., 2022. Study of mass transfer coefficient of CO<sub>2</sub> capture in different solvents using microchannel: a comparative study. *Comput. Aid. Chem. Eng.* 49, 691–696. <https://doi.org/10.1016/B978-0-323-85159-6.50115-9>. Elsevier.
- Kiani, S., Taghizade, A., Ramezani, R., Di, F.R., Molekwa, G.F., Mazinani, S., 2022. Enhancement of CO<sub>2</sub> removal by promoted MDEA solution in a hollow fiber membrane contactor: a numerical and experimental study. *Carbon Capt. Sci. Technol.* 2, 100028. <https://doi.org/10.1016/j.ccst.2022.100028>.
- Kim, G.H., Park, S.Y., You, J.K., Hong, W.H., Kim, J.-N., Kim, J.-D., 2014. CO<sub>2</sub> absorption kinetics in a CO<sub>2</sub>-free and partially loaded aqueous ammonia solution. *Chem. Eng. J.* 250, 83–90. <https://doi.org/10.1016/j.cej.2014.03.120>.
- Kim, Y.J., You, J.K., Hong, W.H., Yi, K.B., Ko, C.H., Kim, J.N., 2008. Characteristics of CO<sub>2</sub> absorption into aqueous ammonia. *Sep. Sci. Technol.* 43 (4), 766–777. <https://doi.org/10.1080/01496390701870606>.
- Kittiampon, N., Kaewchada, A., Jaree, A., 2017. Carbon dioxide absorption using ammonia solution in a microchannel. *Int. J. Greenh. Gas Control* 63, 431–441. <https://doi.org/10.1016/j.ijggc.2017.06.014>.
- Koronaki, I., Prentza, L., Papaefthimiou, V., 2015. Modeling of CO<sub>2</sub> capture via chemical absorption processes—An extensive literature review. *Renew. Sustain. Energy Rev.* 50, 547–566. <https://doi.org/10.1016/j.rser.2015.04.124>.
- Krop, J., 1999. New approach to simplify the equation for the excess Gibbs free energy of aqueous solutions of electrolytes applied to the modelling of the NH<sub>3</sub>–CO<sub>2</sub>–H<sub>2</sub>O vapour–liquid equilibria. *Fluid Phase Equilib.* 163 (2), 209–229. [https://doi.org/10.1016/S0378-3812\(99\)00225-3](https://doi.org/10.1016/S0378-3812(99)00225-3).
- Kuntz, J., Aroonwilas, A., 2009. Mass-transfer efficiency of a spray column for CO<sub>2</sub> capture by MEA. *Energy Proc.* 1 (1), 205–209. <https://doi.org/10.1016/j.egypro.2009.01.029>.
- Kurz, F., Rumpf, B., Maurer, G., 1995. Vapor-liquid-solid equilibria in the system NH<sub>3</sub>–CO<sub>2</sub>–H<sub>2</sub>O from around 310 to 470 K: new experimental data and modeling. *Fluid Phase Equilib.* 104, 261–275. [https://doi.org/10.1016/0378-3812\(94\)02653-I](https://doi.org/10.1016/0378-3812(94)02653-I).
- Lam, K.F., Sorensen, E., Gavriliidis, A., 2013. Review on gas–liquid separations in microchannel devices. *Chem. Eng. Res. Des.* 91 (10), 1941–1953. <https://doi.org/10.1016/j.cherd.2013.07.031>.
- Le Moulec, Y., Kanniche, M., 2011. Optimization of MEA based post combustion CO<sub>2</sub> capture process: flowsheeting and energetic integration. *Energy Proc.* 4, 1303–1309. <https://doi.org/10.1016/j.egypro.2011.01.187>.
- Le Moulec, Y., Neveux, T., Al Azki, A., Chikukwa, A., Hoff, K.A., 2014. Process modifications for solvent-based post-combustion CO<sub>2</sub> capture. *Int. J. Greenh. Gas Control* 31, 96–112. <https://doi.org/10.1016/j.ijggc.2014.09.024>.
- Lewis, W., Whitman, W., 1924. Absorption symposium. *Ind. Eng. Chem.* 16, 1215–1220. <https://doi.org/10.1021/ie50180a002>.
- Li, J.-L., Chen, B.-H., 2005. Review of CO<sub>2</sub> absorption using chemical solvents in hollow fiber membrane contactors. *Sep. Purif. Technol.* 41 (2), 109–122. <https://doi.org/10.1016/j.seppur.2004.09.008>.
- Li, K., Leigh, W., Feron, P., Yu, H., Tade, M., 2016a. Systematic study of aqueous monoethanolamine (MEA)-based CO<sub>2</sub> capture process: techno-economic assessment of the MEA process and its improvements. *Appl. Energy* 165, 648–659. <https://doi.org/10.1016/j.apenergy.2015.12.109>.
- Li, K., Yu, H., Feron, P., Tade, M., 2014a. Modelling and experimental study of SO<sub>2</sub> removal and NH<sub>3</sub> recycling in an ammonia based CO<sub>2</sub> capture process. *Energy Proc.* 63, 1162–1170. <https://doi.org/10.1016/j.egypro.2014.11.126>.
- Li, K., Yu, H., Feron, P., Tade, M., Wardhaugh, L., 2015a. Technical and energy performance of an advanced, aqueous ammonia-based CO<sub>2</sub> capture technology for a 500 MW coal-fired power station. *Environ. Sci. Technol.* 49 (16), 10243–10252. <https://doi.org/10.1012/acs.est.5b02258>.
- Li, K., Yu, H., Feron, P., Wardhaugh, L., Tade, M., 2016b. Techno-economic assessment of stripping modifications in an ammonia-based post-combustion capture process. *Int. J. Greenh. Gas Control* 53, 319–327. <https://doi.org/10.1016/j.ijggc.2016.08.016>.
- Li, K., Yu, H., Qi, G., Feron, P., Tade, M., Yu, J., et al., 2015b. Rate-based modelling of combined SO<sub>2</sub> removal and NH<sub>3</sub> recycling integrated with an aqueous NH<sub>3</sub>-based CO<sub>2</sub> capture process. *Appl. Energ.* 148, 66–77. <https://doi.org/10.1016/j.apenergy.2015.03.060>.
- Li, K., Yu, H., Yan, S., Feron, P., Wardhaugh, L., Tade, M., 2016c. Technoeconomic assessment of an advanced aqueous ammonia-based postcombustion capture process integrated with a 650-MW coal-fired power station. *Environ. Sci. Technol.* 50 (19), 10746–10755. <https://doi.org/10.1012/acs.est.6b02737>.
- Li, L., Conway, W., Puxty, G., Burns, R., Clifford, S., Maeder, M., et al., 2015c. The effect of piperazine (PZ) on CO<sub>2</sub> absorption kinetics into aqueous ammonia solutions at 25.0 C. *Int. J. Greenh. Gas Control* 36, 135–143. <https://doi.org/10.1016/j.ijggc.2015.02.015>.
- Li, L., Han, W., Yu, H., Tang, H., 2013. CO<sub>2</sub> absorption by piperazine promoted aqueous ammonia solution: absorption kinetics and ammonia loss. *Greenh. Gas.: Sci. Technol.* 3 (3), 231–245. <https://doi.org/10.1002/ghg.1347>.
- Li, L., Puxty, G., Maeder, M., Burns, R., Yu, H., Conway, W., 2019. Kinetic absorption of CO<sub>2</sub> into blended ammonia (NH<sub>3</sub>) solutions with a new cyclic amine 4-aminomethyltetrahydropyran (4-AMTHP). *Energ. Fuel* 33 (6), 5377–5383. <https://doi.org/10.1021/acs.energyfuels.9b00394>.
- Li, W., Zhao, X., Liu, B., Tang, Z., 2014b. Mass transfer coefficients for CO<sub>2</sub> absorption into aqueous ammonia using structured packing. *Ind. Eng. Chem. Res.* 53 (14), 6185–6196. <https://doi.org/10.1016/j.ie403097h>.
- Liang, Z., Fu, K., Idem, R., Tontiwachwuthikul, P., 2016. Review on current advances, future challenges and consideration issues for post-combustion CO<sub>2</sub> capture using amine-based absorbents. *Chin. J. Chem. Eng.* 24 (2), 278–288. <https://doi.org/10.1016/j.cjche.2015.06.013>.
- Lichtfors, U., Rumpf, B., 2004. Thermodynamic properties of complex fluid mixtures. 5, An Infrared Spectroscopic Investigation of the Species Distribution in the System NH<sub>3</sub>+ CO<sub>2</sub>+ H<sub>2</sub>O, 92.
- Lillia, S., Bonalumi, D., Fosbøl, P.L., Thomsen, K., Valenti, G., 2018. Experimental study of the aqueous CO<sub>2</sub>–NH<sub>3</sub> rate of reaction for temperatures from 15°C to 35°C, NH<sub>3</sub> concentrations from 5% to 15% and CO<sub>2</sub> loadings from 0.2 to 0.6. *Int. J. Greenh. Gas Control* 70, 117–127. <https://doi.org/10.1016/j.ijggc.2018.01.009>.
- Lillia, S., Bonalumi, D., Valenti, G., 2016. Rate-based approaches for the carbon capture with aqueous ammonia without salt precipitation. *Energy Proc.* 101, 400–407. <https://doi.org/10.1016/j.egypro.2016.11.051>.
- Lim, Y., Choi, M., Han, K., Yi, M., Lee, J., 2013. Performance characteristics of CO<sub>2</sub> capture using aqueous ammonia in a single-nozzle spray tower. *Ind. Eng. Chem. Res.* 52 (43), 15131–15137. <https://doi.org/10.1021/ie401981u>.
- Lin, C.-C., Kuo, Y.-W., 2016. Mass transfer performance of rotating packed beds with blade packings in absorption of CO<sub>2</sub> into MEA solution. *Int. J. Heat Mass Tran.* 97, 712–718. <https://doi.org/10.1016/j.ijheatmasstransfer.2016.02.033>.
- Lin, S.-H., Hsieh, C.-F., Li, M.-H., Tung, K.-L., 2009. Determination of mass transfer resistance during absorption of carbon dioxide by mixed absorbents in PVDF and PP membrane contactor. *Desalination* 249 (2), 647–653. <https://doi.org/10.1016/j.desal.2008.08.019>.
- Lin J., Chen D.-S. 2017, Process design of aqueous ammonia-based post-combustion CO<sub>2</sub> capture, 2017 6th International Symposium on Advanced Control of Industrial Processes (AdCONIP). <https://doi.org/10.1109/ADCONIP.2017.7983810>.

- Liu, J., Gao, H.-C., Peng, C.-C., Wong, D.S.-H., Jang, S.-S., Shen, J.-F., 2015. Aspen plus rate-based modeling for reconciling laboratory scale and pilot scale CO<sub>2</sub> absorption using aqueous ammonia. *Int. J. Greenh. Gas Control* 34, 117–128. <https://doi.org/10.1016/j.ijggc.2015.01.009>.
- Liu, J., Wang, S., Hartono, A., Svendsen, H.F., Kim, I., Chen, C., 2011a. Vapor–liquid equilibria of NH<sub>3</sub> in (NH<sub>3</sub>+ H<sub>2</sub>O) and (NH<sub>3</sub>+ PZ+ H<sub>2</sub>O) system. *Fluid Phase Equilib.* 311, 30–35. <https://doi.org/10.1016/j.fluid.2011.08.017>.
- Liu, J., Wang, S., Qi, G., Zhao, B., Chen, C., 2011b. Kinetics and mass transfer of carbon dioxide absorption into aqueous ammonia. *Energy Proc.* 4, 525–532. <https://doi.org/10.1016/j.egypro.2011.01.084>.
- Liu, J., Wang, S., Svendsen, H.F., Idrees, M.U., Kim, I., Chen, C., 2012a. Heat of absorption of CO<sub>2</sub> in aqueous ammonia, piperazine solutions and their mixtures. *Int. J. Greenh. Gas Control* 9, 148–159. <https://doi.org/10.1016/j.ijggc.2012.03.013>.
- Liu, J., Wang, S., Zhao, B., Qi, G., Chen, C., 2012b. Study on mass transfer and kinetics of CO<sub>2</sub> absorption into aqueous ammonia and piperazine blended solutions. *Chem. Eng. Sci.* 75, 298–308. <https://doi.org/10.1016/j.ces.2012.03.047>.
- Liu, J., Wong, D.S.-H., Chen, D.-S., 2020. Energy-saving performance of advanced stripper configurations for CO<sub>2</sub> capture by ammonia-based solvents. *J. Taiwan Inst. Chem. Eng.* 113, 273–284. <https://doi.org/10.1016/j.jitec.2020.08.024>.
- Liu, Y., Chu, F., Yang, L., Du, X., Yang, Y., 2018. CO<sub>2</sub> absorption characteristics in a random packed column with various geometric structures and working conditions. *Greenh. Gas.: Sci. Technol.* 8 (1), 120–132. <https://doi.org/10.1002/ghg.1725>.
- Lu, R., Li, K., Chen, J., Yu, H., Tade, M., 2017. CO<sub>2</sub> capture using piperazine-promoted, aqueous ammonia solution: rate-based modelling and process simulation. *Int. J. Greenh. Gas Control* 65, 65–75. <https://doi.org/10.1016/j.ijggc.2017.08.018>.
- Ma, S., Chen, G., Zhu, S., Han, T., Yu, W., 2016. Mass transfer of ammonia escape and CO<sub>2</sub> absorption in CO<sub>2</sub> capture using ammonia solution in bubbling reactor. *Appl. Energ.* 162, 354–362. <https://doi.org/10.1016/j.apenergy.2015.10.089>.
- Ma, S., Song, H., Wang, M., Yang, J., Zang, B., 2013a. Research on mechanism of ammonia escaping and control in the process of CO<sub>2</sub> capture using ammonia solution. *Chem. Eng. Res. Des.* 91 (7), 1327–1334. <https://doi.org/10.1016/j.cherd.2013.01.020>.
- Ma, S., Zang, B., Song, H., Chen, G., Yang, J., 2013b. Research on mass transfer of CO<sub>2</sub> absorption using ammonia solution in spray tower. *Int. J. Heat Mass Transf.* 67, 696–703. <https://doi.org/10.1016/j.ijheatmasstransfer.2013.08.090>.
- Makhlooufi, C., Lasseguette, E., Remigy, J.C., Belaissaoui, B., Roizard, D., Favre, E., 2014. Ammonia based CO<sub>2</sub> capture process using hollow fiber membrane contactors. *J. Membr. Sci.* 455, 236–246. <https://doi.org/10.1016/j.memsci.2013.12.063>.
- Mani, F., Peruzzini, M., Stoppioni, P., 2006. CO<sub>2</sub> absorption by aqueous NH<sub>3</sub> solutions: speciation of ammonium carbamate, bicarbonate and carbonate by a <sup>13</sup>C NMR study. *Green. Chem.* 8 (11), 995–1000. <https://doi.org/10.1039/B602051H>.
- Mathias, P.M., Reddy, S., O'Connell, J.P., 2010. Quantitative evaluation of the chilled-ammonia process for CO<sub>2</sub> capture using thermodynamic analysis and process simulation. *Int. J. Greenh. Gas Control* 4 (2), 174–179. <https://doi.org/10.1016/j.ijggc.2009.09.016>.
- McLarnon, C.R., Duncan, J.L., 2009. Testing of ammonia based CO<sub>2</sub> capture with multi-pollutant control technology. *Energy Proc.* 1 (1), 1027–1034. <https://doi.org/10.1016/j.egypro.2009.01.136>.
- McLeod, A., Jefferson, B., McAdam, E.J., 2014. Biogas upgrading by chemical absorption using ammonia rich absorbents derived from wastewater. *Water Res.* 67, 175–186. <https://doi.org/10.1016/j.watres.2014.09.010>.
- Mehdipour, M., Keshavarz, P., Seraji, A., Masoumi, S., 2014. Performance analysis of ammonia solution for CO<sub>2</sub> capture using microporous membrane contactors. *Int. J. Greenh. Gas Control* 31, 16–24. <https://doi.org/10.1016/j.ijggc.2014.09.017>.
- Molina, C.T., Bouallou, C., 2015. Assessment of different methods of CO<sub>2</sub> capture in post-combustion using ammonia as solvent. *J. Clean. Prod.* 103, 463–468. <https://doi.org/10.1016/j.jclepro.2014.03.024>.
- Mores, P.L., Manassaldi, J.I., Scenna, N.J., Caballero, J.A., Mussati, M.C., Mussati, S.F., 2018. Optimization of the design, operating conditions, and coupling configuration of combined cycle power plants and CO<sub>2</sub> capture processes by minimizing the mitigation cost. *Chem. Eng. J.* 331, 870–894. <https://doi.org/10.1016/j.cej.2017.08.111>.
- Müller, G., Bender, E., Maurer, G., 1988. Das Dampf-Flüssigkeitsgleichgewicht des ternären Systems Ammoniak-Kohlendioxid-Wasser bei hohen Wassergehalten im Bereich zwischen 373 und 473 Kelvin. Berichte der Bunsengesellschaft für physikalische Chemie 92 (2), 148–160. <https://doi.org/10.1002/bbpc.198800036>.
- Nair P.S., Selvi P.P. 2014, Absorption of carbondioxide in packed column, <https://api.semanticscholar.org/CorpusID:10364008>.
- Nakamura, R., Breedveld, G.J., Prausnitz, J.M., 1976. Thermodynamic properties of gas mixtures containing common polar and nonpolar components. *Ind. Eng. Chem. Proc. Des. Develop.* 15 (4), 557–564.
- Nguyen, H.L.Q., Wong, D.S.-H., 2019. Eliminating steam requirement of aqueous ammonia capture process by lean solution flash and vapor recompression. *Proc. Integr. Optimiz. Sustain.* 3, 307–319. <https://doi.org/10.1007/s41660-018-0074-x>.
- Nguyen, H.L.Q., Wong, D.S.-H., 2021. Integration of rich and lean vapor recompression configurations for aqueous ammonia-based CO<sub>2</sub> capture process. *Chem. Eng. Res. Des.* 169, 86–96. <https://doi.org/10.1016/j.cherd.2021.02.020>.
- Nguyen, P., Lasseguette, E., Medina-Gonzalez, Y., Remigy, J.-C., Roizard, D., Favre, E., 2011. A dense membrane contactor for intensified CO<sub>2</sub> gas/liquid absorption in post-combustion capture. *J. Membr. Sci.* 377 (1-2), 261–272. <https://doi.org/10.1016/j.memsci.2011.05.003>.
- Niu, Z., Guo, Y., Lin, W., 2010. Experimental studies on removal of carbon dioxide by aqueous ammonia fine spray. *Sci. China Ser. E: Technol. Sci.* 53 (1), 117–122. <https://doi.org/10.1007/s11431-010-0023-6>.
- Niu, Z., Guo, Y., Zeng, Q., Lin, W., 2012. Experimental studies and rate-based process simulations of CO<sub>2</sub> absorption with aqueous ammonia solutions. *Ind. Eng. Chem. Res.* 51 (14), 5309–5319. <https://doi.org/10.1021/ie2030536>.
- Obek C.A., Ayittey F.K., Saptoro A., 2019. Improved process modifications of aqueous ammonia-based CO<sub>2</sub> capture system, MATEC Web of Conferences. <https://doi.org/10.1051/matecconf/201926802004>.
- Oexmann, J., Kather, A., Linnenberg, S., Liebenthal, U., 2012. Post-combustion CO<sub>2</sub> capture: chemical absorption processes in coal-fired steam power plants. *Greenh. Gas.: Sci. Technol.* 2 (2), 80–98. <https://doi.org/10.1002/ghg.1273>.
- Oh, S.-Y., Binns, M., Cho, H., Kim, J.-K., 2016. Energy minimization of MEA-based CO<sub>2</sub> capture process. *Appl. Energ.* 169, 353–362. <https://doi.org/10.1016/j.apenergy.2016.02.046>.
- Park, H., Jung, Y.M., You, J.K., Hong, W.H., Kim, J.-N., 2008. Analysis of the CO<sub>2</sub> and NH<sub>3</sub> reaction in an aqueous solution by 2D IR COS: formation of bicarbonate and carbamate. *J. Phys. Chem. A* 112 (29), 6558–6562. <https://doi.org/10.1021/jp80091d>.
- Pawlowski, E.M., Newman, J., Prausnitz, J.M., 1982. Phase equilibria for aqueous solutions of ammonia and carbon dioxide. *Ind. Eng. Chem. Proc. Des. Develop.* 21 (4), 764–770.
- Pelkie, J.E., Concannon, P.J., Manley, D.B., Poling, B.E., 1992. Product distributions in the carbon dioxide-ammonia-water system from liquid conductivity measurements. *Ind. Eng. Chem. Res.* 31 (9), 2209–2215. <https://doi.org/10.1021/ie00009a018>.
- Pérez-Calvo, J.-F., Milella, F., Ammann, K., Mazzotti, M., 2021a. Density and viscosity of aqueous (ammonia+ carbon dioxide) solutions at atmospheric pressure and temperatures between 278.15 and 318.15 K. *J. Chem. Eng. Data* 66 (4), 1787–1801. <https://doi.org/10.1021/acs.jcd.0c01090>.
- Pérez-Calvo, J.-F., Sutter, D., Gazzani, M., Mazzotti, M., 2017. Application of a chilled ammonia-based process for CO<sub>2</sub> capture to cement plants. *Energy Proc.* 114, 6197–6205. <http://creativecommons.org/licenses/by-nc-nd/4.0/>.
- Pérez-Calvo, J.-F., Sutter, D., Gazzani, M., Mazzotti, M., 2020. A methodology for the heuristic optimization of solvent-based CO<sub>2</sub> capture processes when applied to new flue gas compositions: a case study of the chilled ammonia process for capture in cement plants. *Chem. Eng. Sci.* X 8, 100074. <https://doi.org/10.1016/j.chema.2020.100074>.
- Pérez-Calvo, J.-F., Sutter, D., Gazzani, M., Mazzotti, M., 2021b. Advanced configurations for post-combustion CO<sub>2</sub> capture processes using an aqueous ammonia solution as absorbent. *Sep. Purif. Technol.* 274, 118959 <https://doi.org/10.1016/j.seppur.2021.118959>.
- Pérez-Calvo J.F., Sutter D., Gazzani M., Mazzotti M., 2018, Pilot tests and rate-based modelling of CO<sub>2</sub> capture in cement plants using an aqueous ammonia solution, [10.3303/CET1869025](https://doi.org/10.3303/CET1869025).
- Pinsett, B., Pearson, L., Roughton, F., 1956. The kinetics of combination of carbon dioxide with ammonia. *Trans. Faraday Soc.* 52, 1594–1598. <https://doi.org/10.1039/tf9565201594>.
- Puxty, G., Rowland, R., Attalla, M., 2010. Comparison of the rate of CO<sub>2</sub> absorption into aqueous ammonia and monoethanolamine. *Chem. Eng. Sci.* 65 (2), 915–922. <https://doi.org/10.1016/j.ces.2009.09.042>.
- Qi, G., Wang, S., 2017a. Experimental study and rate-based modeling on combined CO<sub>2</sub> and SO<sub>2</sub> absorption using aqueous NH<sub>3</sub> in packed column. *Appl. Energ.* 206, 1532–1543. <https://doi.org/10.1016/j.apenergy.2017.09.110>.
- Qi, G., Wang, S., 2017b. Thermodynamic modeling of NH<sub>3</sub>-CO<sub>2</sub>-SO<sub>2</sub>-K<sub>2</sub>SO<sub>4</sub>-H<sub>2</sub>O system for combined CO<sub>2</sub> and SO<sub>2</sub> capture using aqueous NH<sub>3</sub>. *Appl. Energ.* 191, 549–558. <https://doi.org/10.1016/j.apenergy.2017.01.083>.
- Qi, G., Wang, S., Liu, J., Zhao, B., Zhuo, Y., Chen, C., 2012. Impact of SO<sub>2</sub> on CO<sub>2</sub> capture in coal-fired flue gas using aqueous ammonia. *J. Chem. Ind. Eng.* 63 (7), 2203–2209. <https://doi.org/10.3969/j.issn.0438-1157.2012.07.030>.
- Qi, G., Wang, S., Lu, W., Yu, J., Chen, C., 2015a. Vapor–liquid equilibrium of CO<sub>2</sub> in NH<sub>3</sub>-CO<sub>2</sub>-SO<sub>2</sub>-H<sub>2</sub>O system. *Fluid Phase Equilib.* 386, 47–55. <https://doi.org/10.1016/j.fluid.2014.11.015>.
- Qi, G., Wang, S., Xu, Z., Zhao, B., Chen, C., 2015b. Mass transfer and kinetics study on combined CO<sub>2</sub> and SO<sub>2</sub> absorption using aqueous ammonia. *Int. J. Greenh. Gas Control* 41, 60–67. <https://doi.org/10.1016/j.ijggc.2015.06.023>.
- Qi, G., Wang, S., Yu, H., Wardhaugh, L., Feron, P., Chen, C., 2013. Development of a rate-based model for CO<sub>2</sub> absorption using aqueous NH<sub>3</sub> in a packed column. *Int. J. Greenh. Gas Control* 17, 450–461. <https://doi.org/10.1016/j.ijggc.2013.05.027>.
- Qin, F., Wang, S., Hartono, A., Svendsen, H.F., Chen, C., 2010. Kinetics of CO<sub>2</sub> absorption in aqueous ammonia solution. *Int. J. Greenh. Gas Control* 4 (5), 729–738. <https://doi.org/10.1016/j.ijggc.2010.04.010>.
- Qing, Z., Yin Cheng, G., Zhenqi, N., 2011. Experimental studies on removal capacity of carbon dioxide by a packed reactor and a spray column using aqueous ammonia. *Energy Proc.* 4, 519–524. <https://doi.org/10.1016/j.egypro.2011.01.083>.
- Qiu, Z.-Z., Gong, S.-L., Zheng, C.-R., Zhang, L., Li, H., Li, P., et al., 2011. Simultaneous absorption of SO<sub>(2)</sub> and CO<sub>(2)</sub> by aqueous ammonia in a packed column. *Dongli Gongcheng Xuebaog (J. Chin. Soc. Pow. Eng.)* 31 (9), 700–704. <https://doi.org/10.1621/j.cnki.qhxxb.2016.25.030>.
- Que, H., Chen, C.-C., 2011. Thermodynamic modeling of the NH<sub>3</sub>-CO<sub>2</sub>-H<sub>2</sub>O system with electrolyte NRTL model. *Ind. Eng. Chem. Res.* 50 (19), 11406–11421. <https://doi.org/10.1021/ie201276m>.
- Ramshaw, C., 1983. HIGEE distillation—an example of process intensification. *Chem. Engr.* 389, 13–14. <https://cir.nii.ac.jp/crid/1574231873792372864>.
- Rashidi, H., Rasouli, P., Azimi, H., 2022. A green vapor suppressing agent for aqueous ammonia carbon dioxide capture solvent: micro contactor mass transfer study. *Energy* 244, 122711. <https://doi.org/10.1016/j.energy.2021.122711>.
- Rejl, F., Hajdl, J., Valenč, L., Moucha, T., Schultes, M., 2016. Analogy of absorption and distillation processes. Wetted-wall column study. *Chem. Eng. Sci.* 153, 146–154. <https://doi.org/10.1016/j.ces.2016.07.021>.

- Resnik, K.P., Yeh, J.T., Pennline, H.W., 2004. Aqua ammonia process for simultaneous removal of CO<sub>2</sub>, SO<sub>2</sub> and NO<sub>x</sub>. Int. J. Environ. Technol. Manage. 4 (1-2), 89–104. <https://doi.org/10.1504/IJETM.2004.004634>.
- Rhee, C.H., Kim, J.Y., Han, K., Ahn, C.K., Chun, H.D., 2011. Process analysis for ammonia-based CO<sub>2</sub> capture in ironmaking industry. Energy Proc. 4, 1486–1493. <https://doi.org/10.1016/j.egypro.2011.02.015>. <https://www.sciencedirect.com/science/article/pii/S1876610211002128>.
- Rivera-Tinoco, R., Bouallou, C., 2010. Comparison of absorption rates and absorption capacity of ammonia solvents with MEA and MDEA aqueous blends for CO<sub>2</sub> capture. J. Clean. Prod. 18 (9), 875–880. <https://doi.org/10.1016/j.jclepro.2009.12.006>.
- Rochelle, G., 2016. Conventional amine scrubbing for CO<sub>2</sub> capture. Absorption-based Post-Combustion Capture of Carbon dioxide. Elsevier, pp. 35–67. <https://doi.org/10.1016/B978-0-08-100514-9.00003-2>.
- Rochelle, G.T., 2009. Amine scrubbing for CO<sub>2</sub> capture. Science (1979) 325 (5948), 1652–1654. <https://doi.org/10.1126/science.1176731>.
- Rosa, L.P., Cruz, N., Costa, G.M., Pontes, K.V., 2021. A comparative study of thermodynamic models to describe the VLE of the ternary electrolytic mixture H<sub>2</sub>O–NH<sub>3</sub>–CO<sub>2</sub>. Chem. Prod. Process. Model. 17 (3), 255–271, 0000-0002-4662-5933.
- Rowland, R., Yang, Q., Jackson, P., Attalla, M., 2011. Amine mixtures and the effect of additives on the CO<sub>2</sub> capture rate. Energy Proc. 4, 195–200. <https://doi.org/10.1016/j.egypro.2011.01.041>.
- Sander, B., 1984. Extended UNIFAC/UNIQUAC Models for (1) Gas Solubilities and (2) Electrolyte Solutions. Department of Chemical Engineering, Technical University of ... Ph. D. Thesis.
- Sander, B., Fredenslund, A., Rasmussen, P., 1986. Calculation of vapour-liquid equilibria in mixed solvent/salt systems using an extended UNIQUAC equation. Chem. Eng. Sci. 41 (5), 1171–1183. [https://doi.org/10.1016/0009-2509\(86\)87090-7](https://doi.org/10.1016/0009-2509(86)87090-7).
- Sehgal, S., Alvarado, J.L., Hassan, I.G., Kadam, S.T., 2021. A comprehensive review of recent developments in falling-film, spray, bubble and microchannel absorbers for absorption systems. Renew. Sustain. Energy Rev. 142, 110807 <https://doi.org/10.1016/j.rser.2021.110807>.
- Shale, C., 1971. Removal of sulphur and nitrogen oxides from stack gases by ammonia. AIChE Symp. Ser.
- Shokrollahi, F., Lau, K., Partoon, B., Smith, A., 2022. A review on the selection criteria for slow and medium kinetic solvents used in CO<sub>2</sub> absorption for natural gas purification. J. Nat. Gas. Sci. Eng. 98, 104390 <https://doi.org/10.1016/j.jngse.2021.104390>.
- Simons, K., Nijmeijer, K., Wessling, M., 2009. Gas-liquid membrane contactors for CO<sub>2</sub> removal. J. Membr. Sci. 340 (1-2), 214–220. <https://doi.org/10.1016/j.memsci.2009.05.035>.
- Soave, G., 1972. Equilibrium constants from a modified Redlich-Kwong equation of state. Chem. Eng. Sci. 27 (6), 1197–1203. [https://doi.org/10.1016/0009-2509\(72\)80096-4](https://doi.org/10.1016/0009-2509(72)80096-4).
- Songolzadeh, M., Soleimani, M., Takht Ravanchi, M., Songolzadeh, R., 2014. Carbon dioxide separation from flue gases: a technological review emphasizing reduction in greenhouse gas emissions. Sci. World J. 2014 <https://doi.org/10.1155/2014/828131>.
- Stec, M., Spietz, T., Chwola, T., Tatarczuk, A., Krótki, A., 2019. Simple method for determining CO<sub>2</sub> loading of partially carbonated aqueous ammonia solutions using pH and density measurements. Int. J. Greenh. Gas Control 87, 80–88. <https://doi.org/10.1016/j.ijggc.2019.05.015>.
- Strigle, R.F., 1987. Random Packings and Packed Towers: Design and Applications. Gulf Publishing Company, Book Division. <https://books.google.com/books?id=eZdTAAQAAJ>.
- Sultan, H., Quach, T.-Q., Muhammad, H.A., Bhatti, U.H., Lee, Y.D., Hong, M.G., et al., 2021. Advanced post combustion CO<sub>2</sub> capture process—A systematic approach to minimize thermal energy requirement. Appl. Therm. Eng. 184, 116285 <https://doi.org/10.1016/j.applthermaleng.2020.116285>.
- Sutter, D., Gazzani, M., Mazzotti, M., 2015. Formation of solids in ammonia-based CO<sub>2</sub> capture processes—Identification of criticalities through thermodynamic analysis of the CO<sub>2</sub>–NH<sub>3</sub>–H<sub>2</sub>O system. Chem. Eng. Sci. 133, 170–180. <https://doi.org/10.1016/j.ces.2014.12.064>.
- Sutter, D., Gazzani, M., Mazzotti, M., 2016. A low-energy chilled ammonia process exploiting controlled solid formation for post-combustion CO<sub>2</sub> capture. Faraday Discuss. 192, 59–83. <https://doi.org/10.1039/C6FD00044D>.
- Sutter, D., Gazzani, M., Pérez-Calvo, J.-F., Leopold, C., Milella, F., Mazzotti, M., 2017. Solid formation in ammonia-based processes for CO<sub>2</sub> capture—turning a challenge into an opportunity. Energy Proc. 114, 866–872. <https://doi.org/10.1016/j.egypro.2017.03.1229>.
- Tay, W., Lau, K., Lai, L., Shariff, A., Wang, T., 2019. Current development and challenges in the intensified absorption technology for natural gas purification at offshore condition. J. Nat. Gas. Sci. Eng. 71, 102977 <https://doi.org/10.1016/j.jngse.2019.102977>.
- Tay, W., Lau, K., Shariff, A., 2016. High frequency ultrasonic-assisted CO<sub>2</sub> absorption in a high pressure water batch system. Ultrason. Sonochem. 33, 190–196. <https://doi.org/10.1016/j.ulsonch.2016.04.004>.
- Taylor, R., Krishna, R., 1993. Multicomponent Mass Transfer. Wiley. <https://books.google.com/books?id=FrpX9dNjWc0C>.
- Telikapalli, V., Kozak, F., Francois, J., Sherrick, B., Black, J., Muraskin, D., et al., 2011. CCS with the Alstom chilled ammonia process development program—Field pilot results. Energy Proc. 4, 273–281. <https://doi.org/10.1016/j.egypro.2011.01.052>.
- Thomsen, K., Rasmussen, P., 1999. Modeling of vapor-liquid-solid equilibrium in gas-aqueous electrolyte systems. Chem. Eng. Sci. 54 (12), 1787–1802. [https://doi.org/10.1016/S0009-2509\(99\)00019-6](https://doi.org/10.1016/S0009-2509(99)00019-6).
- Toro Molina, C., Bouallou, C., 2016. Carbon dioxide absorption by ammonia intensified with membrane contactors. Clean. Technol. Environ. Policy 18 (7), 2133–2146. <https://doi.org/10.1007/s10098-016-1140-0>.
- Ullah, A., Soomro, M.I., Kim, W.-S., 2019. Analysis of a rich vapor compression method for an ammonia-based CO<sub>2</sub> capture process and freshwater production using membrane distillation technology. Chem. Eng. Res. Des. 147, 244–258. <https://doi.org/10.1016/j.cherd.2019.05.005>.
- Vaidya, P.D., Kenig, E.Y., 2010. Termolecular kinetic model for CO<sub>2</sub>-alkanolamine reactions: an overview. Chem. Eng. Technol. 33 (10), 1577–1581. <https://doi.org/10.1002/ceat.201000050>.
- Verbrugge, P., 1979. Vapour-liquid Equilibria of the Ammonia-Carbon dioxide-Water System. Citeseer.
- Versteeg, P., Rubin, E.S., 2011. Technical and economic assessment of ammonia-based post-combustion CO<sub>2</sub> capture. Energy Proc. 4, 1957–1964. <https://doi.org/10.1016/j.egypro.2011.02.076>.
- Villeneuve, K., Zaidiza, D.A., Roizard, D., Rode, S., 2018. Modeling and simulation of CO<sub>2</sub> capture in aqueous ammonia with hollow fiber composite membrane contactors using a selective dense layer. Chem. Eng. Sci. 190, 345–360. <https://doi.org/10.1016/j.ces.2018.06.016>.
- Wang, F., Deng, S., Zhao, J., Yan, J., 2017a. A novel ammonia-based CO<sub>2</sub> capture process hybrid ammonia absorption refrigeration. Energy Proc. 142, 3734–3740. <https://doi.org/10.1016/j.egypro.2017.12.269>.
- Wang, F., Zhao, J., Miao, H., Zhao, J., Zhang, H., Yuan, J., et al., 2018. Current status and challenges of the ammonia escape inhibition technologies in ammonia-based CO<sub>2</sub> capture process. Appl. Energy 230, 734–749. <https://doi.org/10.1016/j.apenergy.2018.08.116>.
- Wang, M., Joel, A.S., Ramshaw, C., Eimer, D., Musa, N.M., 2015. Process intensification for post-combustion CO<sub>2</sub> capture with chemical absorption: a critical review. Appl. Energ. 158, 275–291. <https://doi.org/10.1016/j.apenergy.2015.08.083>.
- Wang, R., Zhang, H., Feron, P., Liang, D., 2005. Influence of membrane wetting on CO<sub>2</sub> capture in microporous hollow fiber membrane contactors. Sep. Purif. Technol. 46 (1-2), 33–40. <https://doi.org/10.1016/j.seppur.2005.04.007>.
- Wang, X., Conway, W., Fernandes, D., Lawrence, G., Burns, R., Puxty, G., et al., 2011. Kinetics of the reversible reaction of CO<sub>2</sub> (aq) with ammonia in aqueous solution. J. Phys. Chem. A 115 (24), 6405–6412. <https://doi.org/10.1021/jp108491a>.
- Wang, Y., Zhao, L., Otto, A., Robinius, M., Stolten, D., 2017b. A review of post-combustion CO<sub>2</sub> capture technologies from coal-fired power plants. Energy Proc. 114, 650–665. <https://doi.org/10.1016/j.egypro.2017.03.1209>.
- Wen, N., Brooker, M.H., 1995. Ammonium carbonate, ammonium bicarbonate, and ammonium carbamate equilibria: a Raman study. J. Phys. Chem. 99 (1), 359–368. <https://doi.org/10.1021/100001a054>.
- Xiang, Q., Fang, M., Maeder, M., Yu, H., 2013. Effect of sarcosinate on the absorption kinetics of CO<sub>2</sub> into aqueous ammonia solution. Ind. Eng. Chem. Res. 52 (19), 6382–6389. <https://doi.org/10.1021/i1e4006063>.
- Xu, Y., Chen, X., Zhao, Y., Jin, B., 2021. Modeling and analysis of CO<sub>2</sub> capture by aqueous ammonia+piperazine blended solution in a spray column. Sep. Purif. Technol. 267, 118655 <https://doi.org/10.1016/j.seppur.2021.118655>.
- Xu, Y., Jin, B., Chen, X., Zhao, Y., 2019. Performance of CO<sub>2</sub> absorption in a spray tower using blended ammonia and piperazine solution: experimental studies and comparisons. Int. J. Greenh. Gas Control 82, 152–161. <https://doi.org/10.1016/j.ijggc.2019.01.008>.
- Xu, Y., Jin, B., Zhao, Y., Hu, E.J., Chen, X., Li, X., 2018. Numerical simulation of aqueous ammonia-based CO<sub>2</sub> absorption in a sprayer tower: An integrated model combining gas-liquid hydrodynamics and chemistry. Appl. Energ. 211, 318–333.
- Xu, Y., Wang, Z., Liu, X., Jin, B., 2014. Modeling of the NH<sub>3</sub>–CO<sub>2</sub>–H<sub>2</sub>O vapor-liquid equilibria behavior with species-group Pitzer activity coefficient model. Int. J. Greenh. Gas Control 31, 113–120. <https://doi.org/10.1016/j.ijggc.2014.09.018>.
- Xu, Y., Zhao, J., Wu, W., Jin, B., 2015. Experimental and theoretical studies on the influence of ionic liquids as additives on ammonia-based CO<sub>2</sub> capture. Int. J. Greenh. Gas Control 42, 454–460. <https://doi.org/10.1016/j.ijggc.2015.08.023>.
- Yang, J., Yu, X., Yan, J., Tu, S.-T., 2014a. CO<sub>2</sub> capture using amine solution mixed with ionic liquid. Ind. Eng. Chem. Res. 53 (7), 2790–2799. <https://doi.org/10.1021/ie4040658>.
- Yang, N., Xu, D., Yang, Q., Wardhaugh, L., Feron, P., Li, K., et al., 2013. Aqueous ammonia and amino acid salts blends for CO<sub>2</sub> capture. In: 30th Annual International Pittsburgh Coal Conference 2013. PCC, p. 2013.
- Yang, N., Xu, D.Y., Liu, X., Jin, B., 2014b. Potassium sarcosinate promoted aqueous ammonia solution for post-combustion capture of CO<sub>2</sub>. Greenh. Gas.: Sci. Technol. 4 (4), 555–567. <https://doi.org/10.1002/ghg.1426>.
- Yang, N., Yu, H., Li, L., Xu, D., Han, W., Feron, P., 2014c. Aqueous ammonia (NH<sub>3</sub>) based post combustion CO<sub>2</sub> capture: a review. Oil. Gas Sci. Technol.–Revue d'IPF Energ. Nouvelles 69 (5), 931–945. <https://doi.org/10.2516/ogst/2013160>.
- Yang, N., Yu, H., Dy, Xu, Conway, W., Maeder, M., Feron, P., 2014d. Amino acids/NH<sub>3</sub> mixtures for CO<sub>2</sub> capture: effect of neutralization methods on CO<sub>2</sub> mass transfer and NH<sub>3</sub> vapour loss. Energy Proc. 63, 773–780. <https://doi.org/10.1016/j.egypro.2014.11.086>.
- Yeh, A.C., Bai, H., 1999. Comparison of ammonia and monoethanolamine solvents to reduce CO<sub>2</sub> greenhouse gas emissions. Sci. Total Environ. 228 (2-3), 121–133. [https://doi.org/10.1016/S0048-9697\(99\)00025-X](https://doi.org/10.1016/S0048-9697(99)00025-X).
- Yeh, J.T., Resnik, K.P., Rygle, K., Pennline, H.W., 2005. Semi-batch absorption and regeneration studies for CO<sub>2</sub> capture by aqueous ammonia. Fuel Process. Technol. 86 (14-15), 1533–1546. <https://doi.org/10.1016/j.fuproc.2005.01.015>.
- You, J.K., Park, H., Yang, S.H., Hong, W.H., Shin, W., Kang, J.K., et al., 2008. Influence of additives including amine and hydroxyl groups on aqueous ammonia absorbent for CO<sub>2</sub> capture. J. Phys. Chem. B 112 (14), 4323–4328. <https://doi.org/10.1021/jp711113q>.

- Yu, H., 2018. Recent developments in aqueous ammonia-based post-combustion CO<sub>2</sub> capture technologies. *Chin. J. Chem. Eng.* 26 (11), 2255–2265. <https://doi.org/10.1016/j.cjche.2018.05.024>.
- Yu, H., Morgan, S., Allport, A., Cottrell, A., Do, T., McGregor, J., et al., 2011. Results from trialling aqueous NH<sub>3</sub> based post-combustion capture in a pilot plant at Munmorah power station: absorption. *Chem. Eng. Res. Des.* 89 (8), 1204–1215. <https://doi.org/10.1016/j.cherd.2011.02.036>.
- Yu, H., Morgan, S., Allport, A., Cottrell, A., Do, T., McGregor, J., et al., 2013a. Results from trialling aqueous NH<sub>3</sub> (sub 3) based post combustion capture in a pilot plant at Munmorah power station. *Desorption.* [https://doi.org/10.1007/978-3-642-30445-3\\_152](https://doi.org/10.1007/978-3-642-30445-3_152).
- Yu, H., Qi, G., Wang, S., Morgan, S., Allport, A., Cottrell, A., et al., 2012a. Results from trialling aqueous ammonia-based post-combustion capture in a pilot plant at Munmorah power station: gas purity and solid precipitation in the stripper. *Int. J. Greenh. Gas Control* 10, 15–25. <https://doi.org/10.1016/j.ijggc.2012.04.014>.
- Yu, H., Qi, G., Xiang, Q., Wang, S., Fang, M., Yang, Q., et al., 2013b. Aqueous ammonia based post combustion capture: results from pilot plant operation, challenges and further opportunities. *Energy Proc.* 37, 6256–6264. <https://doi.org/10.1016/j.egypro.2013.06.554>.
- Yu, H., Tan, Z., Thé, J., Feng, X., Croiset, E., Anderson, W.A., 2016a. Kinetics of the absorption of carbon dioxide into aqueous ammonia solutions. *AIChE J.* 62 (10), 3673–3684. <https://doi.org/10.1002/aic.15296>.
- Yu, H., Xiang, Q., Fang, M., Yang, Q., Feron, P., 2012b. Promoted CO<sub>2</sub> absorption in aqueous ammonia. *Greenh. Gas.: Sci. Technol.* 2 (3), 200–208. <https://doi.org/10.1002/ghg.1280>.
- Yu, H., Yang, N., Maeder, M., Feron, P., 2018. Kinetics of the reversible reaction of CO<sub>2</sub> (aq) with taurate in aqueous solution. *Greenh. Gas.: Sci. Technol.* 8 (4), 672–685. <https://doi.org/10.1002/ghg.1771>.
- Yu, H., Zhu, Q., Tan, Z., 2012c. Absorption of nitric oxide from simulated flue gas using different absorbents at room temperature and atmospheric pressure. *Appl. Energ.* 93, 53–58. <https://doi.org/10.1016/j.apenergy.2011.03.039>.
- Yu, J., Wang, S., 2015. Development of a novel process for aqueous ammonia based CO<sub>2</sub> capture. *Int. J. Greenh. Gas Control* 39, 129–138. <https://doi.org/10.1016/j.ijggc.2015.05.008>.
- Yu, J., Wang, S., Yu, H., 2016b. Experimental studies and rate-based simulations of CO<sub>2</sub> absorption with aqueous ammonia and piperazine blended solutions. *Int. J. Greenh. Gas Control* 50, 135–146. <https://doi.org/10.1016/j.ijggc.2016.04.019>.
- Zeng, Q., Guo, Y., Niu, Z., Lin, W., 2011a. Mass transfer coefficients for CO<sub>2</sub> absorption into aqueous ammonia solution using a packed column. *Ind. Eng. Chem. Res.* 50 (17), 10168–10175. <https://doi.org/10.1021/ie101821b>.
- Zeng, Q., Guo, Y., Niu, Z., Lin, W., 2011b. Mass transfer performance of CO<sub>2</sub> absorption into aqueous ammonia in a packed column. *CIESC J.* 62, 146–150.
- Zeng, Q., Guo, Y., Niu, Z., Lin, W., 2013. The absorption rate of CO<sub>2</sub> by aqueous ammonia in a packed column. *Fuel Process. Technol.* 108, 76–81. <https://doi.org/10.1016/j.fuproc.2012.05.005>.
- Zhang, M., Guo, Y., 2013a. Process simulations of large-scale CO<sub>2</sub> capture in coal-fired power plants using aqueous ammonia solution. *Int. J. Greenh. Gas Control* 16, 61–71. <https://doi.org/10.1016/j.ijggc.2013.03.010>.
- Zhang, M., Guo, Y., 2013b. Process simulations of NH<sub>3</sub> abatement system for large-scale CO<sub>2</sub> capture using aqueous ammonia solution. *Int. J. Greenh. Gas Control* 18, 114–127. <https://doi.org/10.1016/j.ijggc.2013.07.005>.
- Zhang, Q., Cheng, C., Wu, T., Xu, G., Liu, W., 2020. The effect of Fe<sub>3</sub>O<sub>4</sub> nanoparticles on the mass transfer of CO<sub>2</sub> absorption into aqueous ammonia solutions. *Chem. Eng. Process.* 154, 108002. <https://doi.org/10.1016/j.cep.2020.108002>.
- Zhao, B., Fang, T., Qian, W., Liu, J., Su, Y., 2021. Process simulation, optimization and assessment of post-combustion carbon dioxide capture with piperazine-activated blended absorbents. *J. Clean. Prod.* 282, 124502. <https://doi.org/10.1016/j.jclepro.2020.124502>.
- Zhao, B., Su, Y., Cui, G., 2016a. Post-combustion CO<sub>2</sub> capture with ammonia by vortex flow-based multistage spraying: process intensification and performance characteristics. *Energy* 102, 106–117. <https://doi.org/10.1016/j.energy.2016.02.056>.
- Zhao, B., Su, Y., Tao, W., Li, L., Peng, Y., 2012. Post-combustion CO<sub>2</sub> capture by aqueous ammonia: a state-of-the-art review. *Int. J. Greenh. Gas Control* 9, 355–371. <https://doi.org/10.1016/j.ijggc.2012.05.006>.
- Zhao, Q., Wang, S., Qin, F., Chen, C., 2011. Composition analysis of CO<sub>2</sub>–NH<sub>3</sub>–H<sub>2</sub>O system based on Raman spectra. *Ind. Eng. Chem. Res.* 50 (9), 5316–5325. <https://doi.org/10.1021/ie1010178>.
- Zhao, S., Feron, P.H., Deng, L., Favre, E., Chabanon, E., Yan, S., et al., 2016b. Status and progress of membrane contactors in post-combustion carbon capture: A state-of-the-art review of new developments. *J. Membr. Sci.* 511, 180–206. <https://doi.org/10.1016/j.memsci.2016.03.051>.
- Zhongli, T., Xingjian, Z., Botan, L., Chunjian, L., Tao, C., Xigang, Y., 2012. Volumetric overall mass transfer coefficients of CO<sub>2</sub> absorption into aqua ammonia in structured packed column. *CIESC J.* 63 (4), 1102–1107. <https://hgxb.cip.com.cn/E/N/Y2012/V63/I4/1102>.
- Zhou, S., Wang, S., Chen, C., 2012. Thermal degradation of monoethanolamine in CO<sub>2</sub> capture with acidic impurities in flue gas. *Ind. Eng. Chem. Res.* 51 (6), 2539–2547. <https://doi.org/10.1021/ie202214y>.